USGS
science for a changing world

Prepared in cooperation with U.S. Fish and Wildlife Service

A Framework for Decision Points to Trigger Adaptive Management Actions in Long-Term Incidental Take Permits

Open-File Report 2015–1227

U.S. Department of the Interior
U.S. Geological Survey

A Framework for Decision Points to Trigger Adaptive Management Actions in Long-Term Incidental Take Permits

By Daniel Dalthorp and Manuela Huso

Prepared in cooperation with U.S. Fish and Wildlife Service

Open-File Report 2015-1227

U.S. Department of the Interior
U.S. Geological Survey

U.S. Department of the Interior
SALLY JEWELL, Secretary

U.S. Geological Survey
Suzette M. Kimball, Acting Director

U.S. Geological Survey, Reston, Virginia: 2015

Suggested citation:
Dalthorp, Daniel, and Huso, Manuela, 2015, A framework for decision points to trigger adaptive management actions in long-term incidental take permits: U.S. Geological Survey Open-File Report 2015-1227, 88 p., http://dx.doi.org/10.3133/ofr20151227.

ISSN 2331-1258 (online)

Contents

Figures

Tables

Conversion Factor

International System of Units to Inch/Pound

	Wind speed	
meter per second (m/s)	2.237	miles per hour (mi/h)

Abbreviations

AMA	adaptive management action
CI	credible interval
EoA	Evidence of Absence
IQR	inter-quartile range (25th through 75th percentiles)
ITP	incidental take permit

A Framework for Decision Points to Trigger Adaptive Management Actions in Long-Term Incidental Take Permits

By Daniel Dalthorp and Manuela Huso

Introduction

Background

The U.S. Fish and Wildlife Service (USFWS) has begun to issue incidental take permits (ITPs) to wind power companies to allow limited take of bird and bat species that are protected under the Endangered Species Act, the Bald and Golden Eagle Protection Act, or the Migratory Bird Treaty Act (Huso and others, 2015). Expected take rates are determined using scientifically based collision-risk models and knowledge about the ecology of the population of interest. ITPs often include mitigation requirements to compensate for estimated take and further describe (1) adaptive management actions (AMAs) that may be required to reduce take rates if permitted rate is exceeded, or (2) additional compensatory mitigation to offset take that exceeds permitted levels.

Confirming the accuracy of predicted take and providing evidence that permitted take levels have not been exceeded can be challenging because carcasses may be detected with probability much less than 1, and often no carcasses are observed. When detection probability is high, finding 0 carcasses can be interpreted as evidence that none (or few) were actually killed. As the probability of observing an individual decreases, the likelihood of missing carcasses increases, making it unclear how to interpret having observed 0 (or few) carcasses. In a practical sense, the consequences of incorrect inference can be significant: overestimating take could result in costly and unjustified mitigation, whereas underestimating could result in unanticipated declines in species populations already at risk.

Huso and others (2015) propose an approach using Bayes' Theorem to construct a posterior distribution of potential take given the observed count and the estimated probability of detecting a carcass. Dalthorp and others (2014) published Evidence of Absence (EoA) software and associated user guide to calculate the posterior distribution of take. These seminal publications originally addressed inferential limits regarding potential take at an individual site in any single year. Subsequent discussions with users led to the idea that these concepts could be expanded and applied over a series of years (the duration of an ITP) and field data could be used to accurately infer whether actual take levels are consistent with, higher than or lower than permitted levels. In response, we have developed a statistical framework for signaling when take levels are inconsistent with permitted levels, both on a short-term (3-year running average) and long-term (cumulative total take) basis.

This document examines the accuracy and precision of these "triggers" and their sensitivity to input parameters, including estimated detection probability (g), level of assurance desired ($1-\alpha$), effectiveness of AMAs (ρ), etc. We present a statistical framework for defining triggers for AMAs when take rates exceed permitted levels, as well as triggers for rescinding previous AMAs when

warranted by low take rates. The triggers (with associated AMAs) are evaluated in terms of the consequences (conservation benefits and operations costs) of various choices about trigger parameters (including permitted take limit, credibility levels, AMA options, and monitoring requirements) against a number of ecological backdrops (including actual take levels and effectiveness of AMAs). The report is strictly statistical and does not make specific recommendations about management or regulatory parameters. Instead, a range of scenarios that span a wide range of possibilities is considered. The purpose is to provide a framework for defining triggers for AMAs and guide decision-making in the management of ITPs with a quantitative consideration of potential consequences.

In the following discussions, an average take rate of τ per year is permitted over the course of n years of operation, and a total take of $T = n\tau$ is allowed over the course of the permit. The methods used to set τ are beyond the scope of this document; we start from the premise that τ has been externally established. Estimated cumulative take is tracked through the years, and when estimated take exceeds the total permitted take (T), a long-term trigger fires and full-avoidance AMAs are implemented to avoid further take. In addition, a moving-average take rate is tracked through the years, and when the average take rate has risen clearly above the permitted level (τ), a short-term trigger fires providing a check against excessive take over the span of a few years and signaling that the long-term take limit is likely to be exceeded unless conditions change. Finally, a reversion trigger may be defined to signal when fatality rates are low enough so that previously implemented AMAs may be reversed without serious risk that future fatality rates will exceed permitted levels.

A program of incremental AMAs may be developed to respond to the firing of the short-term trigger. Such a strategy may involve (1) AMAs to reduce the actual fatality rate (λ) incrementally each time the short-term trigger is fired to keep the fatality rate in line with the expected rate (τ) in future years; (2) an intensification of monitoring to increase precision of estimates; or (3) adjustment of τ to align permitted with actual take rates. AMAs that reduce the fatality rate or increase precision are likely to reduce the chances that the short-term trigger will fire in future years if the short-term trigger remains the same. In addition, after the short-term trigger has fired some predetermined number of times, with or without implementation of incremental AMAs, it may be desirable to implement a full-avoidance AMA to avoid further take (as with the long-term trigger).

Estimation of Fatalities

Because it is difficult to directly observe fatalities as they occur (Pandey and others, 2007; Evans, 2012; Cryan and others, 2014), take is normally estimated indirectly from carcass counts in periodic searches of the ground near turbines over the course of the monitoring season. However, carcasses may be missed in searches for a number of reasons. Most notably, carcasses may land outside the searched area (Huso and Dalthorp, 2014) or be removed by scavengers prior to discovery by search teams (Bispo and others, 2013), and searchers may miss carcasses that are present at time of search (Morrison, 2002). Several researchers have developed fatality estimators that account for imperfect detection and adjust carcass counts accordingly (Erickson and others, 1998; Shoenfeld, 2004; Huso 2011; Korner-Nievergelt and others, 2011; Etterson, 2013; Péron and others, 2013; Wolpert, 2015). These widely used "adjusted counts" estimators are elaborations of the same basic model that estimates the number of fatalities (M) as $\widehat{M} = X/\hat{g}$, where X is the number of carcasses observed and $\hat{g}$ is the estimated probability of detecting a carcass that arrives during the period of interest (after accounting for area searched, carcass removal rate, and searcher efficiency). However, the estimators differ in how the detection probability is estimated and how data from different time periods and different subunits within a site are combined into an overall fatality estimate for the site for the entire study period (Huso and others, in press).

The EoA software (Dalthorp and others, 2014) is based on a semi-periodic estimator for detection probability g that is similar to Wolpert (2015) and includes the estimators for Erickson and others (1998), Shoenfeld (2004), Huso (2011), Korner-Nievergelt and others (2011), as special cases (Huso and others, 2015b; Wolpert, 2015). After estimating g, it uses Bayes' theorem to estimate M in terms of "credible intervals" (CIs) (Huso and others, 2015a), which are analogous to confidence intervals used in classical statistics. For example, after accounting for the numerous sources of imperfect detection and estimating overall detection probability as $\hat{g}$, EoA gives M^* as the upper bound of a $100(1-\alpha)\%$ CI for M. The interpretation is that it can be asserted with $100(1-\alpha)\%$ credibility that the true number of fatalities M is less than or equal to M^*.

The value of α governs how conservative M^* is as an estimate of M, with smaller values of α leading to larger M^* but stronger assurance that the actual number of fatalities M does not exceed M^*. A less formal but intuitive interpretation is to think of M^* as a $100(1-\alpha)\%$ credible upper bound for M (esp. when α is small) or simply as an estimate of M when $\alpha = 0.5$ and $X > 0$, giving a median point; that is, it is equally likely in probability that the actual fatality is less than this value as greater than this value.

Yearly take (M) of protected species at any given facility is likely to be small, and the number of observed carcasses (X) is likely to be even smaller. Finding $X = 0$ carcasses is a distinct possibility. However, if detection probability is small, $X = 0$ provides little assurance that the actual number of fatalities was not large. For example, if there are 150 fatalities and detection probability is $g = 0.01$, then the probability of missing all 150 carcasses would be $(1-0.01)^{150} = 22\%$, so $X = 0$ would not be surprising. In this case, finding no carcasses does not rule out the possibility that large numbers of individuals were killed but were simply missed in the searches. Higher detection probabilities give greater power to rule out high fatality rates. If $g = 0.75$, then $X = 0$ provides strong evidence that there were not more than 1 or 2 fatalities, because if there were 3, it is highly improbable that all 3 would have been missed $[P(X = 0|M = 3) = (1-0.75)^3 = 0.016]$. From user input, EoA software (Dalthorp, and others, 2014) estimates the detection probability, and, taking into account both the detection probability and the observed number of carcasses, it provides a credible upper bound on the number of fatalities (with the user-specified degree of credibility = $1-\alpha$).

Triggers for Adaptive Management in Long-Term Incidental Take Permits

The EoA software provides many useful tools for designing monitoring protocols and analyzing results. The user guide for version 1.0 (Dalthorp and others, 2014) provides a tutorial with several examples of how the software can be used to determine whether the number of fatalities in a single year exceeded a specified threshold. It has been argued (Meinke and others, 2014) that it may be impracticable to provide strong assurance on an annual basis of small take numbers when search conditions are difficult and high detection probabilities are not easily attainable due to carcasses that are small and cryptic, extensive areas of unsearchable ground, high scavenging rates, or some other reason.

In the months following publication of the EoA software (Dalthorp and others, 2014), it became clear that a multiyear permit provides a context vastly different from the kinds of single-year scenarios discussed in the user guide and allows for modified approaches to compliance monitoring with substantially reduced annual costs. In particular, long-term take permits may be based on total expected take rates over a span of several years with companies offsetting expected take with mitigation. Take in excess of permitted rates would then require AMAs to reduce take rates to bring them into line with expectations or require adjusting permitted take rates upward and additional mitigation. This framework allows two adaptations which are not considered in the original user guide (Dalthorp and others, 2014) but which make it much easier to demonstrate compliance. First, a long-term permit may accommodate

year-to-year variation in take as long as the total take over the course of the n years of the permit does not exceed $T = n\tau$. This is not nearly as strict as requiring that take be less than τ each and every year. Indeed, if the total take over n years is T, the average annual take would be τ, but take would be expected to exceed τ in about one-half of the years, which would be a gross violation of a requirement that annual take never exceed τ but would be permissible for a long-term requirement that cumulative take not exceed $T = n\tau$. Second, for long-term take limits that are based on expected take rates rather than rates that would cause immediate jeopardy to the population if exceeded, lower levels of assurance may be acceptable (for example, allowing $\alpha = 0.2$ or 0.5 instead of requiring a more conservative $\alpha = 0.05$ or 0.10). In particular, although a value of $\alpha = 0.5$ might well allow fatality rates in excess of T to go undetected at a significant fraction of projects, average take across many projects would be unlikely to exceed permitted numbers, provided: (1) AMAs eliminate further take at projects where estimated take exceeds the long-term limit, and (2) AMAs reduce take rates at projects where average rates over several years significantly exceed permitted averages.

Specific Definitions

Define the annual permitted average take rate as τ individuals per year over the course of an n-year permit, and the total permitted cumulative take is $T = n\tau$. Actual take is denoted by M with estimated take denoted by M^*.

Table 1. Glossary of terms.

Ecological parameters—What is actually happening with the protected species?
M = actual number of fatalities
λ = baseline true annual fatality rate at permit issuance
ρ = factor by which an AMA changes fatality rate
ρ_∞ = factor by which the final level of AMA changes fatality rate
Operational parameters—How do we know what is happening?
X = number of carcasses observed
g = overall carcass detection probability after accounting for unsearched area, scavenging, and searcher efficiency
Governing parameters—What is set by regulators and energy companies?
n = number of years of operation covered by permit
τ = permitted annual take rate
T = total permitted take over life of permit ($T = n\tau$)
α = significance level for testing cumulative take (long-term)
α' = significance level for testing take rate (short-term)
α_r = significance level for reversing a previous AMA (including initial prophylactic curtailment)
AMAs = Adaptive Management Actions taken if fatality rates are not in line with expectations
Test statistics
M^* = estimated cumulative number of fatalities
$\lambda^* = 100\alpha'\%$ credible lower bound or $100(1-\alpha_r)\%$ credible upper bound for mean take rate

Long-Term Trigger—Does Total Cumulative Take Exceed Long-Term Authorized? —Test Whether $M^* > \mathrm{T}$

Total take accumulates from year to year. Progress toward the long-term take limit of T is tracked using the "Multiple Year Total" module in the EoA software. Because actual cumulative take (M) is not known, estimated cumulative total (M^*) must be used instead. Exceedance of the long-term limit ($M^* > \mathrm{T}$) triggers AMA to avoid further take. The value of M^* is strongly tied to choice of required significance level α, which must be agreed on before monitoring begins. Small values of α (for example, 0.1 or 0.2) give relatively strong assurance that take does not exceed the permitted limit at any given project, but triggering will tend to occur well before $M > \mathrm{T}$. A value of $\alpha = 0.5$ results in more accurate tracking of actual fatality rates with triggering tending to occur after $M > \mathrm{T}$, in which case the trigger is not designed to prevent exceedance but to signal when exceedance has occurred.

As an example, suppose the long-term authorized take is $\mathrm{T} = 60$ for a 30-year permit. Ideally, if we knew exactly the number of fatalities each year, we could track the cumulative number of fatalities through the years and implement full-avoidance AMA when the cumulative total exceeded T. But in practice, the number of fatalities is estimated from carcass counts, after accounting for estimated detection probability, with varying degrees of certainty (fig. 1). A conservative approach using a small value of α, for example, α=0.1, would (1) give greater assurance that fatality rates do not exceed permitted levels, (2) provide a buffer against potential underestimation of fatality resulting from inadvertent mischaracterization of detection probability, and (3) provide a margin of safety against a full-avoidance AMA that is less than 100% effective. But it would also result in a higher likelihood of triggering well before the limit of 60 has been reached. If the factors that contribute to imperfect detection—most notably coverage (that is, the fraction of total carcasses that arrive in the search area during the monitoring period), carcass persistence, searcher efficiency, and change in searcher efficiency with carcass age—are properly accounted for and g accurately reflects overall detection probability for the species of concern, then 0.5 will generally be the most accurate choice for α.

In the scenario portrayed in figure 1, the actual number of fatalities, first exceeds T in year 25, and the estimated number of fatalities M^* with $\alpha = 0.5$ first exceeds T to fire the long-term trigger in year 26 (fig. 1), 1 year after the actual number of fatalities first exceeded T. A value of $\alpha = 0.2$ would result in triggering in year 14 when the actual fatality rate was 39—well below the limit of 60, providing some assurance that T had not been exceeded and some assurance that T will not be greatly exceeded if fatalities continue to accumulate after the AMA is implemented. An even more conservative approach would be to base M^* on $\alpha = 0.1$, which, in this example, would induce triggering in year 10 when the number of fatalities was 30 (fig. 1).

The long-term trigger with $\alpha = 0.5$ is designed to signal when take exceeds permitted limits, but it is not designed to prevent exceedance. Indeed, the long-term trigger does not guard against the possibility that the take permitted for the entire life of the project occurs within just a few years or give any indication when annual take rates are well above τ. The conservation effect of a total take of T may be more severe if it occurs in a short period rather than being spread out over the course of the project. In addition, the long-term trigger does not provide a mechanism for detecting changes in fatality rates over time. Finally, the AMAs associated with the long-term trigger may be costly. Advance warning of impending long-term triggers coupled with less onerous AMAs to prevent exceedance may be desirable. To remedy these limitations of relying strictly on a long-term trigger, a short-term trigger can work in concert with the long-term trigger to give advance warning of possible exceedance, to detect changes in fatality rates, and to provide a framework for incremental AMAs to prevent eventual exceedance.

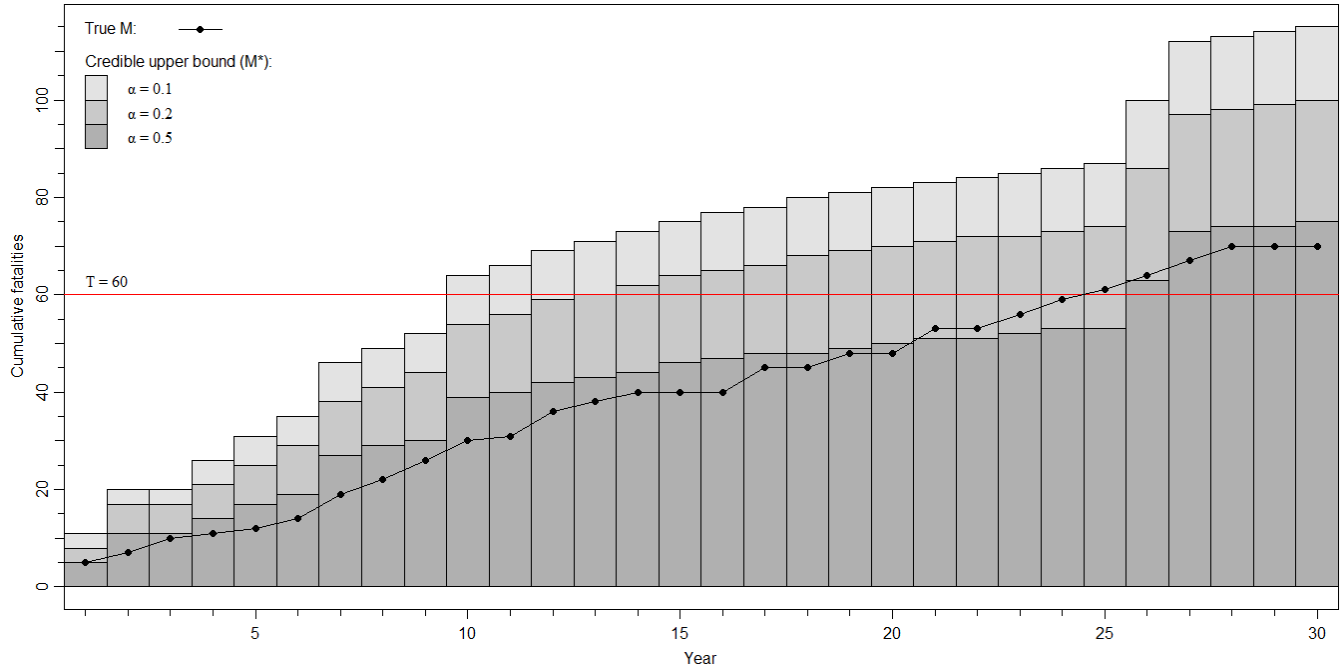

Figure 1. Operation of the long-term trigger. Simulated yearly fatalities were generated from a Poisson distribution with an annual rate of $\lambda = 2$. Carcass counts were generated from the fatalities as binomial random variables with probability of success equal to the detection probability g, which was taken as 0.3 in the first 3 years and 0.08 in years 4–30. Credible intervals were calculated using the Multiple Years module in the Evidence of Absence software. See table 1 for explanation of terms used here.

Short-Term Trigger—Is Actual Average Take Rate Larger Than Expected? —Test Whether $\lambda > \tau$

The short-term trigger is designed to fire when the number of carcasses over the course of a few years combined with the estimated detection probability indicate that an average rate of $\tau = \mathrm{T}/n$ per year has likely been exceeded. The short-term trigger acts as a precaution against unexpectedly high fatality rates, as a warning signal that the long-term authorized take is likely to be exceeded unless additional measures are taken to reduce take rate, and as a mechanism to signal significant changes in fatality rates. In response to short-term trigger firing, incremental AMAs may be implemented to improve the precision of estimates by more intensive monitoring, to reduce take rates to bring them more in line with expectations (minimization), or to adjust permitted take levels to align with actual take and offset the increase in permitted take with additional mitigation.

Even though the average permitted annual take at a site, τ, might be "correct" and reflect the true annual take rate, the actual number of fatalities that occur will not be exactly the same every year, due simply to natural variation and random chance. The short-term trigger is designed to allow for some annual variation in actual take and to guard against "hair-trigger" decision points. The trigger fires when the observed data (carcass counts combined with detection probabilities) are incompatible with the permitted rate. In other words, if it is too unlikely ($\leq\alpha'$) that the number of carcasses counted would be as high as observed if the true fatality rate really were in line with the permitted rate, then the short-term trigger would fire. The test is conducted each year on a 3-year running average basis. If the total number of carcasses observed in any consecutive 3 years is not compatible with what would be expected if the rate were equal to permitted level, the trigger fires.

Specifically, let X be the 3-year total carcass count for years $i-2, i-1$, and i, that is $X = \sum_{j=i-2}^{i} X_j$ (with $X_j = 0$ for $j < 1$). For purposes of the trigger, suppose the total number of fatalities in three years is $M \sim \text{Poisson}(3\lambda)$. Estimate λ via a posterior distribution conditioned on the observed carcass count and the estimated detection probability ($\hat{g}$):

$$P(\lambda|\hat{g}, X) = \frac{P(X|\lambda,\hat{g})P(\lambda)}{\int P(X|\lambda,\hat{g})P(\lambda)d\lambda},$$

where $X \sim \text{binomial}(M, \hat{g})$, $\hat{g} \sim \text{beta}(a, b)$, a and b are the parameters for a beta distribution with mean and variance of $\hat{g}$ as estimated for multiple year totals (Dalthorp and others, 2014), and $P(\lambda) \propto 1/\sqrt{\lambda}$ is the Jeffreys prior for Poisson rate. The trigger fires when $P(\lambda \leq \tau|\hat{g}, X) < \alpha'$, indicating that there is little chance that actual fatality rate λ is less than the permitted τ. Equivalently, if the lower bound of the $100(1-2\alpha')\%$ credibility interval for λ exceeds permitted τ, the short-term trigger is fired.

For example, suppose the permitted take total is $\text{T} = 60$ over the course of a 30-year permit and the annual permitted rate is $\tau = 2$, and we define $\alpha' = 0.01$ for the short-term trigger. With a detection probability of $g = 0.3$ [or $\hat{g} \sim \text{beta}(62999999.7, 146999999.3)$], the 98% CI [that is, $100(1-2\alpha')\%$ CI cuts off the upper and lower 1% of the posterior distribution] for the annual rate (λ) when a total of $X = 5$ carcasses are observed over 3 years would be [1.98, 14.6]. Because the interval includes 2, we cannot conclude that the permitted take rate is outside the credible range for actual take, and the short-term trigger does not fire. Although at first glance an estimated 3-year total of $X/g = 16.7$ may appear substantially greater than the permitted rate of 2 per year or 6 in 3 years, it is not clearly beyond what could occur with an average rate of 2 per year and a detection probability of 0.3. By contrast, if $X = 6$, the short-term trigger is fired because the 98% CI is [2.59, 16.2], indicating that $\tau = 2$ is outside the credible range of fatality rates that are compatible with the observed data.

The value of α' is approximately the probability of the trigger firing when $\lambda = \tau$. Thus, larger values of α' result in a more sensitive trigger because they require weaker evidence to conclude $\lambda > \tau$. A small value of α' (for example, 0.01) may be necessary to protect against the trigger firing unnecessarily when $\lambda \leq \tau$.

The test is based on a 3-year running total, so the trigger is especially unlikely to fire in the first 2 years unless $\lambda \gg \tau$ because firing would mean that the take allotted for the first 3 years arrives before the 3 years are finished. Thus, a short-term trigger firing in the first 2 years is a stronger signal of exceedance than a later triggering. This may help justify (1) applying more stringent AMAs for short-term triggers in the first 2 years than in later years, or (2) using a slightly higher value of α' for the first 2 years compared to later years to improve the chances of detecting an excessively high take rate while only slightly increasing the risk of wrongly flagging a rate that is not out of line with permitted τ.

Reversion Trigger—Is Actual Average Take Rate Small Enough to Safely Reverse an Existing Operational Constraint? —Test Whether $\lambda < \tau\,\rho$

If a facility is operating under constraints that are expected to reduce fatality rates by a factor of $\rho, (0 < \rho \leq 1)$ compared with rates expected under operations free from the constraints (that is, the fatality rate would be λ for operations without the constraints and $\rho\lambda$ with the constraints), then the reversion trigger is designed to signal when fatality rates are low enough so that removal of the operational constraints would not be likely to result in annual fatality rates that exceed τ. One possible use of the reversion trigger would be to relax an initial prophylactic constraint if fatality rates are well below expected rates. For example, if, from the beginning of a project, turbines are required to be curtailed at wind speeds <5.0 m/s to minimize bat fatalities, the reversion trigger could be used to determine if fatality rates are low enough to allow unconstrained operations and still remain within the permitted fatality rate.

In particular, a previous, operational constraint or restrictive AMA implemented to reduce fatalities by a factor of ρ can be reversed when take rate is demonstrated to be lower than $\tau\rho$ at a credibility level of $1 - \alpha_r$ according to a test on average rate over the years since the AMA was implemented. The rationale is that reversing an AMA with effectiveness of ρ would have the effect of increasing the fatality rate to λ/ρ, so an initial fatality rate of $\lambda \leq \tau\rho$ would result in a rate $\lambda/\rho \leq \tau$ after reversion.

To conduct the test, define the required significance level α_r and calculate a posterior distribution of the actual take rate λ with the (non-informative) Jeffreys prior. Specifically, let X be the cumulative total carcass count for year 1 through year i. For purposes of the trigger, suppose the total number of fatalities over i years is $M \sim \text{Poisson}(i\lambda)$. Estimate λ via a posterior distribution conditioned on the observed carcass count and the estimated detection probability ($\hat{g}$):

$$P(\lambda|\hat{g}, X) = \frac{P(X|\lambda,\hat{g})P(\lambda)}{\int P(X|\lambda,\hat{g})P(\lambda)d\lambda},$$

where $X \sim \text{binomial}(M, \hat{g})$, $\hat{g} \sim \text{beta}(a, b)$, a and b are the parameters for a beta distribution with mean and variance of $\hat{g}$ as estimated for multiple year totals (Dalthorp and others, 2014), and $P(\lambda) \propto 1/\sqrt{\lambda}$ is the Jeffreys prior for Poisson rate. The trigger fires when $P(\lambda < \tau\rho|\hat{g}, X) > 1 - \alpha_r$ indicating that that actual fatality rate λ is less that $\tau\rho$ and reversion is not likely to result in a fatality rate greater than the permitted τ.

Evaluating Trigger Performance

The dual triggering framework consists of a long-term trigger to signal when take limits have been exceeded and a short-term trigger to give advance warning when take rate is not in line with expectations or when it changes unexpectedly during the life of the permit. The short- and long-term triggers are intended to trigger adaptive management when warranted by the monitoring data, which include count of observed carcasses as well as estimated carcass-detection probability. The basic framework is highly flexible, with several options for balancing the competing objectives of conservation of protected species and efficiency of operations.

Extensive simulations were performed to evaluate the performance of the triggers for a 30-year permit under various combinations of (1) governing parameters (τ = 0.5, 1, 2, 4 and 8; α = 0.5, 0.2 and 0.1; α' = 0.01, 0.05 and 0.10); (2) operational parameters (g = 1, 0.8, 0.3, 0.15, 0.12, and 0.08 under an array of year-to-year patterns that reflect conditions encountered in monitoring fatalities of bats, small birds, or eagles); (3) ecological parameters (ratio of actual take rate to permitted rate λ/τ = 0.5, 0.75, 1, 1.5, 2, and 3; (4) effectiveness of incremental AMA after the short-term trigger has fired n times = ρ_0^n , where ρ_0 is the factor by which fatality is changed with each successive increment in AMA, and ρ_0= 1, 0.841, 0.707, and 0.5; and (5) effectiveness of the avoidance AMA after the long-term trigger is fired or the short-term trigger has fired a specified number times, ρ_∞= 0 and 0.05). Simulations and figures were produced using the R statistical software (R Core Team, 2013) with custom packages VGAM (Yee, 2010) and pBrackets (Schulz, 2014).

In practice, specific values of governing parameters (τ, α, α') and effectiveness of AMAs (ρ_0, ρ_∞) have direct and pronounced effects on trigger performance. Their values are decided upon by industry and government representatives through negotiation and then written into the ITP after agreement is reached. In defining the values of the governing parameters, consideration should be given to balancing the inherent tradeoffs between conservation and operations. Parameter values that provide weaker assurance that set limits have not been exceeded will likely be less costly to implement but may fail to detect fatality rates of conservation concern. Conversely, parameter choices aimed at providing strong assurance that fatality rates have not been exceeded are likely to be more costly and may lead to unnecessary restrictions on operations with no tangible conservation benefit. Throughout this document, the consequences of various choices of governing parameters on fatality rates and on operations are given in tandem to facilitate comparisons between costs in terms of both conservation and operational efficiency.

Values of operational parameters (g for each year) are determined by a combination of the monitoring protocol (for example, frequency and spatial extent of monitoring) and environmental conditions on the ground (for example, scavenger activity, effectiveness of field crews, ground texture, vegetation, weather). The value of g can only be crudely predicted in advance and must be estimated at each site in each year. For bats in the Midwest, intensive monitoring may result in g near 0.3 whereas road and pad searches may result in g of 0.1 or less. By contrast, detection probabilities of $g = 0.8$ may be possible with extensive monitoring for eagles, which are much larger and persist longer than bats and tend to be found in areas with sparser vegetation and more visible ground. Detection probabilities may be increased in a number of ways, for example, by:

1. increasing the number of turbines searched;
2. expanding the search radius around turbines;
3. stratifying the search area and allocating limited search efforts to the areas with the greatest detection probabilities and the highest carcass densities;
4. increasing the frequency of searches;
5. decreasing the activity of scavengers;
6. using specially trained dogs to aid searchers; or
7. improving the visibility on the ground via clearing vegetation, smoothing the surface, or lightening its color.

Specific values for ecological parameters—actual take rates (λ) and actual effectiveness of AMAs (ρ)—are not known in practice, but specific values are assumed in the simulations to explore trigger performance under various hypothetical scenarios. The effectiveness and advisability of specific sets of AMAs to use in conjunction with the triggers are not addressed in this report.

Simulated annual fatalities (M) were generated from random draws from a Poisson(λ) distribution, where λ is a fixed value that varies by scenario. Given M fatalities, simulated carcass counts (X) were generated as random draws from a binomial(M, g)[1]. Triggers were then tested year-by-year on 30-year sets of counts and detection probabilities, and performance is measured in terms of number of fatalities realized and years of operation under each level of AMA.

Performance of Long-Term Trigger

The long-term trigger is designed to signal when the cumulative fatality (M) has exceeded the permitted take limit of T individuals. Some key characteristics of the long-term trigger are:

1. When the average annual take rate is significantly less than $\tau = \mathrm{T}/n$, the long-term trigger is unlikely to ever fire under most conditions when $\alpha = 0.5$;
2. The trigger with $\alpha = 0.5$ is not designed to prevent exceedance of take limits but to signal when take limits have been exceeded. Thus, when average annual take rates exceed τ, the total take typically will have exceeded the take limit before the trigger is fired. However, smaller values of α result in a more sensitive long-term trigger and can be used to prevent exceedance.
3. Although on average the trigger (with $\alpha = 0.5$) fires when M slightly exceeds T, the trigger will sometimes fire when $M \leq \mathrm{T}$ and sometimes not fire until a few years after $M > \mathrm{T}$. This is due to inherent uncertainties in estimating total fatality when there is imperfect detection. Precision can be improved by reducing uncertainty (for example, by increasing detection probability g though more intensive monitoring or by increasing T). Improvements in precision lead to lower probabilities that M is much greater or much less than T when the trigger fires. Alternatively, the accuracy can be adjusted (for example, by changing α) to increase or decrease the sensitivity of the trigger, leading to earlier or later trigger firings. Adjustments to accuracy necessarily lead to tradeoffs between conservation and operations; that is, a decrease in average fatalities comes at a cost of reduced operations, and extending the years of operation before the trigger fires comes at a cost of greater numbers of fatalities.
4. If the true average annual take rate (λ) is exactly $\tau = \mathrm{T}/n$, odds are about 50-50 that actual take M will exceed T at some point in the n years. However, exceedance is likely to be near the end of permit. For example, suppose $\lambda = \tau$ and the project operates freely throughout the course of the n years of the permit, then the expected total number of fatalities is exactly the permitted limit: $\mathrm{E}[M] = \mathrm{T}$. However, because of random variation in fatalities from year to year, the actual number of fatalities at the end of permit will rarely be T exactly but will be greater than T in about half the projects and less than T in the other half. For example, suppose at each of 100 projects the take limit is $\mathrm{T} = 60$ through 30 years; that is, the annual rate is $\lambda = 2$, and the number of fatalities each year is Poisson distributed. Then the total number of fatalities at a project after 30 years would be a random variable $M \sim \mathrm{Poisson}(60)$. At the end of 30 years, M would exceed T at about 47% of the projects.

[1] For simplicity, in the simulations of the data, g is assumed fixed, and in the estimation, g is assumed known. In practice, there is potentially a large degree of uncertainty in $\hat{g}$ (that is, uncertainty in estimates of g). For values of $\alpha < 0.5$, greater uncertainty in $\hat{g}$ would generally be reflected in larger M^* values and earlier long-term triggering. For values of $\alpha > 0.5$, greater uncertainty in $\hat{g}$ would generally be reflected in smaller M^* values and later long-term triggering. For $\alpha = 0.5$, uncertainty in $\hat{g}$ has relatively minor effect on average M^* values. By contrast, greater uncertainty in $\hat{g}$ would result in wider CIs for λ and less sensitive short-term triggering. The EoA software (v1.0 and later) accounts for uncertainty in estimates of g.

Results representing effects of governing parameters, operational parameters, and ecological parameters on (1) the number of fatalities and (2) the number of years of operation before the long-term trigger fires (or permit expires, whichever comes first) are presented in figures 2–13. In each figure, results from (approximately) 150 different scenarios are shown.

Technical Note on Prior Distributions for M

The M^* estimates in the simulations are calculated using Bayes' theorem with an integrated discretized reference theory prior for M as an objective prior (Berger and others, 2012). Specifically, the posterior distribution of M is calculated as $P(M|x,g) = \frac{P(x|M,g)P(M)}{\sum_m P(x|M=m,g)P(M=m)}$, where $P(M) \propto \int_M^{M+1} 1/\sqrt{m}\, dm = \sqrt{M+1} - \sqrt{M}$. In version 1.0 of the EoA software (Dalthorp and others, 2014), a uniform prior [$P(M) \propto 1$] is used instead. In a broad sense, the two priors are similar, and results derived from one or the other will be negligible in most situations. However, when x is small, the reference prior results in more accurate CI coverage. In practice, compared with uniform prior, the reference prior results in a noticeably less sensitive long-term trigger when τ is small. The authors are planning to use the reference prior for M in software update EoA v2.0.

Number of Fatalities

In figures 2, 4, 5, 7, 8, 10, and 12, the distributions of the total number of fatalities when the long-term trigger fires (or 30 years, whichever comes first) are displayed as transparent boxes representing the inter-quartile range (IQR), or the 25th and 75th percentiles. In other words, of all the projects operating under the given set of parameters (τ, λ/τ, etc.), one-half of the projects will have numbers of fatalities that will fall within the box: 25% will have numbers above the box and 25% will have numbers below the box. The whiskers on the boxes represent the 10th–25th percentiles and the 75th–90th percentiles, and the horizontal lines in the centers of the boxes represent the medians. The blue bars represent take that is lower than T, and yellow represents take that is greater than T.

The *x*-axis is divided into six sections based on the ratio of actual fatality rate to permitted rate, λ/τ. For example, in the right-most section, the actual fatality rate is 3 times the permitted rate. Subdivisions within a given λ/τ section correspond to different values of permitted take τ. Boxes within the τ-subdivisions represent different detection probabilities g, increasing from left to right.

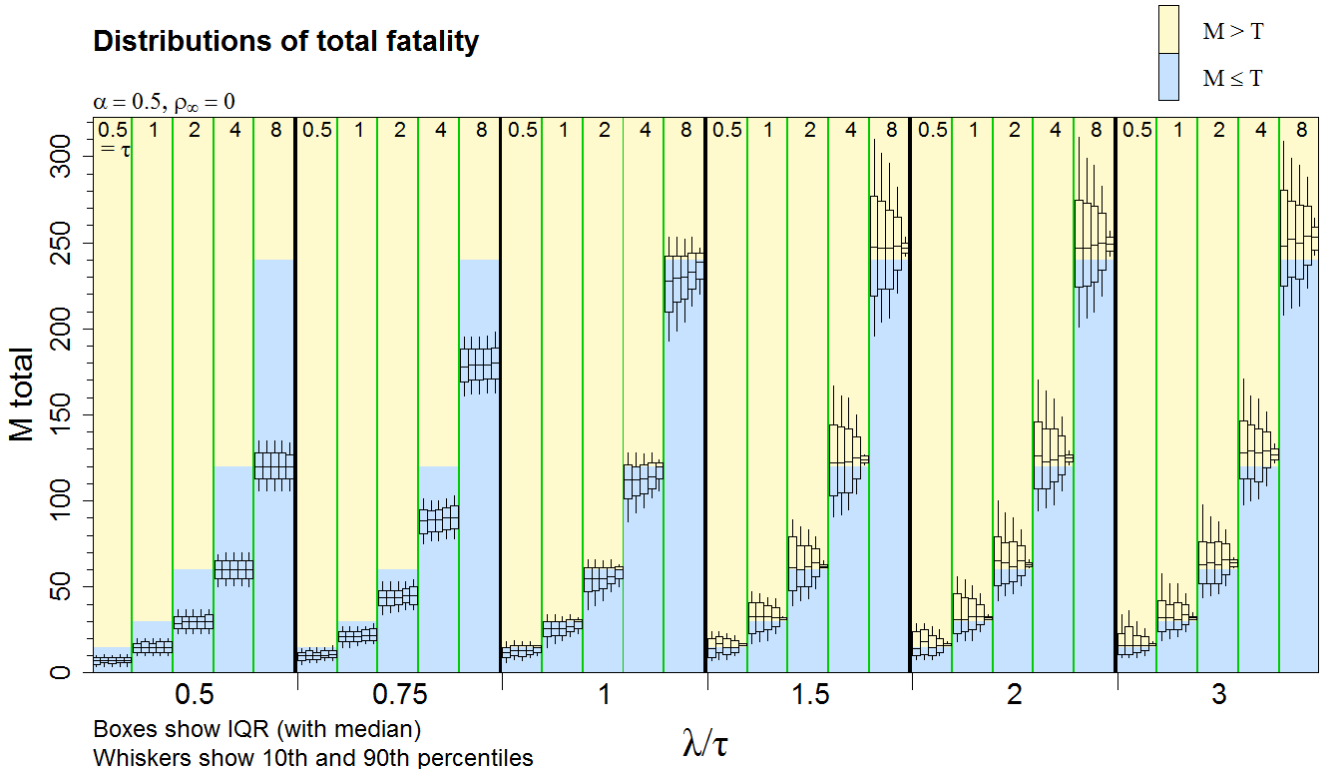

Figure 2. Total number of fatalities under long-term trigger, with $\alpha = 0.5$ and $\rho_\infty = 0$; that is, adaptive management action reduces fatality to 0 after trigger fires. Boxes represent distributions of cumulative total fatalities when long-term trigger fires or 30-year permit expires (whichever comes first). The five boxes within each subgroup represent different monitoring protocols and detection probabilities. In the first four boxes, g is 0.3 for each of the first 3 years and, from left to right, $g = 0.08, 0.12, 0.15,$ and 0.3 in the following 27 years. In the right-most box, detection probability is 1 in all years. See table 1 for explanation of terms used here.

In figure 2, α is set at 0.5, and it is assumed that the avoidance AMAs that are implemented after the long-term trigger fires are successful in reducing the fatality rate to 0 in future years ($\rho_\infty = 0$).

In the scenarios with $\lambda < \tau$, the 90th percentiles of fatalities were consistently well below T. Total fatality was almost entirely independent of g because fatalities rates were low enough that the long-term trigger rarely fired, and AMA was rarely required. However, there appears to be a slight trend toward greater fatality (closer to T) with greater detection probability when $\lambda/\tau = 0.75$, especially when τ is small. This is a result of the greater precision associated with higher detection probability, which results in less uncertainty and less frequent trigger firings when $\lambda < \tau$. The phenomenon is reflected more clearly in the data showing years of operation before the long-term trigger fires (for example, in fig. 3).

In the scenarios with $\lambda > \tau$, average numbers of fatalities are consistently greater than T because the trigger is designed to signal when $M >$ T rather than to prevent exceedance. Increasing the detection probability has little effect on the resulting average fatality rates, but the variance in the number of fatalities consistently decreases.

In the scenarios with $\lambda = \tau$, the average number of fatalities is less than T. This is to be expected. When $\lambda = \tau$ and the turbines operate freely through the entire life of the project, on average there will be T fatalities after 30 years. However, as discussed earlier, the number of fatalities will exceed T nearly one-half of the time. In those cases, the long-term trigger should fire and thereby lower the mean by clipping off the tops of the distributions.

Number of Years Until Trigger Fires

The number of years of operation until the long-term trigger fires is a function of the total take permitted (T), the governing α, fatality rate (λ per year), and the detection probability (g). In figure 3, the distributions of the total number of years of operation before the long-term trigger fires (or 30 years, whichever comes first) are displayed as colored bars representing the 10th, 25th, 50th, 75th, and 90th percentiles along with dots representing the means.

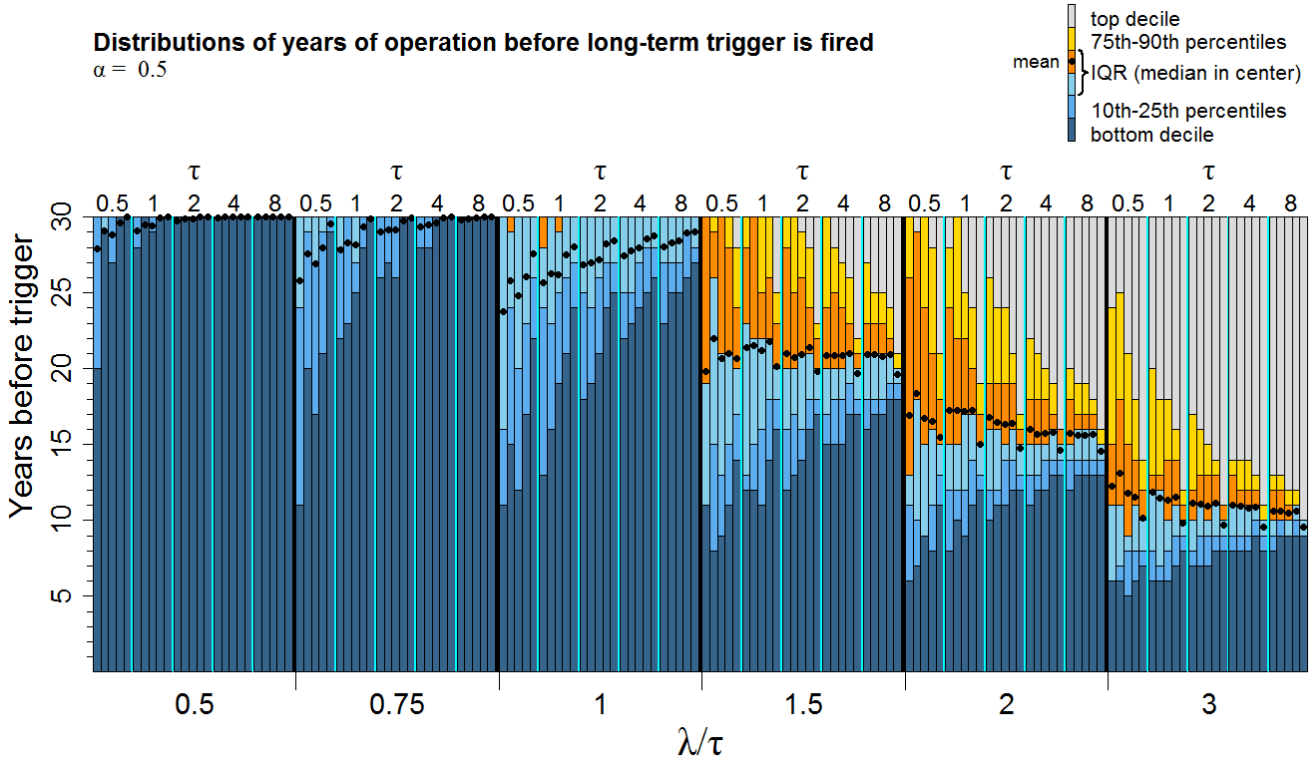

Figure 3. Years of operation before long-term trigger fires, with $\alpha = 0.5$. Color bars represent distributions of years of operation before long-term trigger is fired or 30-year permit expires (whichever comes first). The five boxes within each τ-subgroup represent different monitoring protocols and detection probabilities. In the first four boxes, g is 0.3 for each of the first 3 years and, from left to right, $g = 0.08, 0.12, 0.15$, and 0.3 in the following 27 years. In the right-most box, detection probability is 1 in all years. See table 1 for explanation of terms used here.

Because the number of years of operation is truncated at 30, the average will necessarily be ≤30, resulting in an artificially pessimistic perception of average number of years of operation for scenarios with $\lambda \leq \tau$. A more informative statistic is the median. In scenarios with $\lambda > \tau$ (the three sections on the right half of fig. 3), the median number of years of operation before the long-term trigger fires is approximately $30/(\lambda/\tau)$, which is as expected. For example, in the right-most section, the actual rate is 3 times the permitted rate, and the trigger fires about one-third of the way through the permit when the expected number of fatalities reaches T. Two other general patterns that are apparent in the sections with $\lambda/\tau > 1$ and $g < 1$ are that, although the median number of years of operation is fairly constant regardless of g and τ, the variance decreases markedly as τ and g increase. When $g = 1$, though, the average number of years of operations before triggering tends to be greater than it is when $g < 1$ because with smaller g values, it becomes more likely that exceedance goes undetected for several years, resulting in right-skewed distributions.

In scenarios with $\lambda < \tau$, most projects run the full 30 years without the long-term trigger firing. As with the scenarios where $\lambda > \tau$, lower g and lower τ are reflected in greater variances. However, unlike the $\lambda > \tau$ scenarios, increasing g or τ can have a significant effect on the number of years of operation before the trigger fires. That is because when $\lambda < \tau$, the primary driver of triggering is uncertainty, so decreasing the uncertainty by raising g, can reduce the frequency of trigger firings.

When $\lambda = \tau$, the total fatality M will eventually exceed T in nearly half of the projects. The timing of actual exceedance is reflected in the right-most bar in each subgroup where ($g = 1$ and perfect detection). When τ is large, all the means (including $g = 0.08$) are close to the perfect detection scenario. For smaller τ, detection probability becomes increasingly important.

The years of operation are extended most effectively by increasing g (when τ and λ are small), decreasing λ (when τ and λ are large) or increasing τ.

Effect of Imperfect Avoidance as an Adaptive Management Action after Long-Term Trigger Fires

After the long-term trigger fires, AMAs may be implemented to avoid subsequent take. One scenario might be that projects begin with minimization measures (for example, curtailment at wind speeds lower than 5.0 m/s at night during the season when bats are active) that are expected to reduce fatality rates to 40% of what they would be under free operations. When the long-term trigger is fired, AMA for full avoidance may be required (for example, curtailment at winds <6.9 m/s). The assumption is that the AMA prevents all further fatalities. If the avoidance AMA were only 95% effective ($\rho_\infty = 0.05$) rather than 100% effective at reducing fatalities, total fatality at the end of 30 years would be as shown in figure 4. In each scenario, operations continue at baseline conditions (that is, with prophylactic curtailment at 5.0 m/s and $\rho = 0.4$) until the long-term trigger fires. In subsequent years, fatalities accumulate at 5% of the uncurtailed rate (or 12.5% of baseline).

The effect of imperfect avoidance AMA has negligible effect when $\lambda < \tau$ because the AMA is rarely triggered. When $\lambda = \tau$, avoidance AMA is not infrequently triggered, but triggering would occur late in the project, leaving little opportunity for many additional fatalities to accumulate. When $\lambda/\tau = 3$, however the total number of fatalities may substantially exceed T because there is a long period (about 20 years) of accumulation of additional fatalities after the trigger fires.

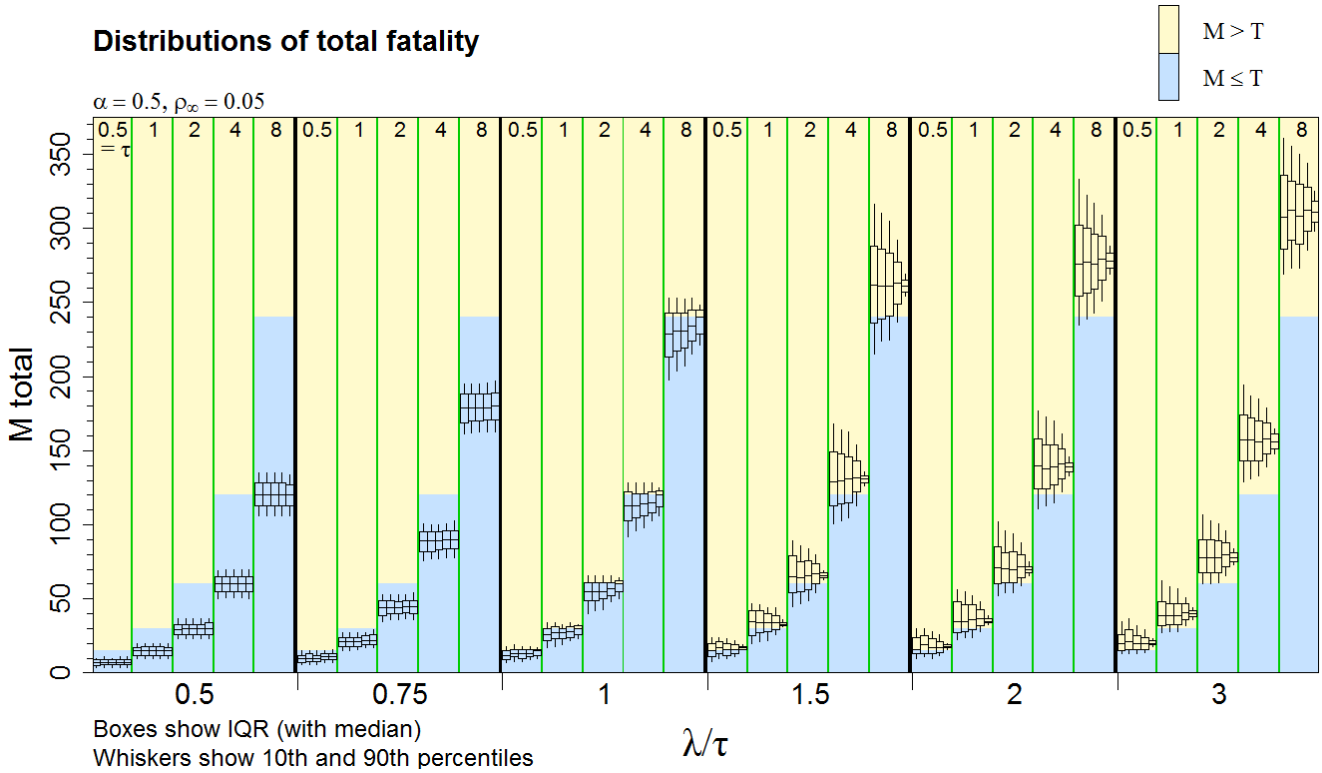

Figure 4. Total number of fatalities under long-term trigger, with $\alpha = 0.5$ and $\rho_\infty = 0.05$. Boxes represent distributions of cumulative total fatalities when long-term trigger fires or 30-year permit expires (whichever comes first). The five boxes within each subgroup represent different monitoring protocols and detection probabilities. In the first four boxes, g is 0.3 for each of the first 3 years and, from left to right, $g = 0.08, 0.12, 0.15$, and 0.3 in the following 27 years. In the right-most box, detection probability is 1 in all years. See table 1 for explanation of terms used here.

Fatalities and Operations with Significance Level (α) Equal to 0.2

Setting $\alpha = 0.5$ gives maximum accuracy but regularly allows exceedance if the baseline fatality rate exceeds τ. By setting $\alpha = 0.2$, the trigger is designed to fire frequently enough to prevent M from exceeding T approximately 80% of the time even when $\lambda > \tau$. This effect is evident in figure 5, which shows the distributions of total fatality with $\alpha = 0.2$. The tops of the IQR boxes for the scenarios with $\lambda > \tau$ are in rough alignment with T (except in the case of perfect detection). Where $\lambda = \tau$, the actual number of fatalites exceeds T in about 10% of projects.

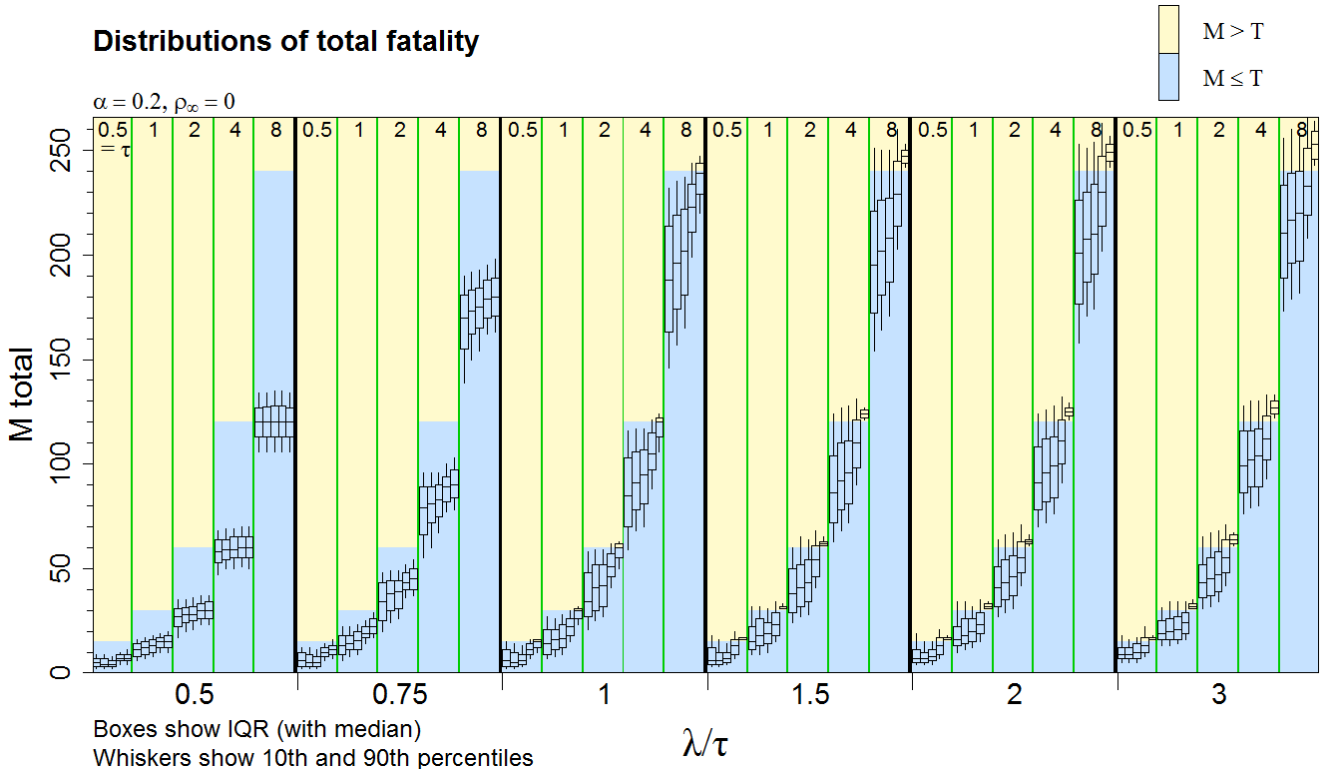

Figure 5. Total number of fatalities under long-term trigger, with $\alpha = 0.2$ and $\rho_\infty = 0$. Boxes represent distributions of cumulative total fatalities when long-term trigger fires or 30-year permit expires (whichever comes first). The five boxes within each subgroup represent different monitoring protocols and detection probabilities. In the first four boxes, g is 0.3 for each of the first 3 years and, from left to right, $g = 0.08, 0.12, 0.15$, and 0.3 in the following 27 years. In the right-most box, detection probability is 1 in all years. See table 1 for explanation of terms used here.

Where $\lambda > \tau$, the effects on operations of using $\alpha = 0.2$ rather than $\alpha = 0.5$ is to reduce both the mean and variance of the number of years of operation before trigger firing (fig. 6). Where $\lambda \leq \tau$, the effect on operations is more substantial, with the average number of years until triggering reduced by approximately 8 years in many scenarios.

Despite the conservative buffer provided by using $\alpha = 0.2$ instead of $\alpha = 0.5$, when the avoidance AMA is only 95% effective (fig. 7), the continued accumulation of fatalities after the long-term trigger firings still resulted in fatalities exceeding T by around 60 (or 25%) in projects where the baseline fatality rate was much higher than the permitted rate ($\lambda = 3\tau$).

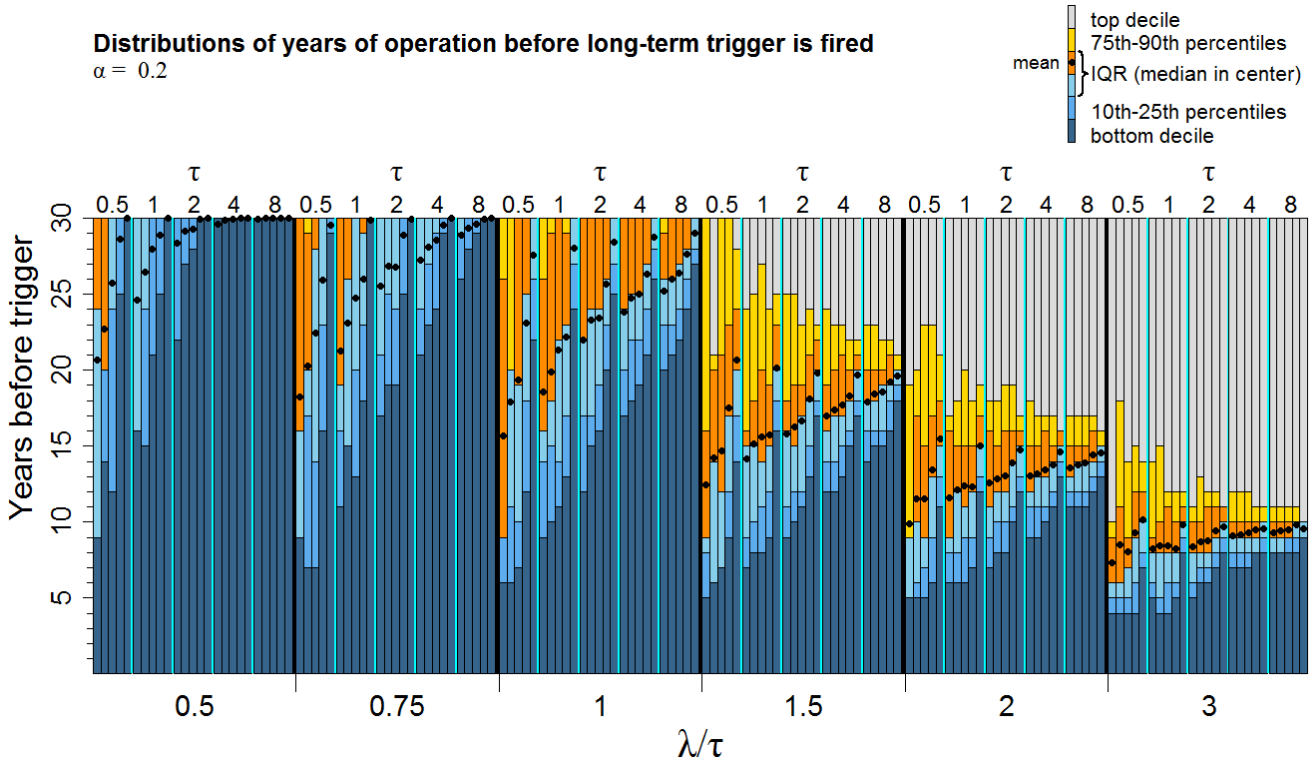

Figure 6. Years of operation before long-term trigger fires, with $\alpha = 0.2$. Color bars represent distributions of years of operation before long-term trigger is fired or 30-year permit expires (whichever comes first). The five boxes within each τ-subgroup represent different monitoring protocols and detection probabilities. In the first four boxes, g is 0.3 for each of the first 3 years and, from left to right, $g = 0.08, 0.12, 0.15$, and 0.3 in the following 27 years. In the right-most box, detection probability is 1 in all years. See table 1 for explanation of terms used here.

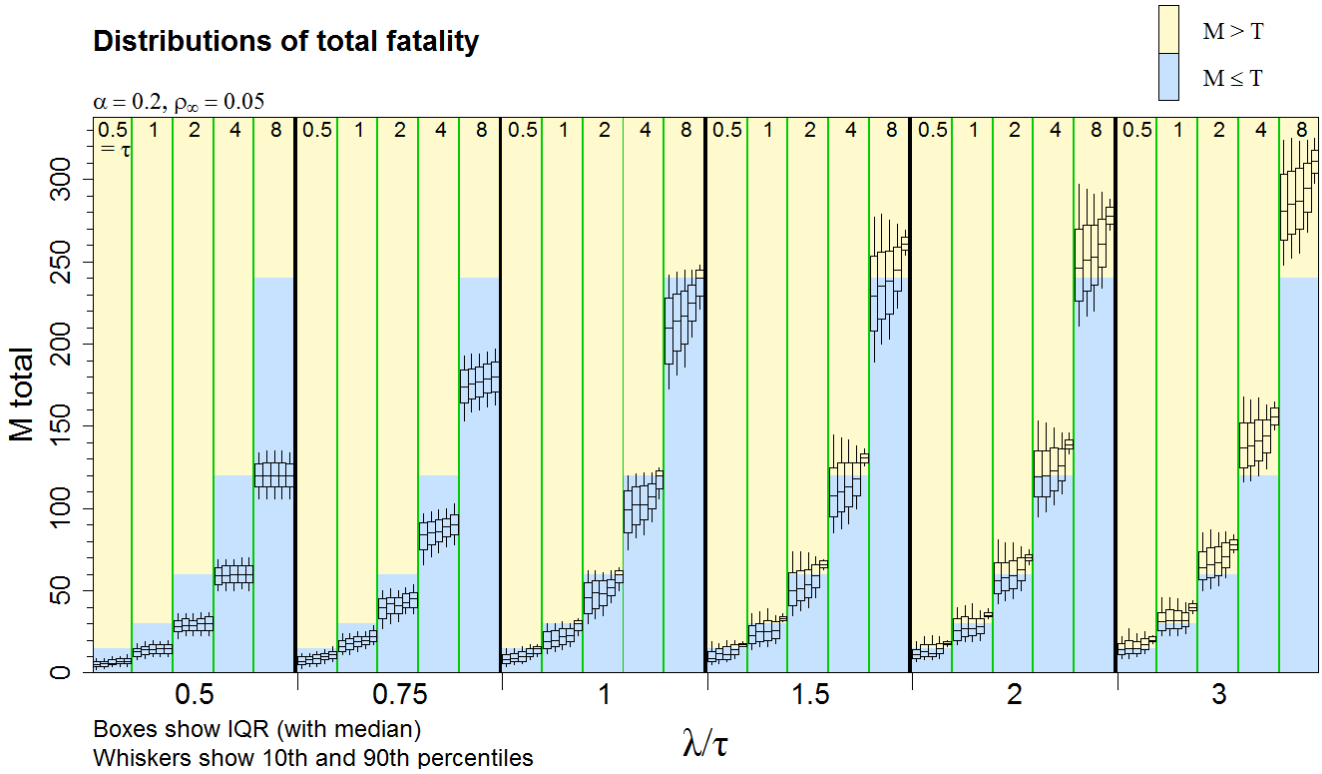

Figure 7. Total number of fatalities under long-term trigger, with $\alpha = 0.2$ and $\rho_\infty = 0.05$. Boxes represent distributions of cumulative total fatalities when long-term trigger fires or 30-year permit expires (whichever comes first). The five boxes within each subgroup represent different monitoring protocols and detection probabilities. In the first four boxes, g is 0.3 for each of the first 3 years and, from left to right, $g = 0.08, 0.12, 0.15$, and 0.3 in the following 27 years. In the right-most box, detection probability is 1 in all years. See table 1 for explanation of terms used here.

Long-Term Trigger with High Detection Probabilities

The low detection probabilities ($g = 0.08, 0.12$, and 0.15) featured in the previous examples are not unusual when monitoring for bats, but much higher detection probabilities are attainable when monitoring for larger, more persistent carcasses like eagles. The following set of figures (8–13) shows what can be expected when detection probabilities are $g = 0.80$ in an initial 3-year monitoring period followed by 27 years of monitoring at $g = 0, 0.3$, or 0.8 in various combinations of repeating 5-year blocks. Specifically, for the full 30 years, the monitoring schedules that were analyzed are (from least intensive to most intensive) are detailed in table 2.

Table 2. Monitoring schedules in simulations with high detection probabilities.

(1) 0.8, 0.8, 0.8 + 0.0, 0.0, 0.0, 0.0, 0.8 …	Punctuated monitoring
(2) 0.8, 0.8, 0.8 + 0.0, 0.0, 0.0, 0.8, 0.8 …	
(3) 0.8, 0.8, 0.8 + 0.3, 0.3, 0.3, 0.3, 0.3 …	Continuous monitoring
(4) 0.8, 0.8, 0.8 + 0.3, 0.3, 0.3, 0.3, 0.8 …	
(5) 0.8, 0.8, 0.8 + 0.3, 0.3, 0.3, 0.8, 0.8 …	

Under the long-term trigger at $\alpha = 0.5$ and with 100% effective avoidance AMA after triggering, the average total number of fatalities at the end of a 30-year permit (fig. 8) had little dependence on the monitoring schedule. However, there were noticeable differences in variability of fatality rates in scenarios with $\lambda \geq \tau$.

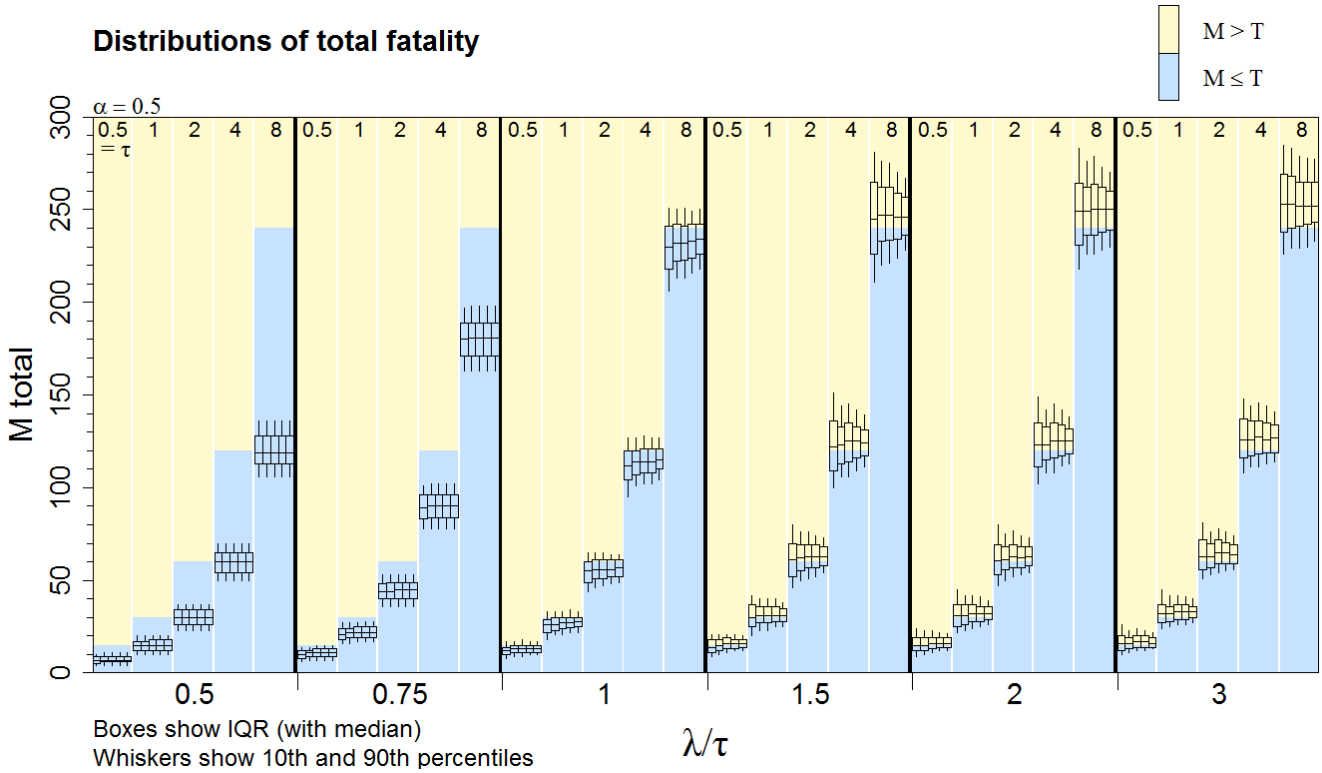

Figure 8. Total number of fatalities under long-term trigger with high detection probabilities, with $\alpha = 0.5$. Boxes represent distributions of cumulative total fatality when long-term trigger fires or 30-year permit expires (whichever comes first). The five boxes within each subgroup represent different monitoring protocols and detection probabilities, corresponding to the five monitoring schedules in table 2, respectively. See table 1 for explanation of terms used here.

Similarly, the average number of years of operation before triggering (fig. 9) also had little dependence on monitoring schedule, except when τ was ≤1. However, in the scenarios with those low permitted take rates, triggering tended to be several years earlier under the punctuated monitoring schedules ($g = 0, 0, 0, 0, 0.8$ and $g = 0, 0, 0, 0.8, 0.8$) than under continuous monitoring schedules ($g = 0.3$ or more each year).

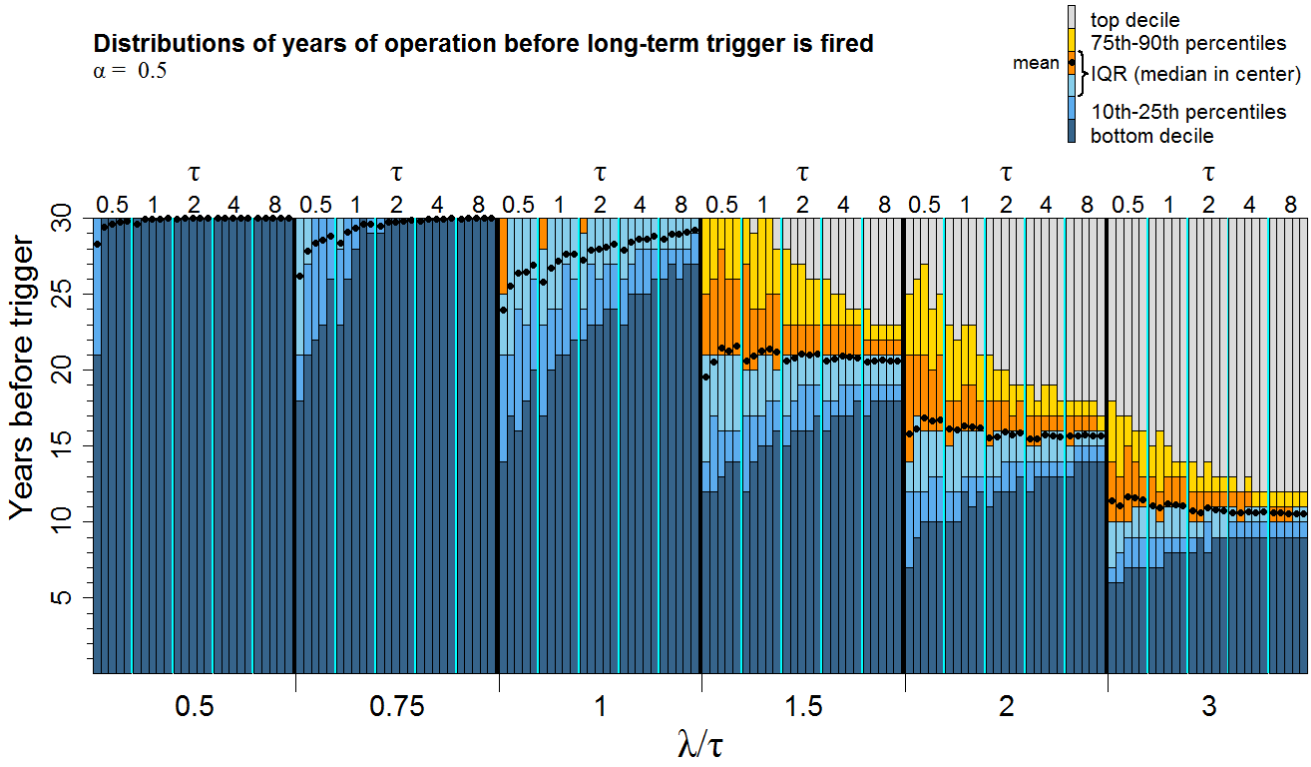

Figure 9. Years of operation before long-term trigger fires with high detection probabilities, with $\alpha = 0.5$. Color bars represent distributions of years of operation before long-term trigger is fired or 30-year permit expires (whichever comes first). From left to right, the five boxes within each τ-subgroup represent increasing levels of monitoring intensity, corresponding to the monitoring schedules listed in table 2. See table 1 for explanation of terms used here.

Under a governing parameter of $\alpha = 0.2$, the differences between puncuated and continuous monitoring schedules were more pronounced than under $\alpha = 0.5$, with the punctuated monitoring schedules associated with lower fatality rates (fig. 10) and substantially earlier trigger firings (fig. 11). In the most extreme case—with a low permitted rate of $\tau = 0.5$ and a baseline fatality rate of $\lambda = 0.5\tau$—light, yearly monitoring at $g = 0.3$ postponed triggering by more than 20 years on average compared with intensive monitoring at $g = 0.8$ one year in five with no monitoring in the intervening years (fig. 11, left-most panel). However, the punctuated monitoring schedules resulted in earlier trigger firing in virtually all scenarios. The only exceptions are where the long-term trigger did not fire under either schedule— namely, $\lambda = \tau/2$ and $\tau \geq 4$.

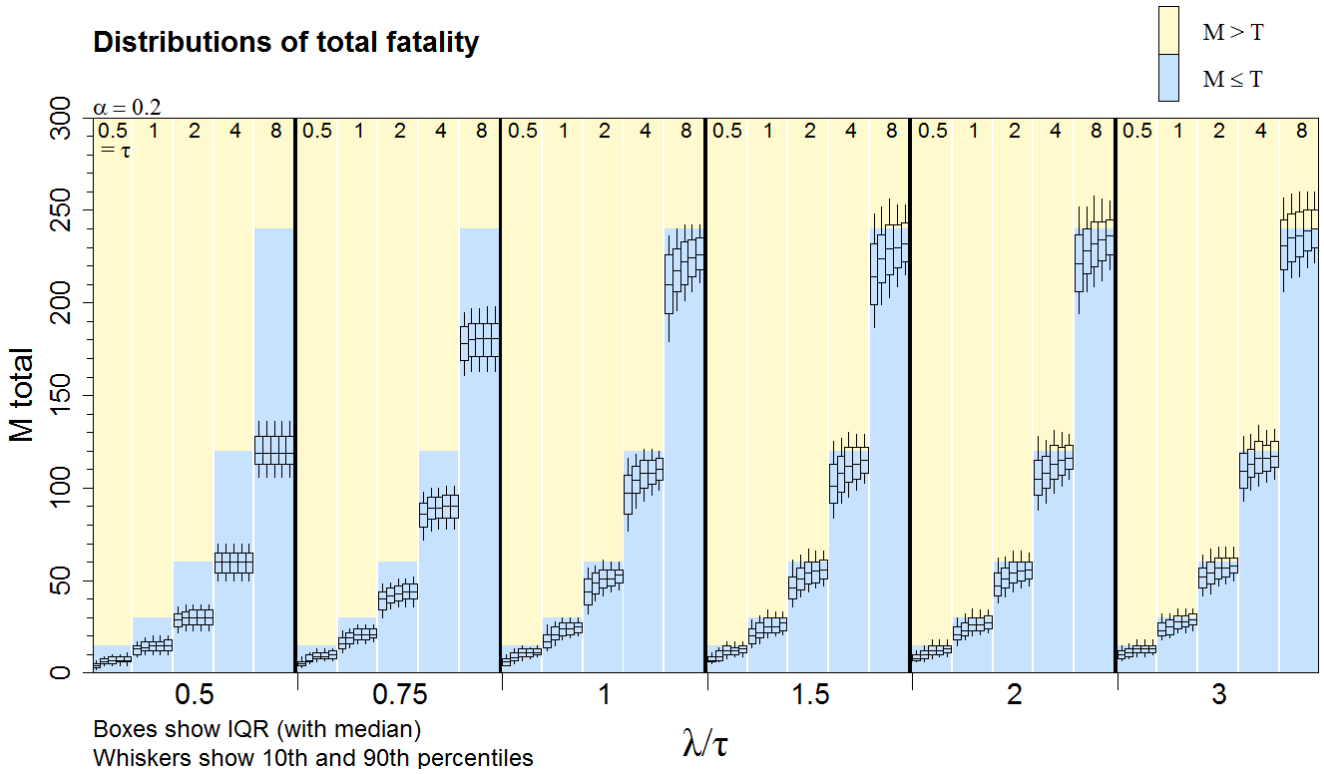

Figure 10. Total number of fatalities under long-term trigger with high detection probabilities, with $\alpha = 0.2$. Boxes represent distributions of cumulative total fatalities when long-term trigger fires or 30-year permit expires (whichever comes first). The five boxes within each subgroup represent different monitoring protocols and detection probabilities, corresponding to the five monitoring schedules in table 2, respectively. See table 1 for explanation of terms used here.

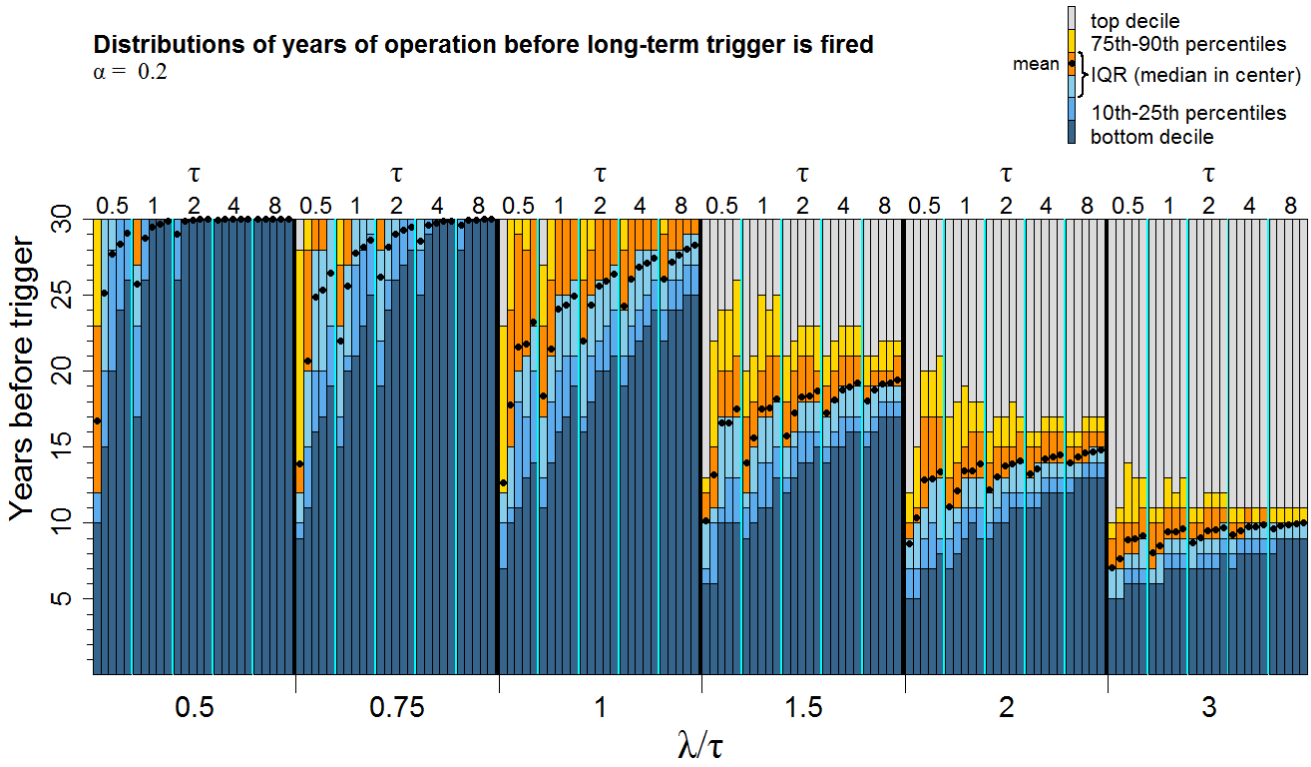

Figure 11. Years of operation before long-term trigger fires with high detection probabilities, with $\alpha = 0.2$. Color bars represent distributions of years of operation before long-term trigger is fired or 30-year permit expires (whichever comes first). From left to right, the five boxes within each τ-subgroup represent increasing levels of monitoring intensity, corresponding to the monitoring schedules listed in table 2. See table 1 for explanation of terms used here. Patterns under scenarios with $\alpha = 0.1$ were qualitatively similar to those with $\alpha = 0.2$, but with earlier triggering in all cases (figs. 12 and 13).

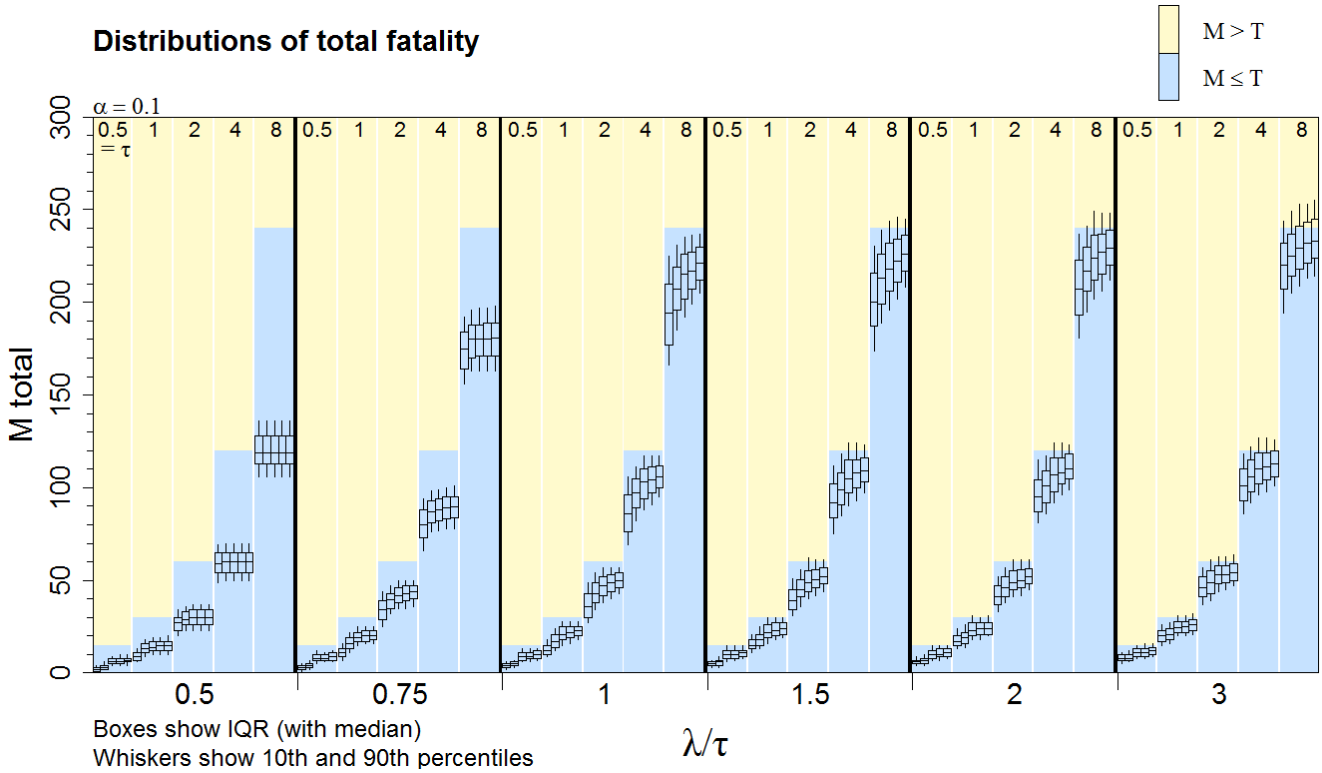

Figure 12. Total number of fatalities under long-term trigger with high detection probabilities, with $\alpha = 0.1$. Boxes represent distributions of cumulative total fatality when long-term trigger fires or 30-year permit expires (whichever comes first). The five boxes within each subgroup represent different monitoring protocols and detection probabilities, corresponding to the five monitoring schedules in table 2, respectively. See table 1 for explanation of terms used here.

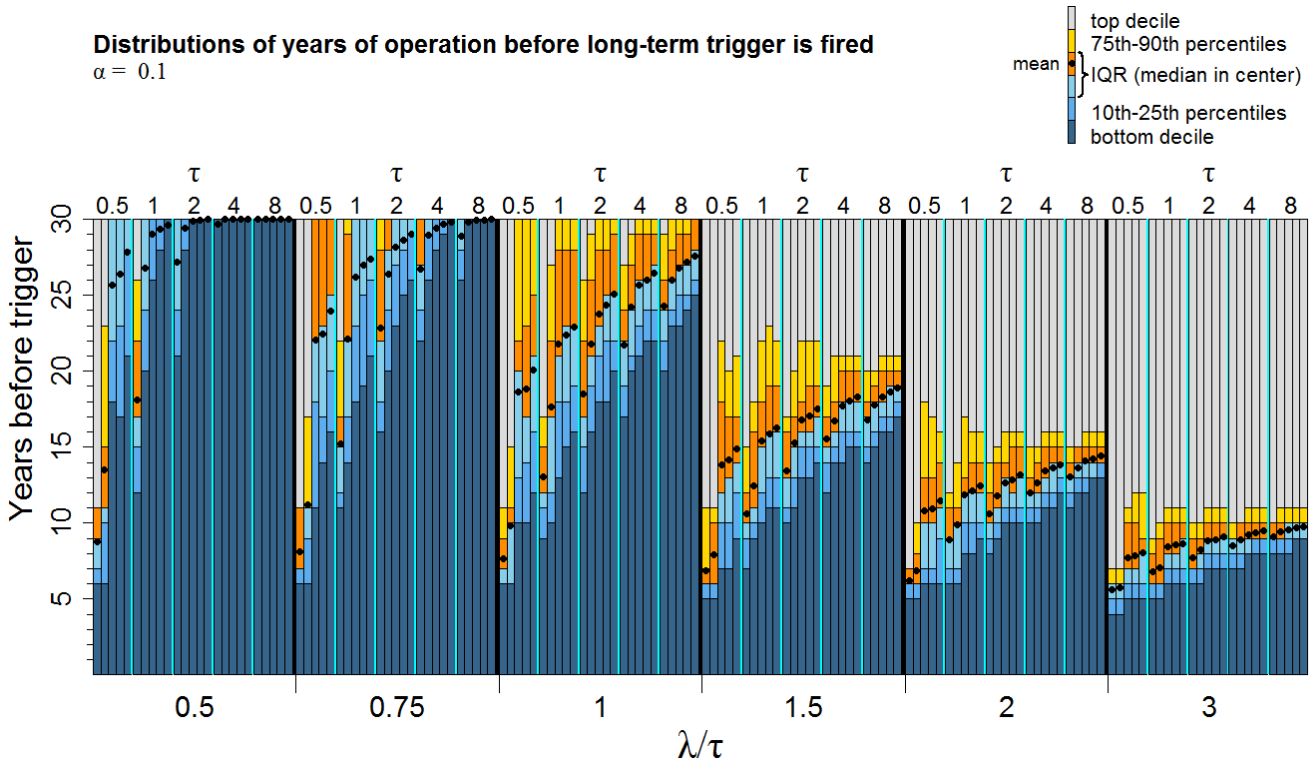

Figure 13. Years of operation before long-term trigger fires with high detection probabilities, with $\alpha = 0.1$. Color bars represent distributions of years of operation before long-term trigger is fired or 30-year permit expires (whichever comes first). From left to right, the five boxes within each τ-subgroup represent increasing levels of monitoring intensity, corresponding to the monitoring schedules listed in table 2. See table 1 for explanation of terms used here.

Effect of Probability of Detection on Years of Operation before Long-Term Trigger

In figures 14–18, the cumulative probability of triggering is plotted as a function of the number of years of operation for scenarios in which monitoring in the initial 3 years of the project is at $g_0 = 0.3$ and at $g_{RP} = 0.08, 0.12, 0.15, 0.3$, and 1 in the 27 remaining years of the project (with different lines for each value of g). For example, in the top left panel of figure 14 illustrating results for $\tau = 0.5, \alpha = 0.5$, and $\lambda/\tau = 0.5$, about 50% of projects operating with $g = 0.08$ in years 4–30 complete the full course of 30 years without triggering (solid black line), whereas less than 10% of projects operating with $g = 0.3$ in the out years trigger within 30 years (blue line). In the scenario with $\tau = 0.5, \alpha = 0.5$, and $\lambda/\tau = 1$, 20% of the projects with $g = 0.08$ trigger within about 10 years, but searching at $g = 0.3$ pushes that 20% mark out to about 20 years.

Greater detection probabilities generally led to longer periods of operation before the long-term trigger fired. The effect was clearest at $\tau = 1$ (fig. 15). For example, at $\alpha = 0.5$, $\tau = 1$, and $\lambda/\tau = 0.75$, the long-term trigger fired within 30 years in about one-fourth of the projects monitored at $g = 0.15$ in the out years (fig. 15, middle left panel, green line), but the trigger fired within 17 years for one-fourth of the projects monitored at $g = 0.08$, indicating that the more intensive monitoring greatly extended the period of baseline operations.

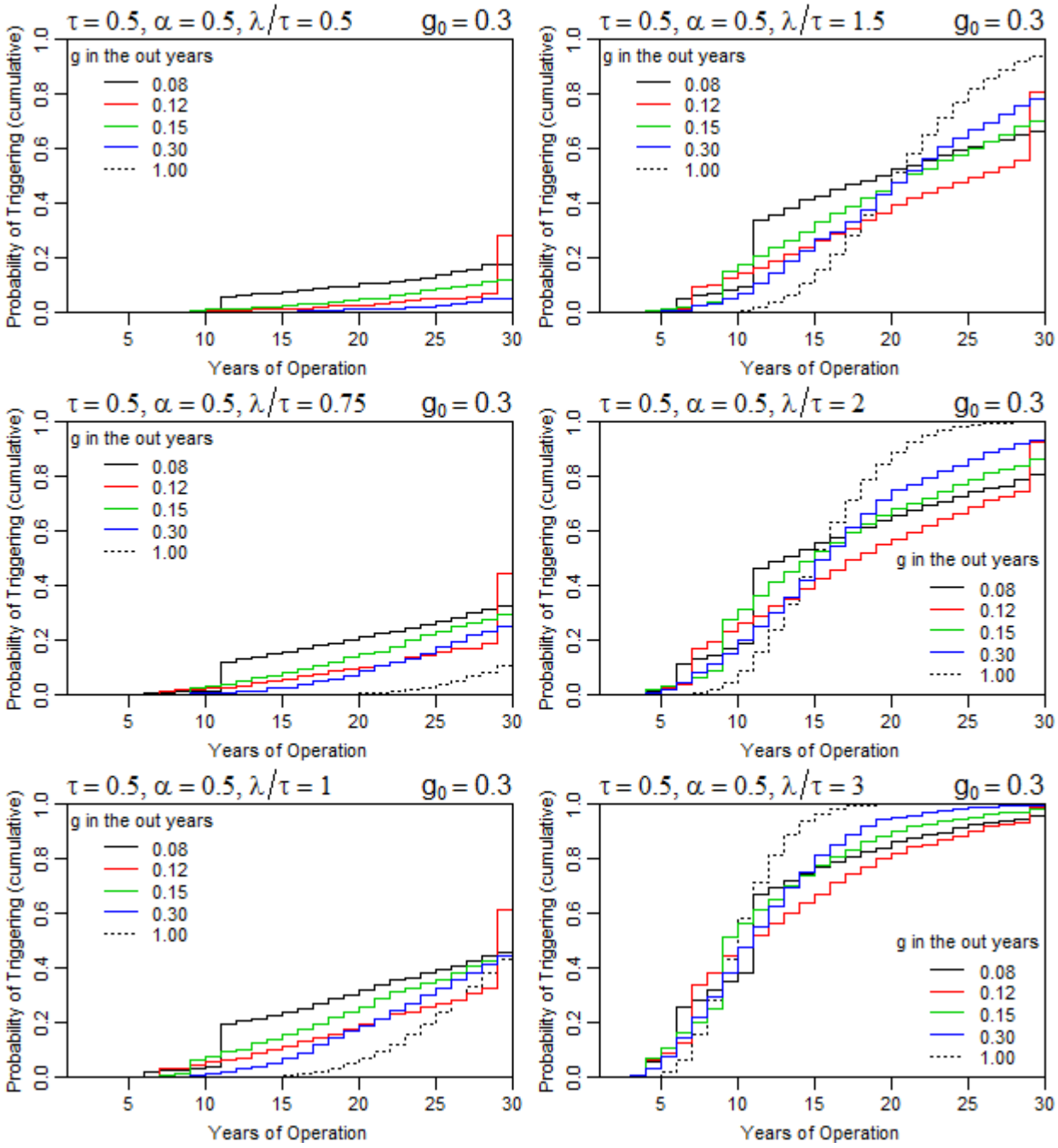

Figure 14. Detection probability (g) and years of operation, with $\tau = 0.5$. See table 1 for explanation of terms used here.

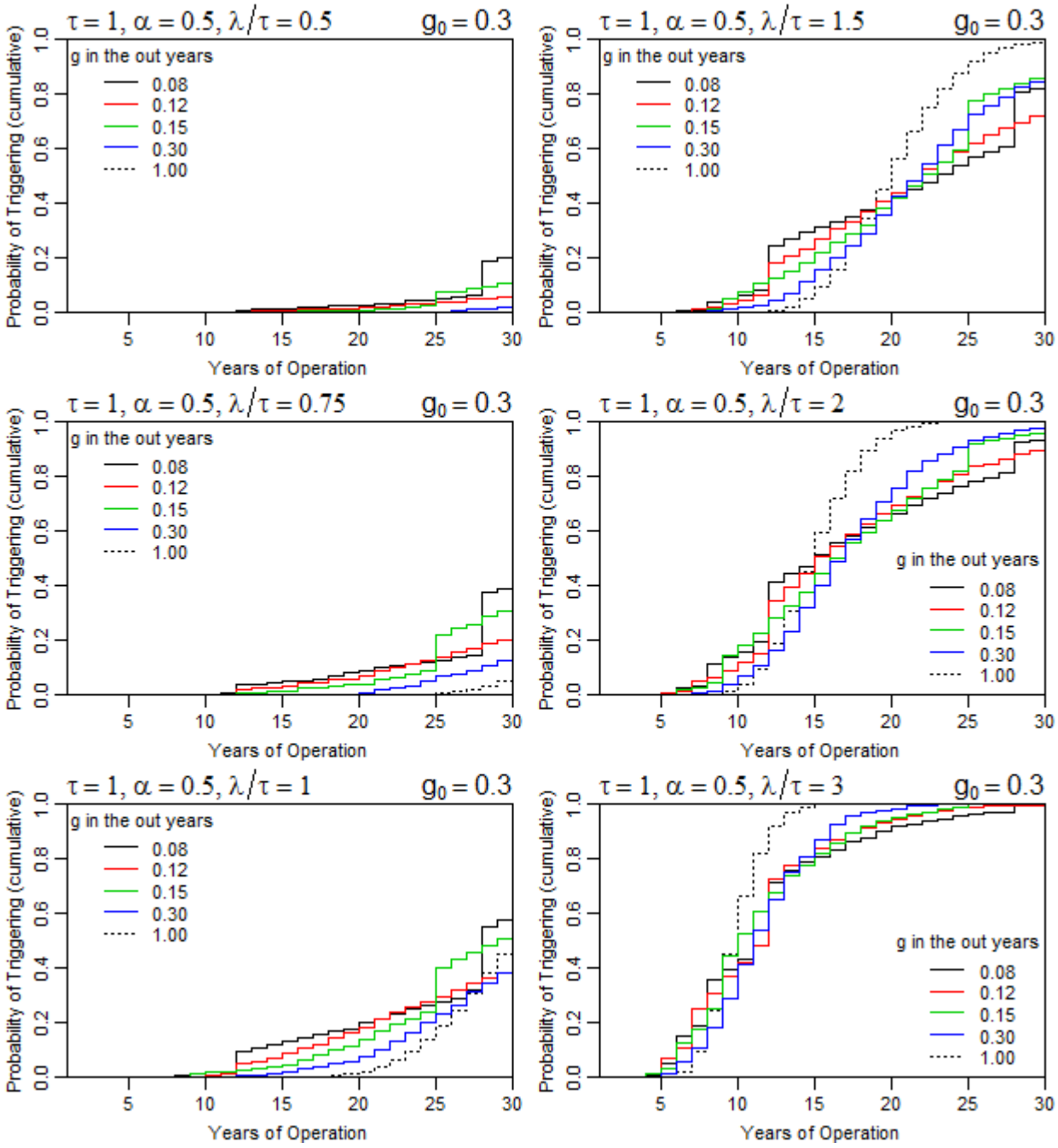

Figure 15. Detection probability (g) and years of operation, with $\tau = 1$. See table 1 for explanation of terms used here.

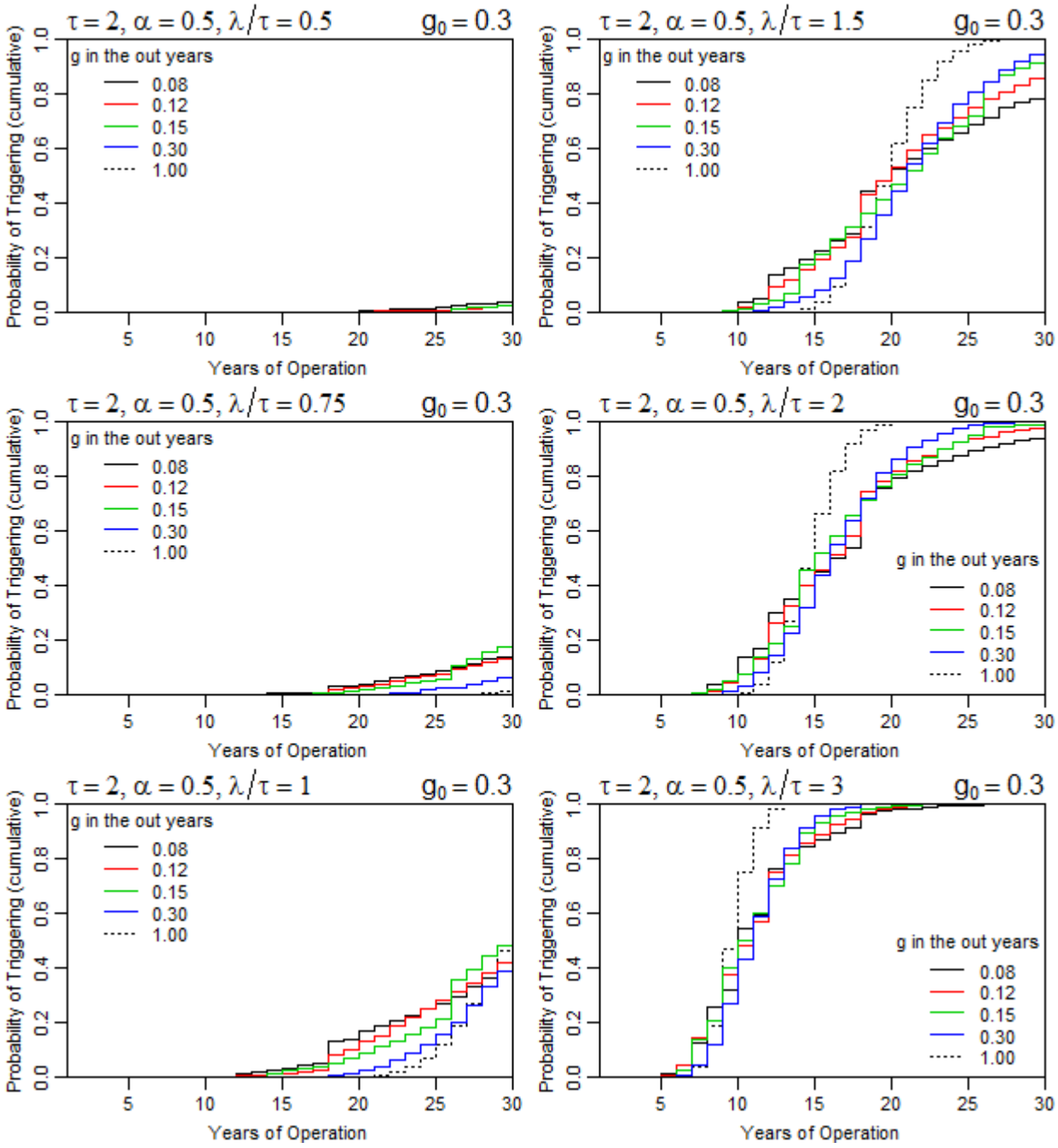

Figure 16. Detection probability (g) and years of operation, with $\tau = 2$. See table 1 for explanation of terms used here.

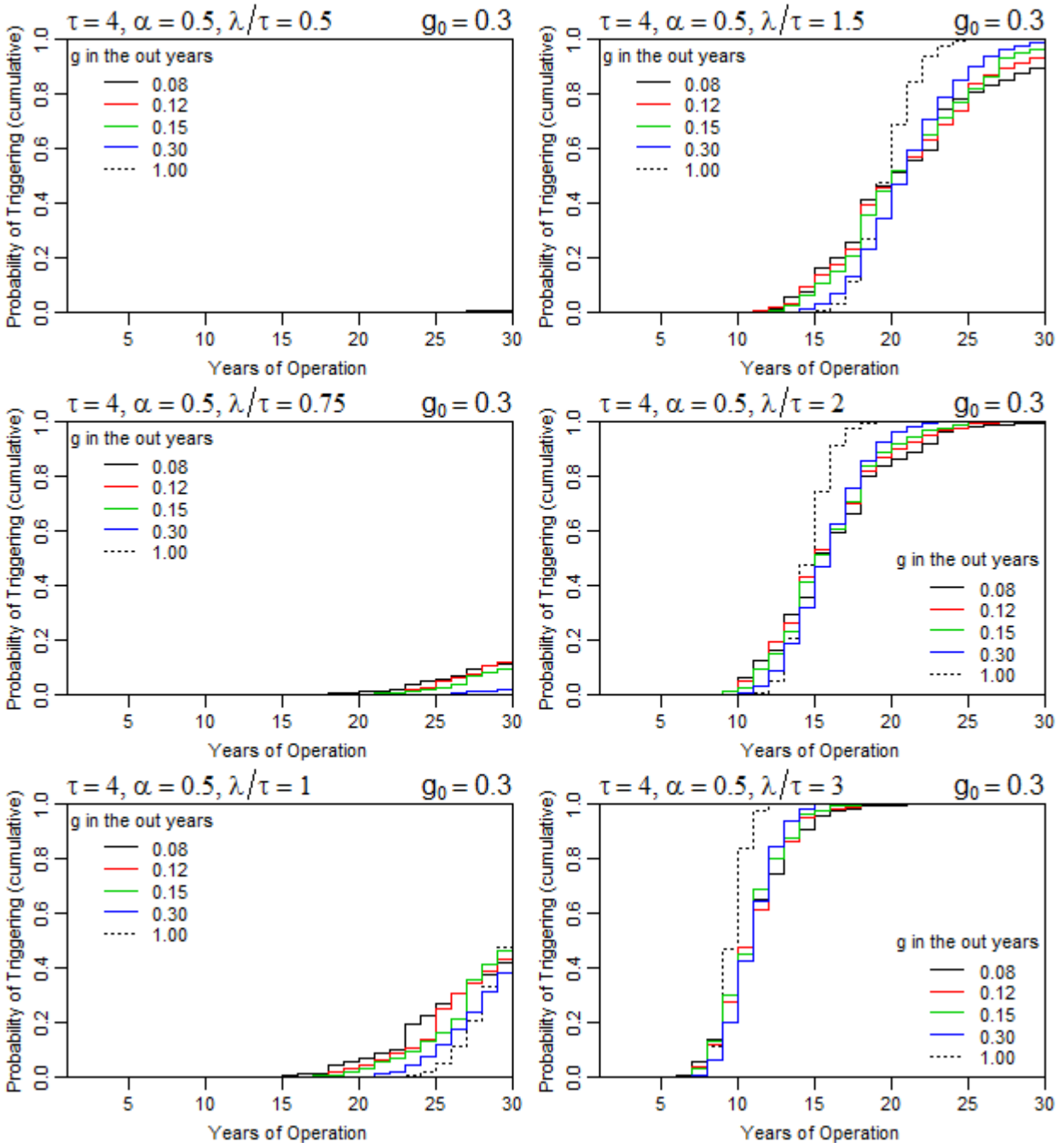

Figure 17. Detection probability (g) and years of operation, with $\tau = 4$. See table 1 for explanation of terms used here.

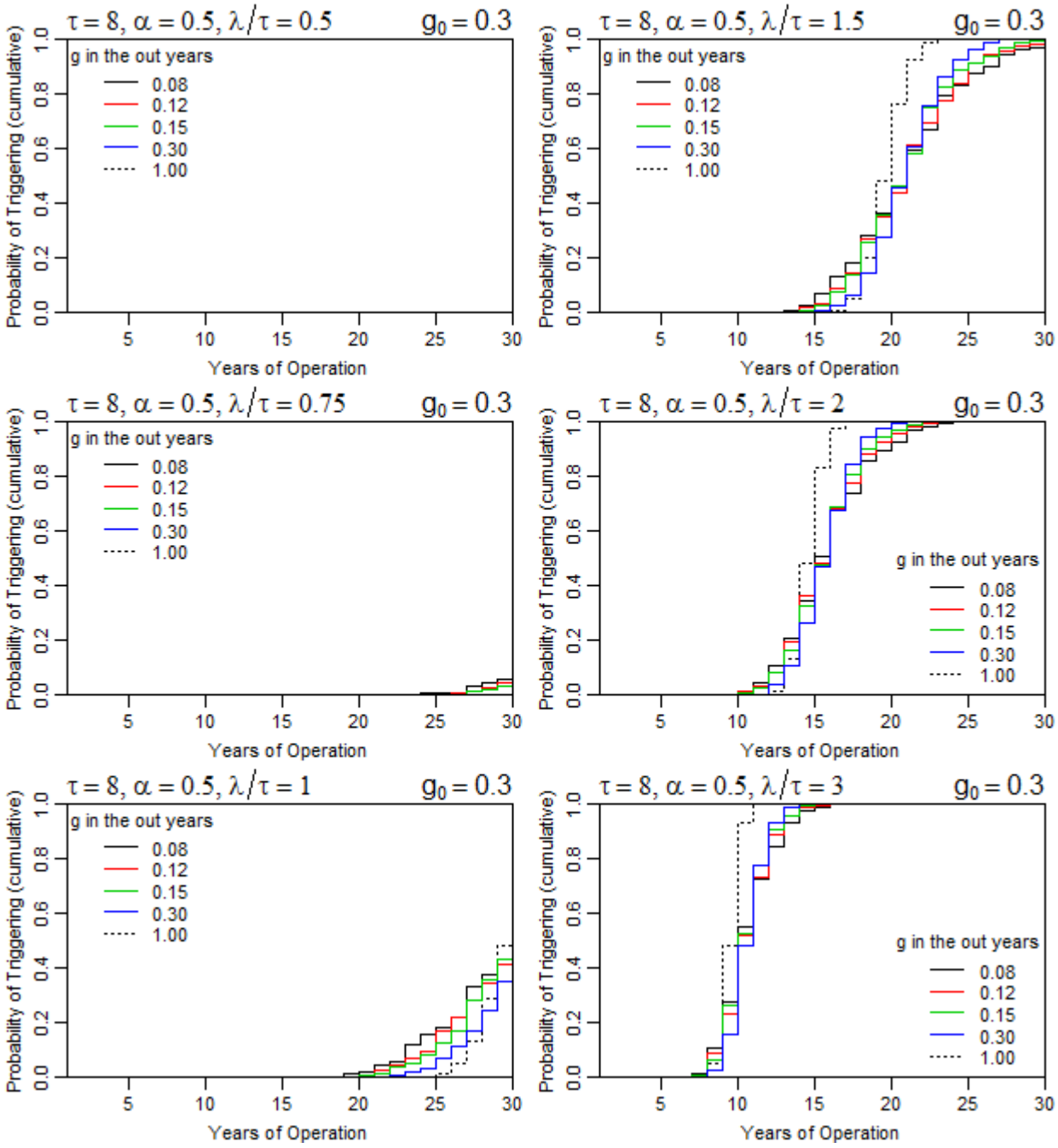

Figure 18. Detection probability (g) and years of operation, with $\tau = 8$. See table 1 for explanation of terms used here.

Performance of Short-Term Trigger

The short-term trigger fires when $P(\lambda \leq \tau) < \alpha'$, indicating that the average annual take rate of τ is being exceeded. The performance of the trigger in terms of how frequently it fires for the same sets of scenarios for which the long-term trigger was analyzed is shown in figures 19–27. The figures show only the frequency of trigger firings and do not assume any program of incremental AMAs is taken. The analyses indicate how well the trigger can distinguish between fatality rates that exceed τ and rates that do not for various combinations of values of governing parameters (α' and τ), detection probabilities (g), and baseline fatality rates (λ). The results can be used to help inform the development of a program of AMAs to respond to evolving information about fatality rates.

In the figures 19–26, green represents the fraction of projects in which the short-term trigger never fires, and gray represents the fraction of projects in which the trigger fires more than three times. Yellow, red, and blue correspond to 1, 2, and 3 trigger fires, respectively. A perfect trigger would yield solid green on the left (never firing when $\lambda \leq \tau$) and solid gray on the right (reliably firing frequently when $\lambda > \tau$), but, in the absence of perfect information, the objective is to define a trigger that strikes an appropriate balance between operational costs and conservation benefits. Higher values of α' result in higher probabilities of the trigger firing and more gray on both halves of the graph. By contrast, higher values of τ give better precision, which increases the gray on the right half and green on the left. Similarly, higher g values give better precision and tend to increase gray on the right half and green on the left. Requiring 2 additional years of intensive monitoring after the short-term trigger fires has no effect on the green, but does increase the frequency of firing on the right half of the graph (more gray) and decreases the frequency on the left (less gray in exchange for more yellow, red, blue).

In all figures, the detection probability in the first 3 years of the project is assumed to be $g_0 = 0.3$. Varying among rows of figures are the detection probabilities in the out years ($g_{RP} = 0.08, 0.12, 0.15, 0.30$ in years 4–30). In the left column of figures, additional intensive monitoring is not required after trigger is fired. In the right column, 2 years of intensive monitoring ($g = 0.3$) is required after trigger fires. The governing α' is 0.01 in figures 19–22 and, $\alpha' = 0.05$ in the figures 23-26. The performance of the trigger depends on the value of α' for which it is defined, the detection probability (g), the permitted take (τ), how well the permitted take reflects actual take rate (λ/τ), and whether or not intensive monitoring is required after the trigger fires.

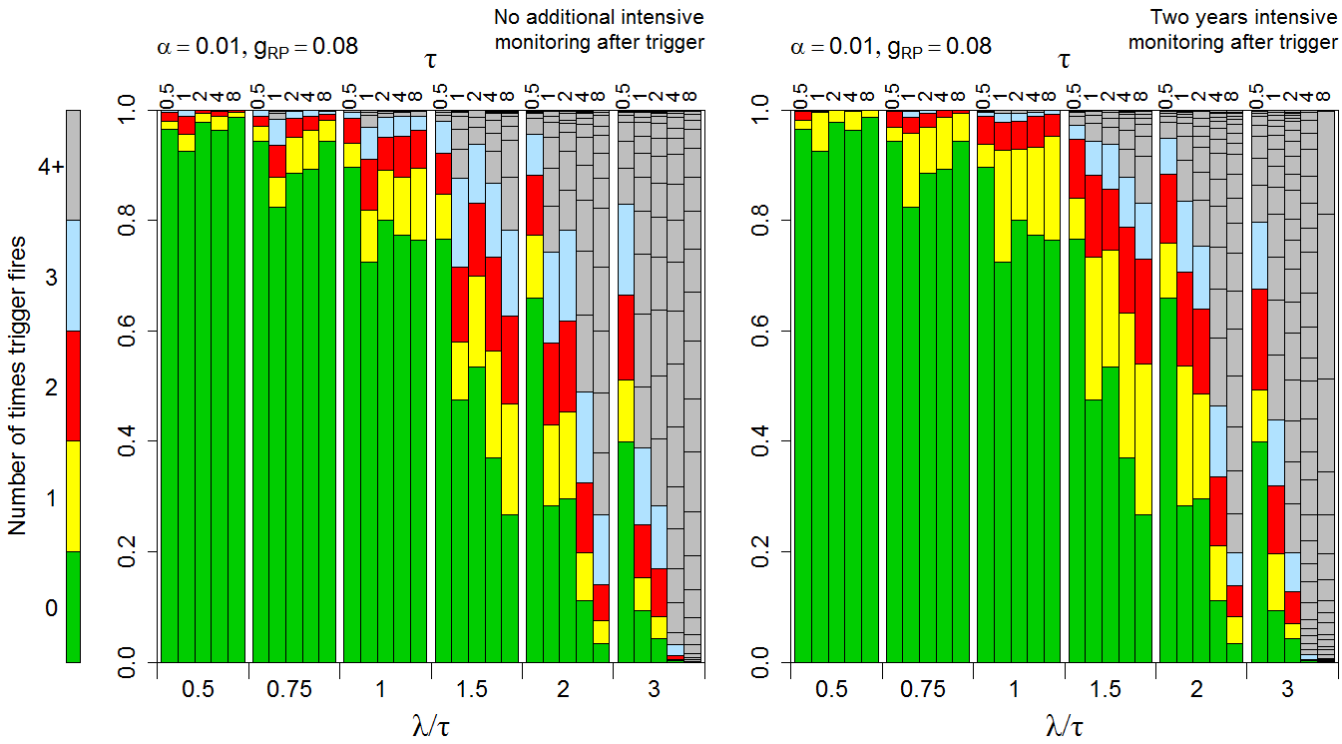

Figure 19. Distribution of number of trigger firings in 30-year projects, with $\alpha = 0.01$; detection probability $g_0 = 0.3$ in years 1–3 and $g_{RP} = 0.08$ in years 4–30. See table 1 for explanation of terms used here.

Distinguishing between Actual Average Take Rate Equal to or Greater Than Permitted Take Rate

For scenarios with $\alpha' = 0.01$ and $g = 0.08$ in the out years, the trigger is unlikely to fire at all in the course of a 30-year permit if $\lambda < \tau$ and $\tau \geq 1$. The probability of the short-term trigger firing a single time during the course of the 30-year permit is roughly 12% both in the $\lambda = \tau$ scenarios and the $\lambda = 1.5\tau$ scenarios, so a single triggering event does not reliably distinguish between $\lambda = \tau$ and $\lambda = 1.5\tau$. However, multiple triggering events are much more likely at $\lambda = 1.5\tau$ than they are at $\lambda = \tau$, and two triggerings may be required to adequately distinguish between $\lambda = \tau$ and $\lambda > \tau$. Two years of intensive monitoring ($g = 0.3$) after the short-term trigger fires has the effect of delaying the second triggering, which is reflected in the differences in size of the yellow bars in the figures in the left column versus those in the right column. Increasing the detection probability improves the precision of the estimates and generally increases the power to distinguish between $\lambda = \tau$ and $\lambda > \tau$ (fig. 19). When $\lambda = 3\tau$, the short-term trigger fires frequently, and it is unlikely that a fatality rate that high would pass undetected for more than a few years.

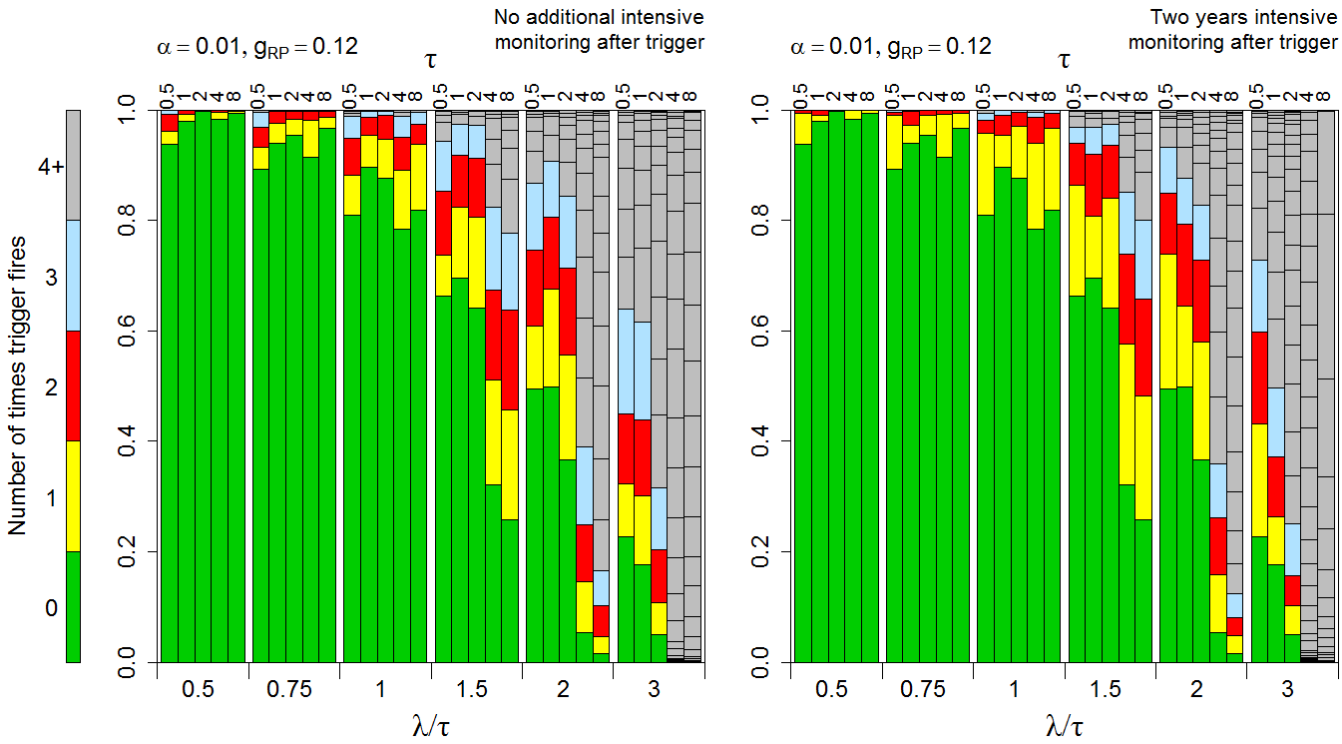

Figure 20. Distribution of number of trigger firings in 30-year projects, with $\alpha = 0.01$; detection probability $g_0 = 0.3$ in years 1–3 and $g_{RP} = 0.12$ in years 4–30. See table 1 for explanation of terms used here.

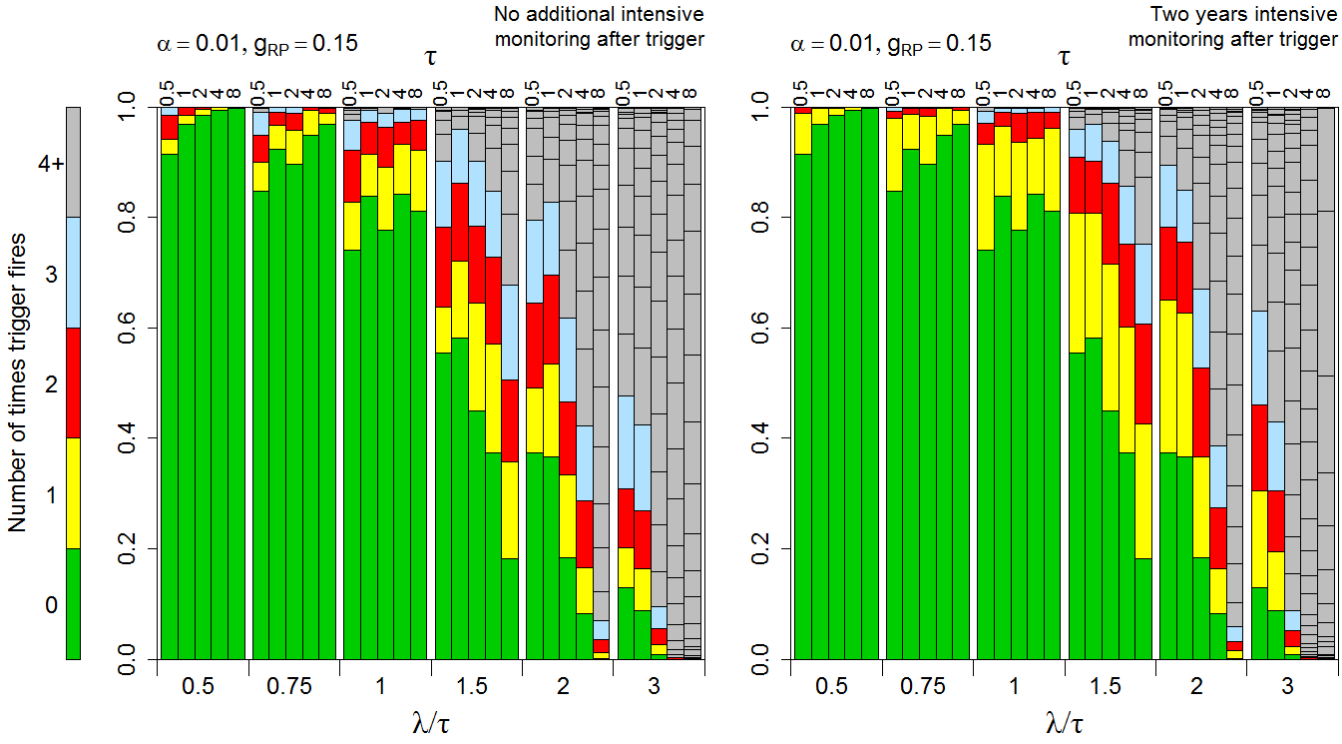

Figure 21. Distribution of number of trigger firings in 30-year projects, with $\alpha = 0.01$; detection probability $g_0 = 0.3$ in years 1–3 and $g_{RP} = 0.15$ in years 4–30. See table 1 for explanation of terms used here.

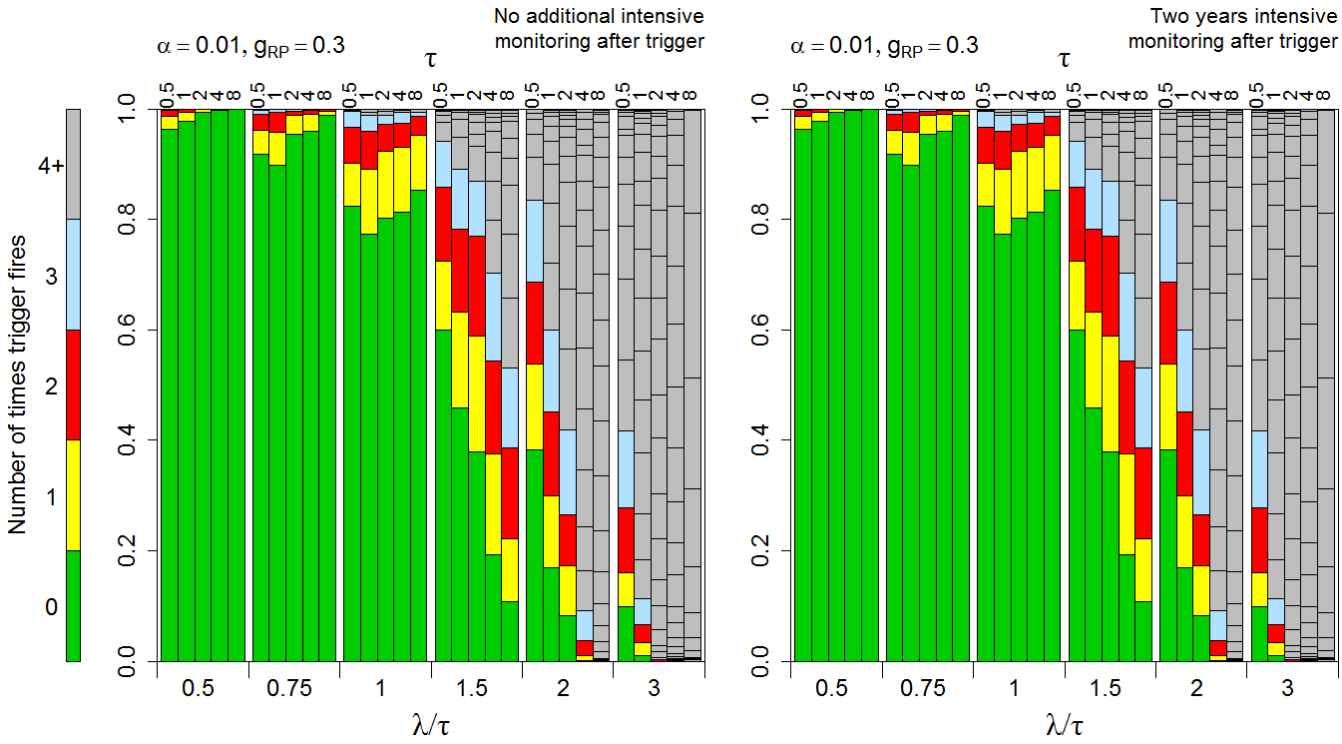

Figure 22. Distribution of number of trigger firings in 30-year projects, with $\alpha = 0.01$; detection probability $g_0 = 0.3$ in years 1–3 and $g_{RP} = 0.3$ in years 4–30. See table 1 for explanation of terms used here.

Increasing the value of α' increases the sensitivity of the trigger. The abundance of gray in the left halves of figures 23–26 indicates that defining $\alpha' = 0.05$ results in frequent trigger firings when $\lambda < \tau$.

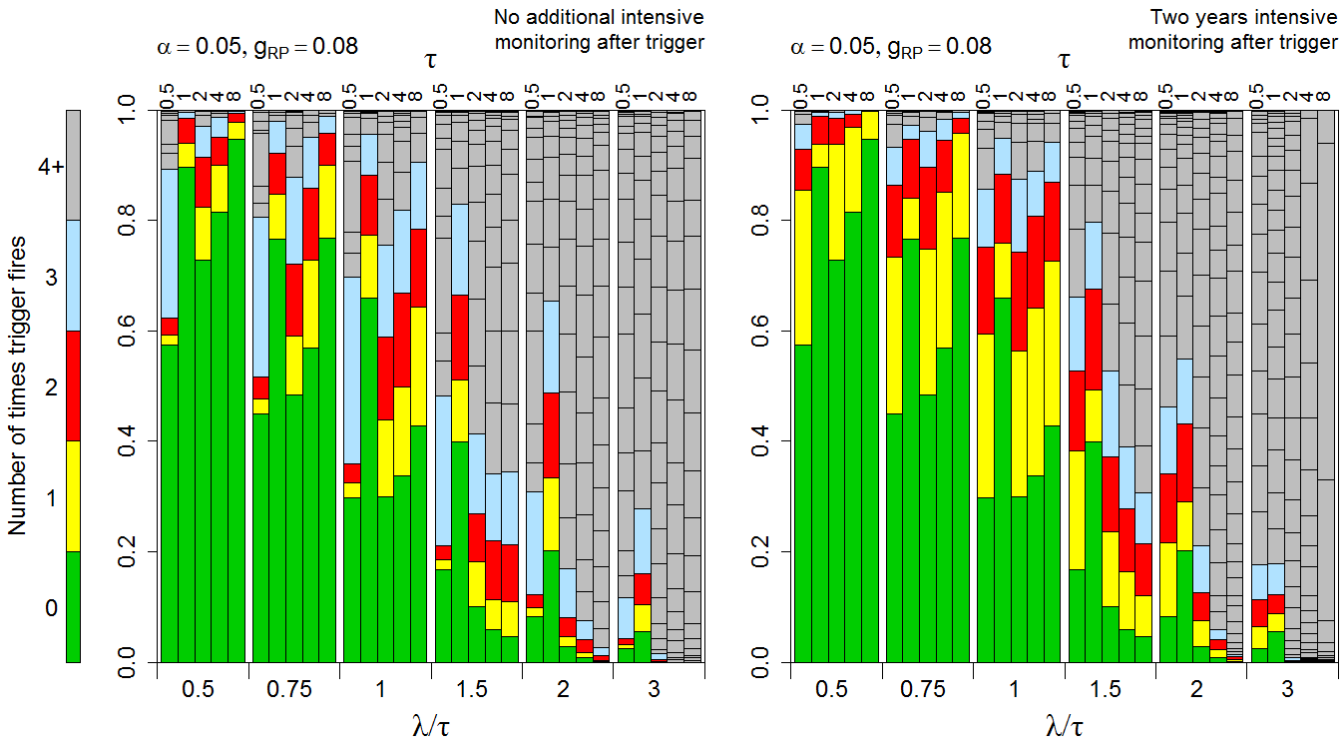

Figure 23. Distribution of number of trigger firings in 30-year projects, with $\alpha = 0.05$; detection probability $g_0 = 0.3$ in years 1–3 and $g_{RP} = 0.08$ in years 4–30. See table 1 for explanation of terms used here.

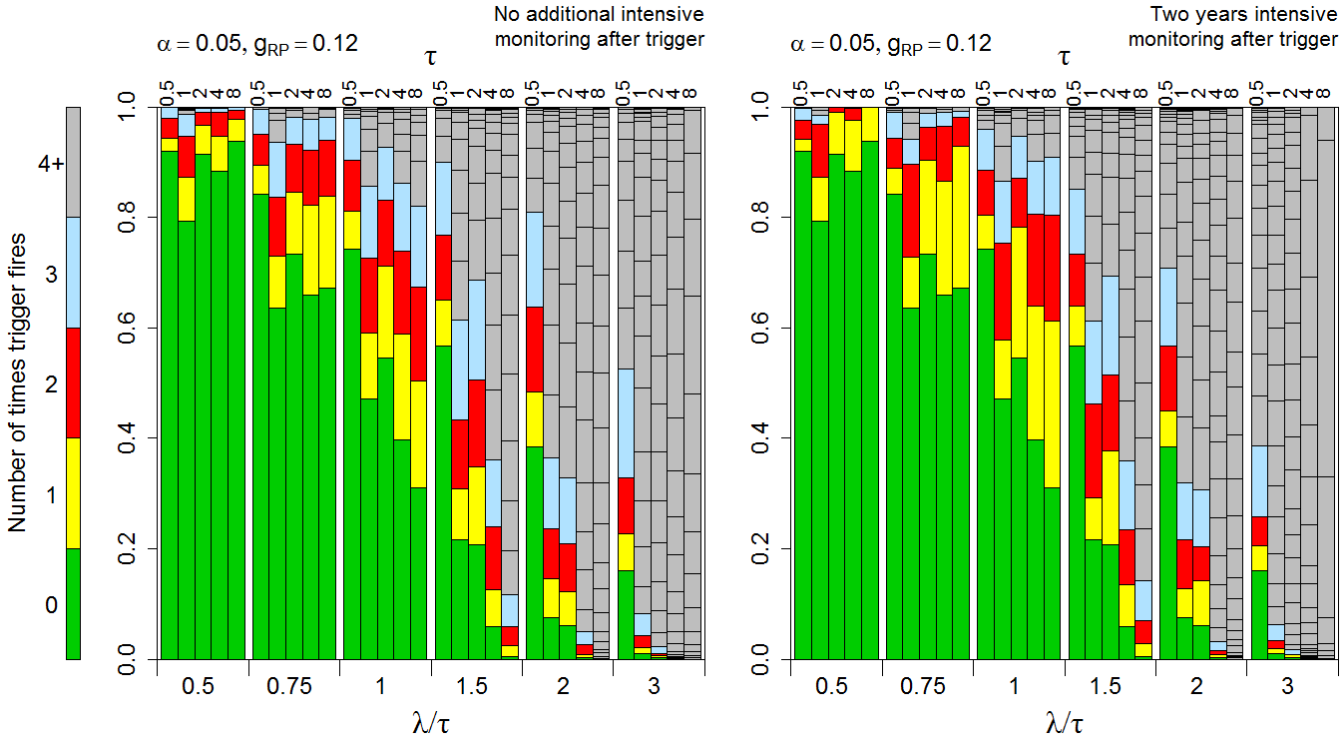

Figure 24. Distribution of number of trigger firings in 30-year projects, with $\alpha = 0.05$; detection probability $g_0 = 0.3$ in years 1–3 and $g_{RP} = 0.12$ in years 4–30. See table 1 for explanation of terms used here.

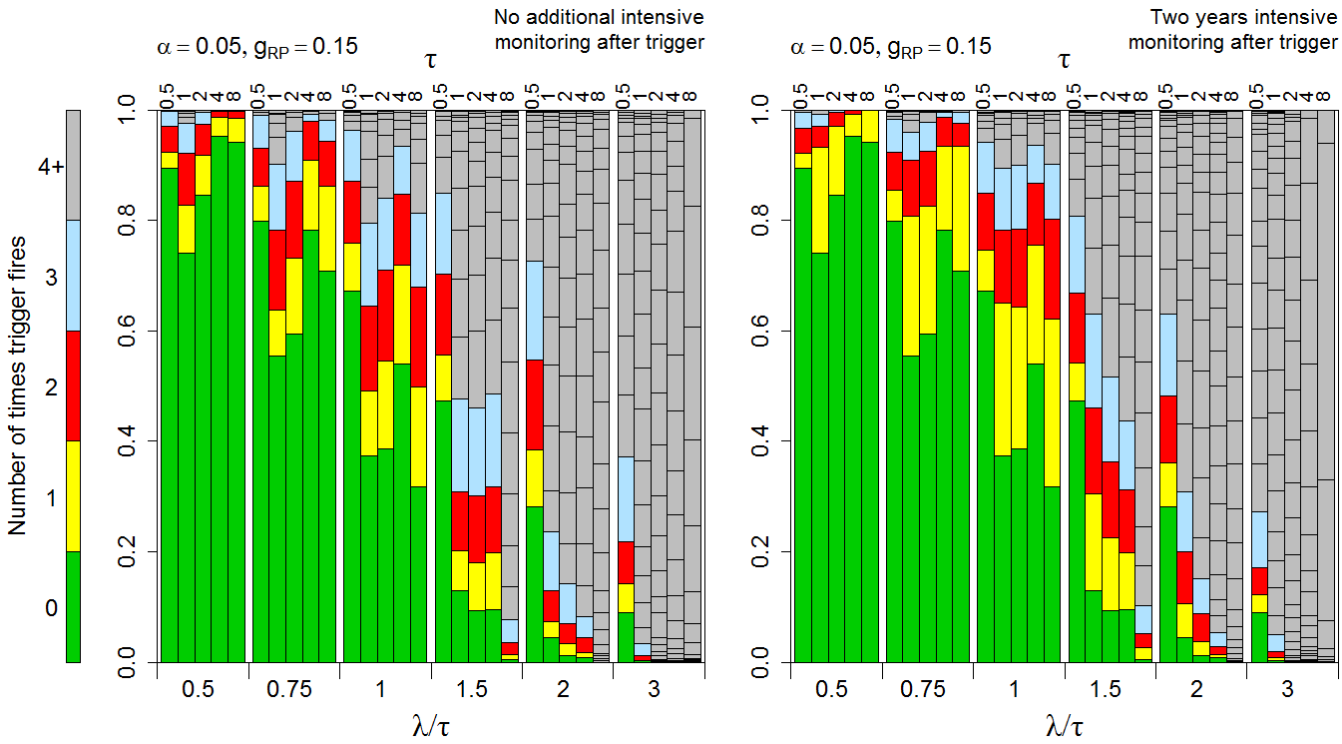

Figure 25. Distribution of number of trigger firings in 30-year projects, with $\alpha = 0.05$; detection probability $g_0 = 0.3$ in years 1–3 and $g_{RP} = 0.15$ in years 4–30. See table 1 for explanation of terms used here.

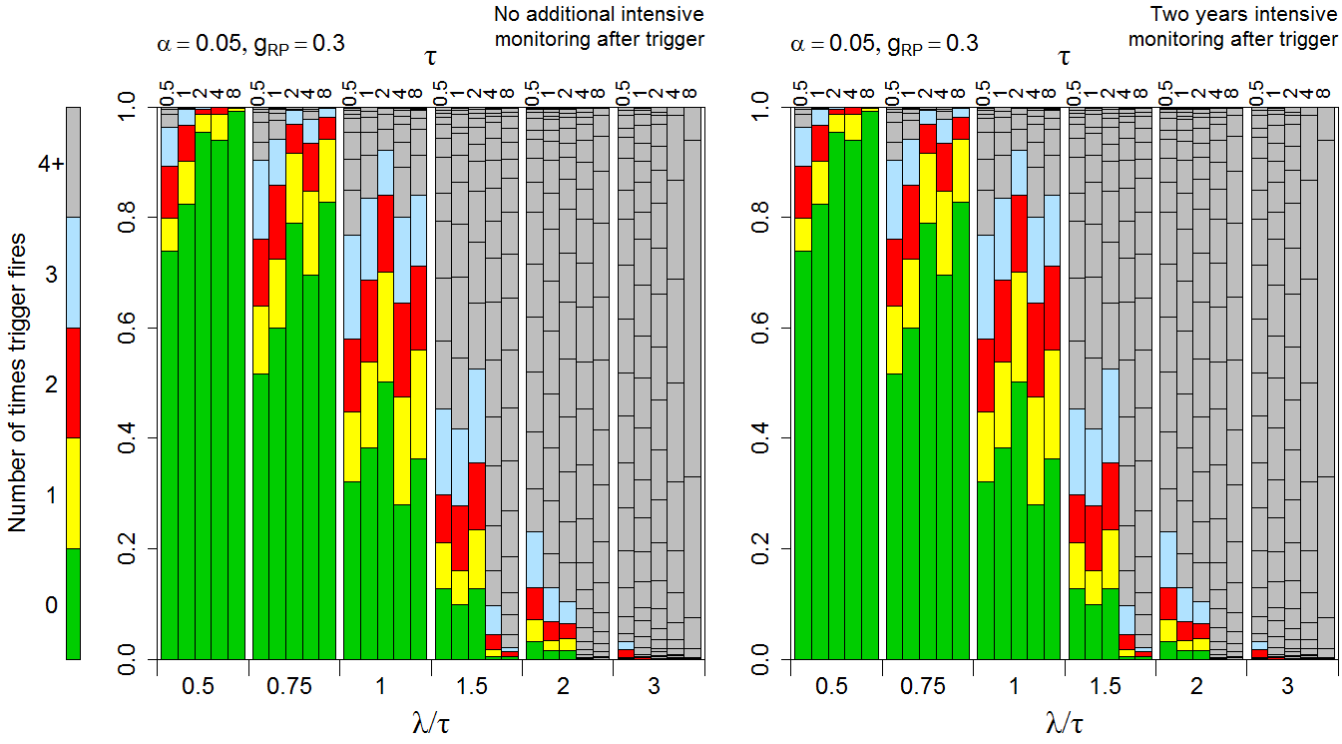

Figure 26. Distribution of number of trigger firings in 30-year projects, with $\alpha = 0.05$; detection probability $g_0 = 0.3$ in years 1–3 and $g_{RP} = 0.3$ in years 4–30. See table 1 for explanation of terms used here.

Behavior of the Short-Term Trigger in the First 2 Years

In the first 2 years of a project, the trigger tests the cumulative total number of observed carcasses X against the 3-year permitted rate. For example, for the trigger to fire in the first year, the number of carcasses found would have to be so large that it would be unusual to see that many in 2 years if the rate were within the permitted range. Thus, the short-term trigger is very unlikely to fire in the first 2 years unless $\lambda \gg \tau$ (fig. 27), and trigger firings in the first 2 years are an especially strong indication of exceedance.

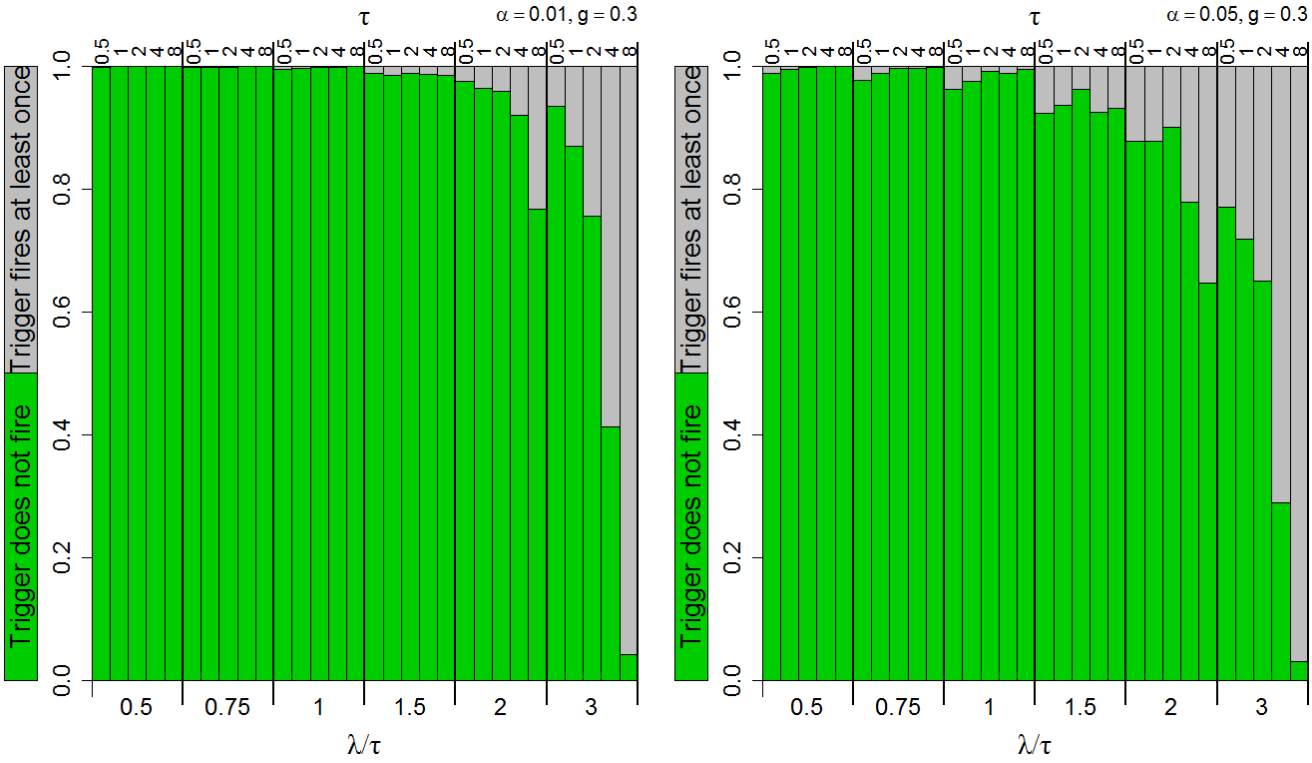

Figure 27. Probability that the short-term trigger fires in 2 years of monitoring at $g = 0.3$. See table 1 for explanation of terms used here.

Interaction of Short- and Long-Term Triggers

The long-term trigger is straightforward in its aims and implementation—to determine when the cumulative number of fatalities (M) has exceeded permitted total (T) and then prevent further fatalities. The short-term trigger is designed to signal when the average take rate (λ) exceeds annual permitted rate (τ). The short-term trigger may be used to detect excessive take rates in the early years of a permit or signal changes in take rates that may warrant AMA. A series of incremental AMAs may be defined to take effect as warranted by the patterns of short-term triggering. Incremental AMAs may include periods of intensive monitoring, actions to reduce fatality rates, adjustment of τ to better match true fatality rates, or other actions. Incremental AMAs can be used to correct initial errors in predicting take (τ), prevent or postpone long-term exceedance, and extend the period of operations before the long-term trigger fires.

There are innumerable possibilities for defining a program of incremental AMAs, and only a small set of possibilities is addressed in this report. The following figures (figs. 28–35) portray the distributions of total fatality and years of operations under each step of incremental AMAs when the long-term and short-term triggers are both acting, and specific programs of incremental AMAs are implemented in conjunction with short-term triggering at $\alpha' = 0.01$. Each of the first two times the short-term trigger is fired, pre-defined AMAs are implemented that change the fatality rate by a factor of ρ (with $\rho = 1, 0.841, 0.707,$ and 0.5 in different scenarios) followed by 2 years of intensive monitoring ($g = 0.3$). The AMA for the third short-term triggering is full avoidance (as with AMA for the long-term trigger). Although the AMAs discussed here are limited to three steps until full avoidance, there could be any number of increments culminating in a final stage that may differ from the full avoidance AMA that is required for the long-term trigger. The actual effectiveness that a given AMA will have cannot be known in advance but must be predicted from previous data, studies, or models. However, compliance with the ITP is based on take estimate rather than the realized effectiveness of a given AMA.

Results are compared for the following programs of incremental AMAs:

1. no short-term trigger and no AMAs,
2. ineffective AMA with $\rho = 1$ for increments 1 and 2; full avoidance for increment 3,
3. AMA with $\rho = 0.841$ for increments 1 and 2 (that is, the first AMA reduces rate to 0.841λ and the second AMA reduces rate to $0.841^2\lambda = 0.707\lambda$),
4. AMA with $\rho = 0.707$ for increments 1 and 2; full avoidance for increment 3,
5. AMA with $\rho = 0.5$ for increments 1 and 2; full avoidance for increment 3.

Programs 2–5 all require 2 years of intensive monitoring ($g = 0.3$) for increments 1 and 2.

The distributions of total fatality at the end of 30 years are represented as boxplots, with programs 1–5 running from left to right, respectively, within each subgroup of parameters.

NOTE: Each subgroup of boxes represents increasing effectiveness of incremental AMAs. There is a separate figure for each g value in the out years (that is, $g = 0.08, 0.12, 0.15,$ or 0.3 for years 4–30).

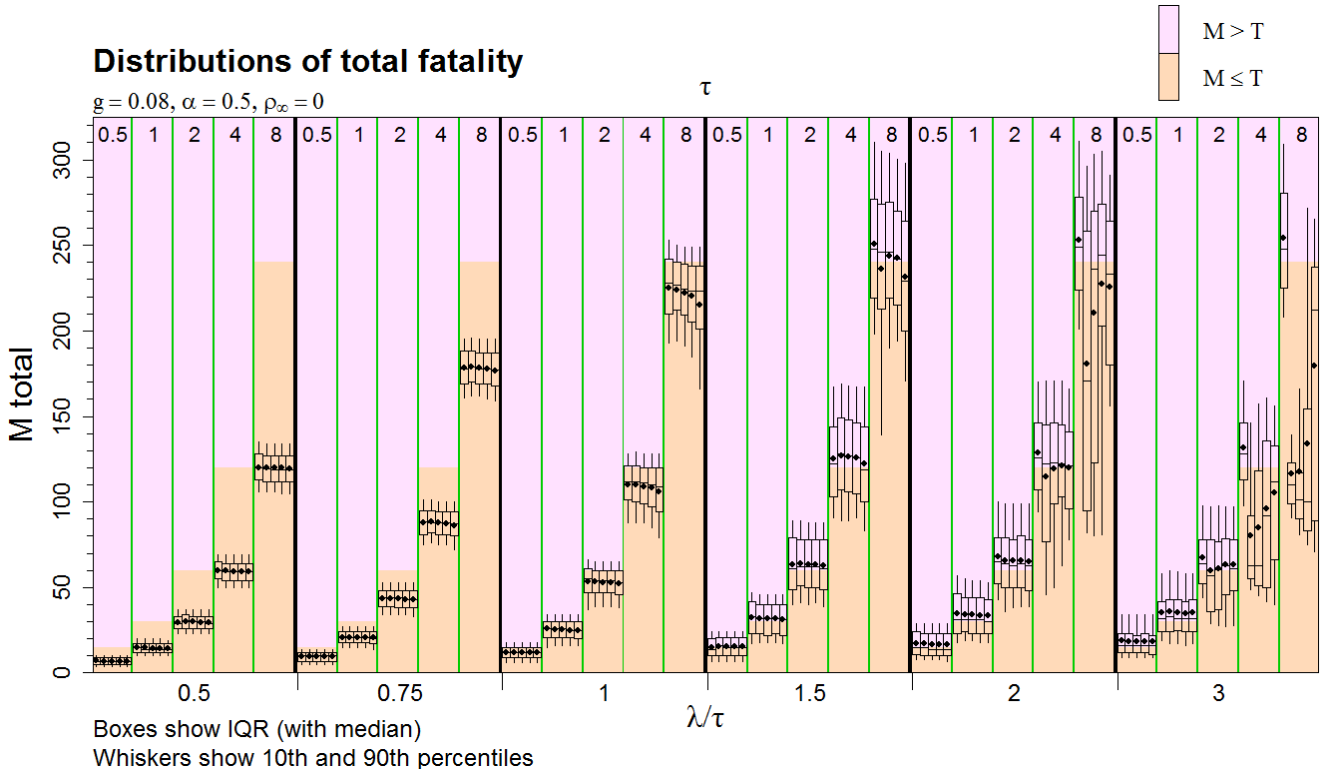

Figure 28. Distributions of fatalities when both short- and long-term triggers are active, with $g = 0.08$ in years 4–30, and $\alpha = 0.5$. Boxes within each subgroup represent increasing effectiveness of adaptive management action (AMAs) applied when the short-term trigger fires, including: (from left to right) no AMAs, $\rho = 1$, $\rho = 0.84$, $\rho = 0.71$, and $\rho = 0.5$. Two years' monitoring at $g = 0.3$ follows any short-term trigger firings. The third short-term trigger firing in a project results in AMAs for avoidance of further fatalities. See table 1 for explanation of terms used here.

When $\lambda \leq \tau$, the effectiveness of the incremental AMAs had little effect on eventual fatality numbers because the short-term trigger was unlikely to fire (fig. 28). However, when $\lambda > \tau$, the short-term triggers and associated AMAs can have a strong effect on eventual fatality numbers. When $\lambda > \tau$ and the AMAs are ineffective ($\rho = 1$, second box from left in each group), the third increment (avoidance AMA) is triggered early enough to result in fatality levels well below the limit. As the effectiveness of the AMAs improves, the fatality rates approach the limit more closely as the induced reductions in fatality rate extend the time until avoidance AMA is required.

This indicates that the short-term trigger has value in identifying excessive take rates more rapidly than does the long-term trigger and prevents eventual exceedance of total allowable take.

When $\lambda \leq \tau$ and τ is small, the 2 years of intensive monitoring following the short-term trigger leads to slight increase in the years of operation before avoidance AMA even when the incremental AMA is ineffective at reducing the fatality rate, which is reflected in slightly shorter gray bars in the second columns of subgroups on the left half of figure 29. Avoidance AMA is reached almost exclusively by the action of the long-term trigger in all scenarios with $\lambda \leq \tau$ because the short-term trigger is extremely unlikely to fire three times. When $\lambda > \tau$, the ineffective AMA does not reduce the fatality rate but the short-term trigger fires three times before the long-term trigger fires, which results in fewer years of operation prior to avoidance AMA. As the effectiveness of the AMAs increases, the years of operation prior to avoidance AMA also increase.

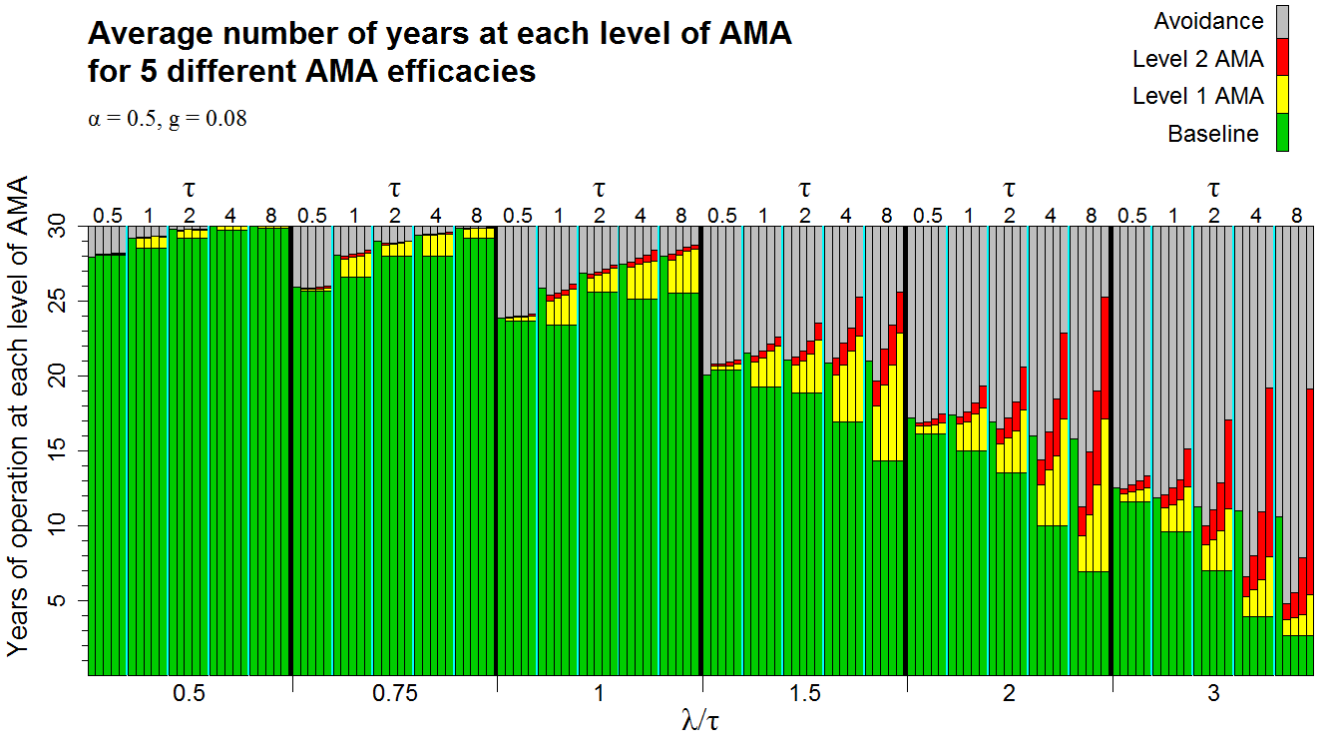

Figure 29. Average number of years at each adaptive management action (AMA) level, with $g = 0.08$ in years 4–30, and $\alpha = 0.5$. Bars within each τ group correspond to effectiveness of AMAs (ρ): from left to right, no short-term trigger, and $\rho = 1$, 0.84, 0.71, and 0.5. AMA levels 1 and 2 each change fatality rate by a factor of ρ. level 3 AMA is full avoidance. Two years' monitoring at g = 0.3 after each increment in AMA. See table 1 for explanation of terms used here.

Qualitatively, the patterns remain similar for $g = 0.12, 0.15, 0.3$ in the out years, but precision improves (figs. 30–35).

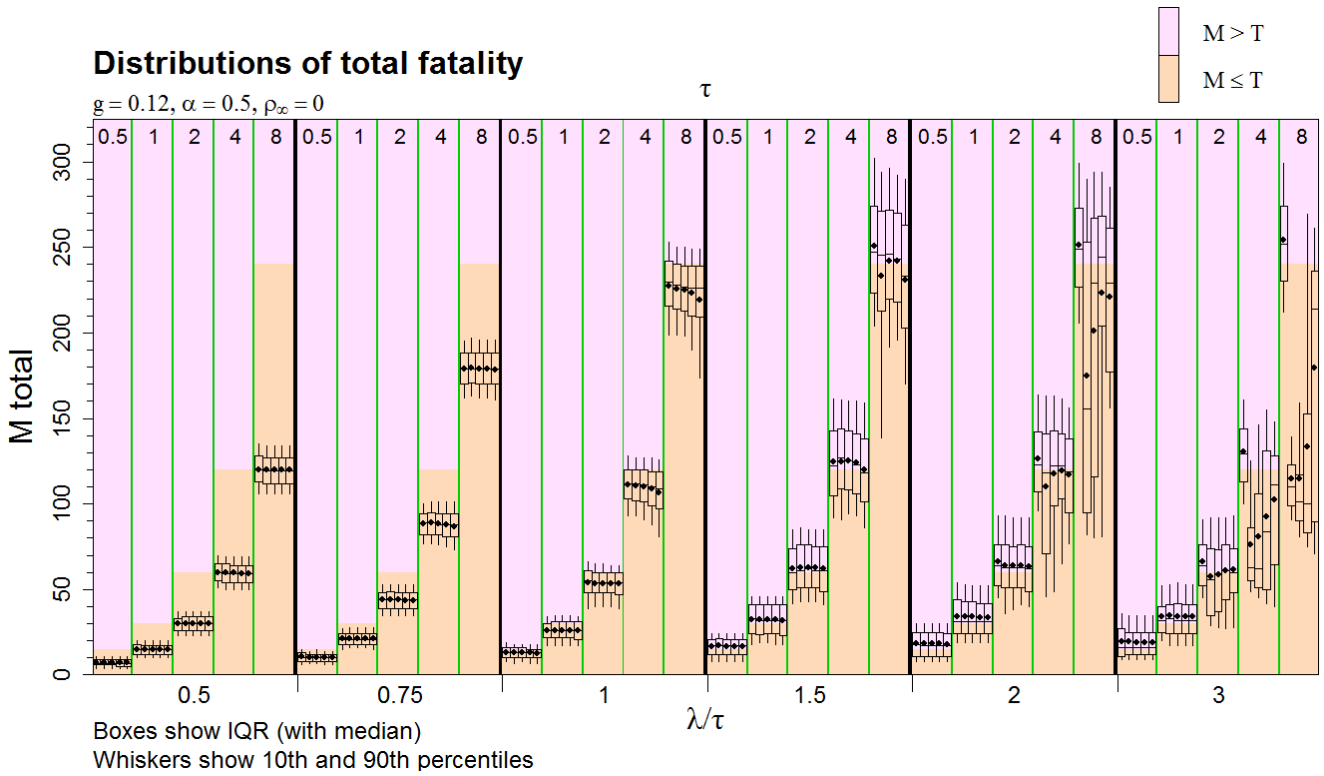

Figure 30. Distributions of fatalities when both short- and long-term triggers are active, with $g = 0.12$ in years 4–30, and $\alpha = 0.5$. Boxes within each subgroup represent increasing effectiveness of adaptive management action (AMAs) applied when the short-term trigger fires, including: (from left to right) no AMAs, $\rho = 1$, $\rho = 0.84$, $\rho = 0.71$, and $\rho = 0.5$. Two years' monitoring at $g = 0.3$ follows any short-term trigger firings. The third short-term trigger firing in a project results in AMAs for avoidance of further fatalities. See table 1 for explanation of terms used here.

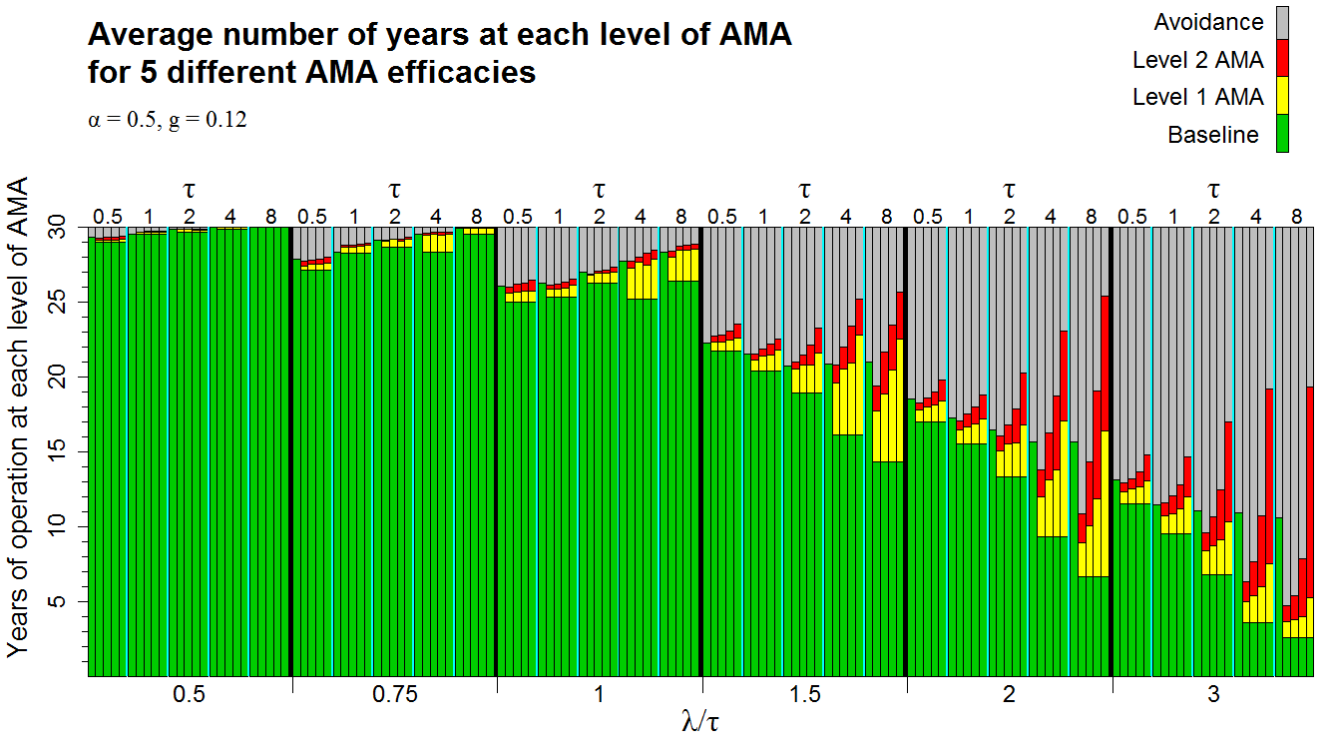

Figure 31. Average number of years at each adaptive management action (AMA) level, with $g = 0.12$ in years 4–30, and $\alpha = 0.5$. Bars within each τ group correspond to effectiveness of AMAs (ρ): from left to right, no short-term trigger, and $\rho = 1$, 0.84, 0.71 and 0.5. AMA levels 1 and 2 each change fatality rate by a factor of ρ. Level 3 AMA is full avoidance. Two years' monitoring at g = 0.3 after each increment in AMA. See table 1 for explanation of terms used here.

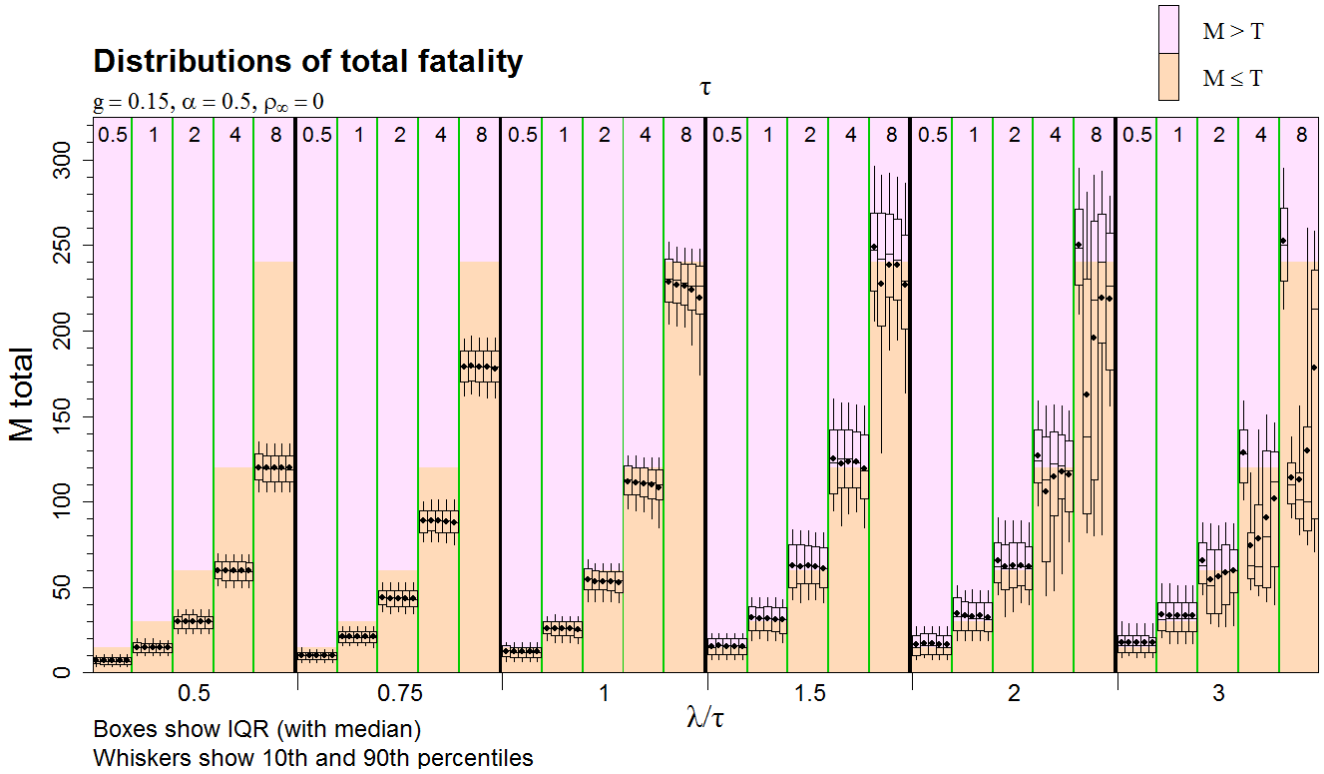

Figure 32. Distributions of fatalities when both short- and long-term triggers are active, with $g = 0.15$ in years 4–30, and $\alpha = 0.5$. Boxes within each subgroup represent increasing effectiveness of adaptive management action (AMAs) applied when the short-term trigger fires, including: (from left to right) no AMAs, $\rho = 1$, $\rho = 0.84$, $\rho = 0.71$, and $\rho = 0.5$. Two years' monitoring at $g = 0.3$ follows any short-term trigger firings. The third short-term trigger firing in a project results in AMAs for avoidance of further fatalities. See table 1 for explanation of terms used here.

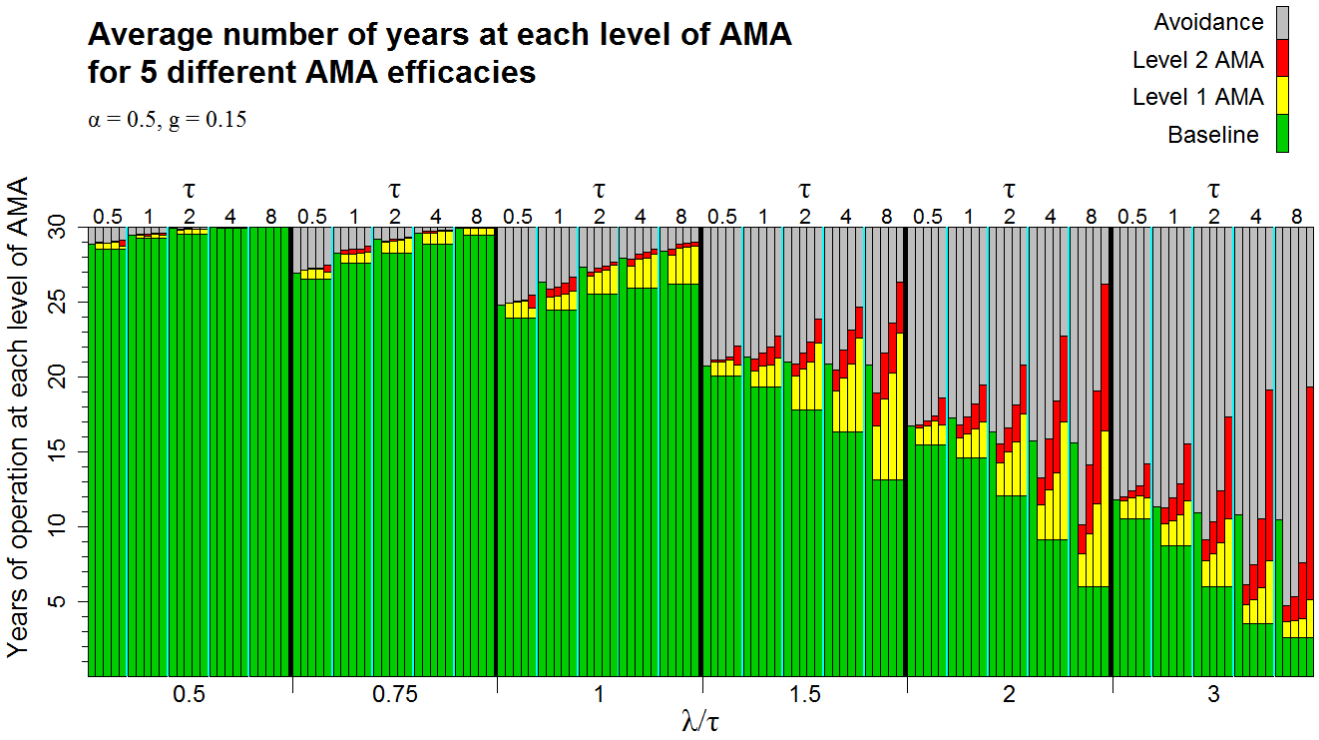

Figure 33. Average number of years at each adaptive management action (AMA) level, with $g = 0.15$ in years 4–30, and $\alpha = 0.5$. Bars within each τ group correspond to effectiveness of AMAs (ρ): from left to right, no short-term trigger, and $\rho = 1$, 0.84, 0.71 and 0.5. AMA levels 1 and 2 each change fatality rate by a factor of ρ. Level 3 AMA is full avoidance. Two years' monitoring at g = 0.3 after each increment in AMA. See table 1 for explanation of terms used here.

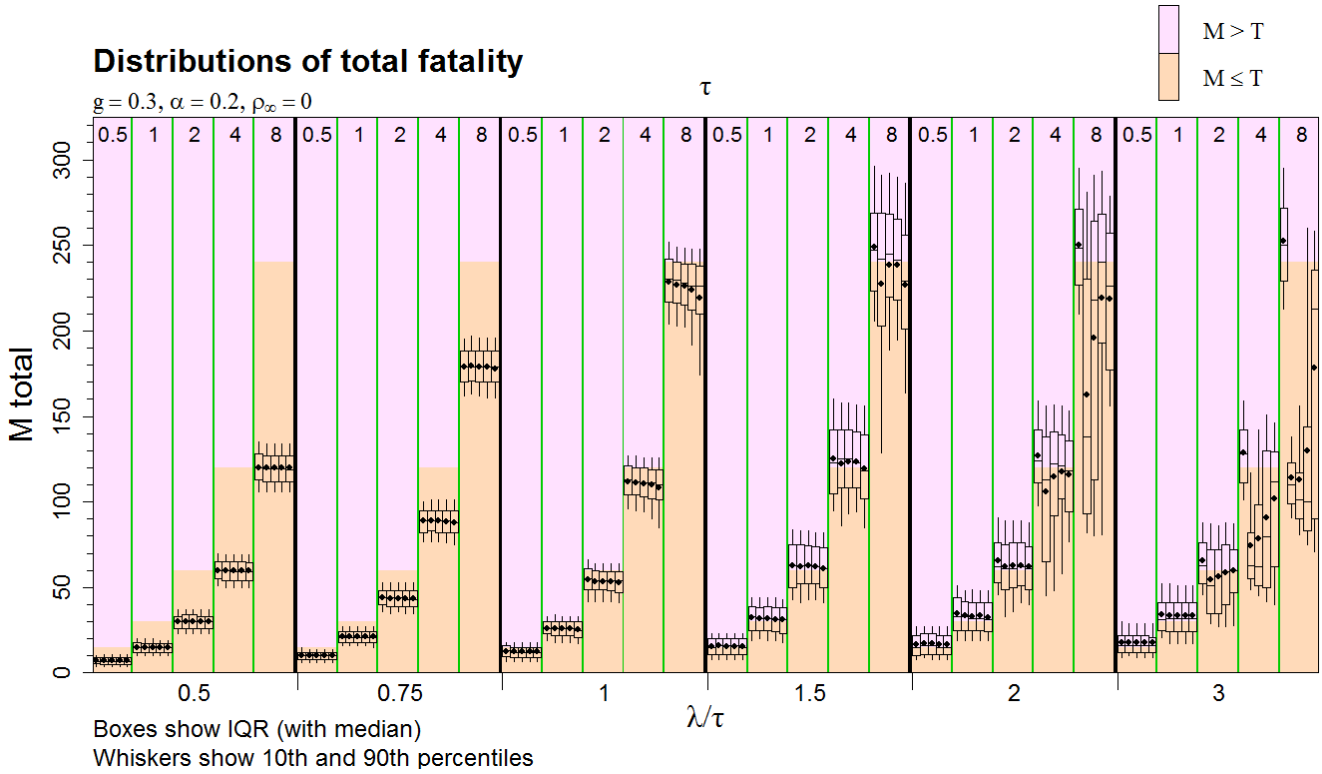

Figure 34. Distributions of fatalities when both short- and long-term triggers are active, with $g = 0.3$ in years 4–30, and $\alpha = 0.5$.Boxes within each subgroup represent increasing effectiveness of adaptive management action (AMAs) applied when the short-term trigger fires, including: (from left to right) no AMAs, $\rho = 1$, $\rho = 0.84$, $\rho = 0.71$, and $\rho = 0.5$. Two years' monitoring at $g = 0.3$ follows any short-term trigger firings. The third short-term trigger firing in a project results in AMAs for avoidance of further fatalities. See table 1 for explanation of terms used here.

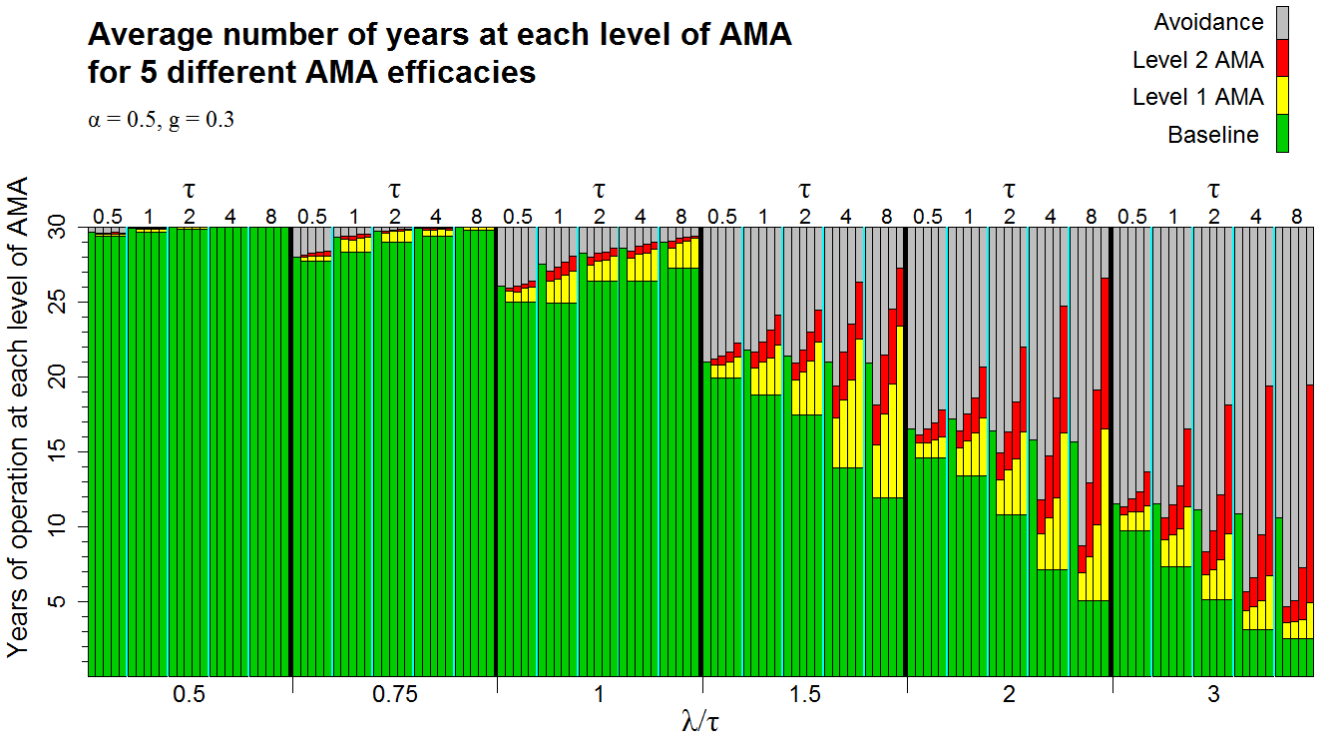

Figure 35. Average number of years at each adaptive management action (AMA) level, with $g = 0.3$ in years 4–30, and $\alpha = 0.5$. Bars within each τ group correspond to effectiveness of AMAs (ρ): from left to right, no short-term trigger, and $\rho = 1$, 0.84, 0.71 and 0.5. AMA levels 1 and 2 each change fatality rate by a factor of ρ. Level 3 AMA is full avoidance. Two years' monitoring at g = 0.3 after each increment in AMA. See table 1 for explanation of terms used here.

Effects of Misspecification of Effectiveness of Incremental Adaptive Management Action in the Model

The effectiveness of incremental AMA is a parameter that is entered as "relative weight" into the EoA model for estimating fatality rates in years after AMAs are implemented. Because of the high degree of variability and uncertainty in fatality rates from year to year, the effectiveness of a particular AMA in a given year is difficult to assess with any useful degree of precision unless fatality rates are high (which, presumably they will not be because the concern is with rare species) and the AMAs are quite effective. The presumption is that fatality rates for the protected species will be low, and surrogates may be used to estimate the realized effectiveness of incremental AMAs (for example, assume that the proportional reduction in fatalities in protected species is the same as it is for total bat fatalities), or the effectiveness may be inferred from previous studies or other supplementary data. If the effectiveness is underestimated (for example, by assuming $\rho = 1$ when it is really 0.7), the long-term trigger will tend to fire earlier than necessary, and if it overestimated (for example, assuming $\rho = 0.8$ when it is really 1), long-term triggering may be slightly delayed. However, as shown below (figs 36-47), it is only under a very limited set of conditions that misspecification of ρ could be a significant issue. In particular, the assumed weights are used in the model only in estimating the weighted average of detection probabilities through the years. If detection probability does not vary from year to year, the assumed weights have no effect whatsoever, and, unless the detection probabilities vary substantially, the potential practical effect of misspecification of ρ is slight. The potential for error also would be greatest when $\lambda \gg \tau$ so that the trigger fires early, and misspecification would have little or no effect in cases where $\lambda < \tau$ because the short-term trigger rarely fires in those cases.

Distributions of total number of fatalities after 30 years are shown in figures 36–47 under an adaptive management plan that involves both short- and long-term triggers with three incremental AMAs implemented after short-term triggers are fired. The first two steps of incremental AMA have true effectiveness of ρ_{true} as indicated at the top of each figure. Boxes reflect actual total fatality numbers after making different assumptions about ρ, with values 1, 0.841, 0.707, and 0.5 (from left to right). The shaded box represents the case where assumed ρ is exactly correct. Assumed effectiveness of AMA influences the estimates of M and λ and thereby affects the timing of AMAs and, ultimately, total take. Figures 36–39 are for $g_{RP} = 0.08$ in the out years (that is, years 4–30); figures 40–43 are for $g_{RP} = 0.12$; and figures 44–47 are for $g = 0.15$. In all cases, $g = 0.3$ for the first 3 years of monitoring.

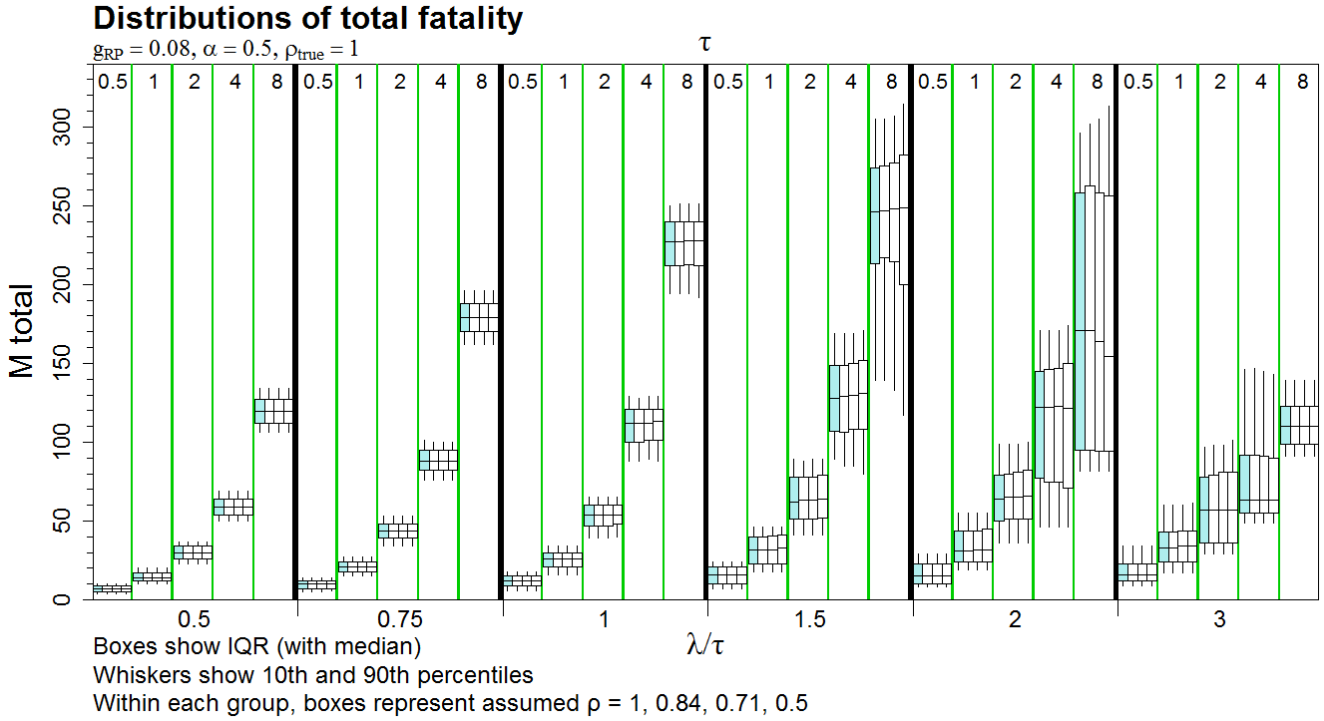

Figure 36. Distribution of total number of fatalities after misspecification of ρ in estimation; $\rho_{\text{true}} = 1$, $\alpha = 0.50$, $g = 0.08$ in years 4–30. In all scenarios, $g = 0.3$ in years 1–3. Boxes with ρ specified correctly are colored blue. See table 1 for explanation of terms used here.

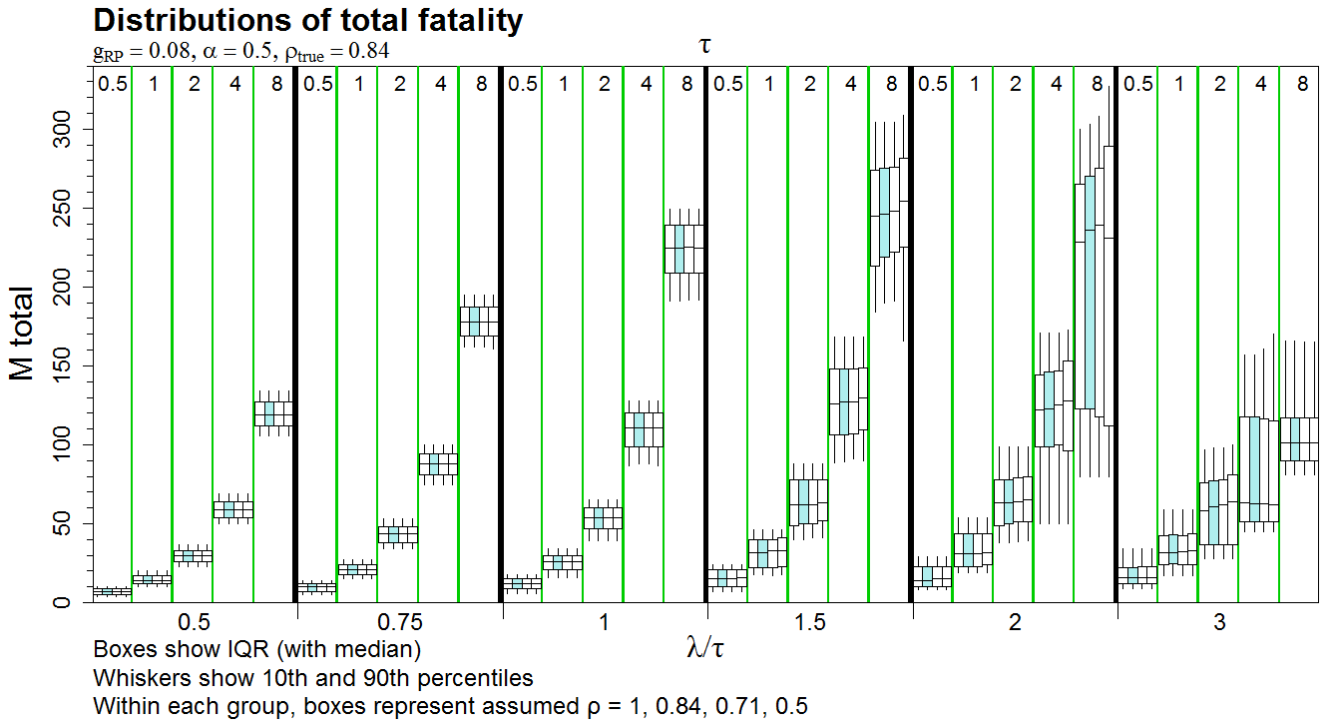

Figure 37. Distribution of total number of fatalities after misspecification of ρ in estimation; $\rho_{\text{true}} = 0.84$, $\alpha = 0.50$, $g = 0.08$ in years 4–30. In all scenarios, $g = 0.3$ in years 1–3. Boxes with ρ specified correctly are colored blue. See table 1 for explanation of terms used here.

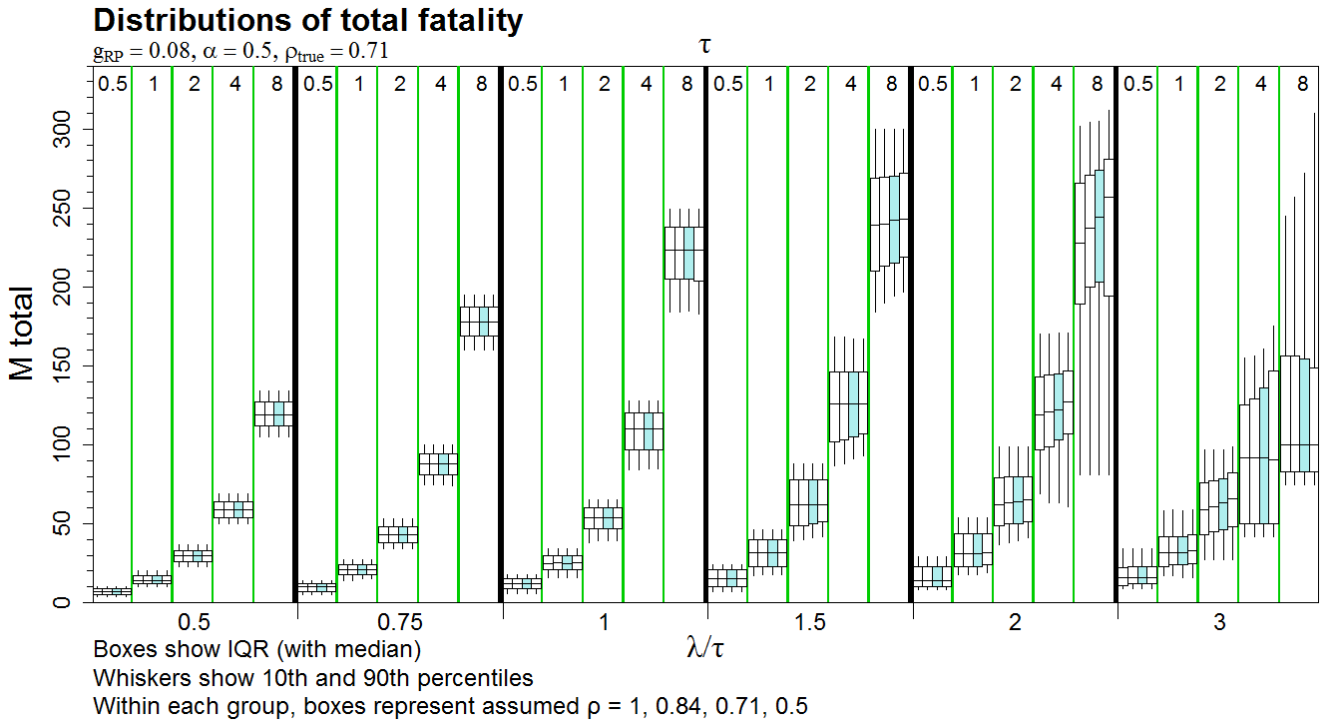

Figure 38. Distribution of total number of fatalities after misspecification of ρ in estimation; $\rho_{\text{true}} = 0.71$, $\alpha = 0.50$, $g = 0.08$ in years 4–30. In all scenarios, $g = 0.3$ in years 1–3. Boxes with ρ specified correctly are colored blue. See table 1 for explanation of terms used here.

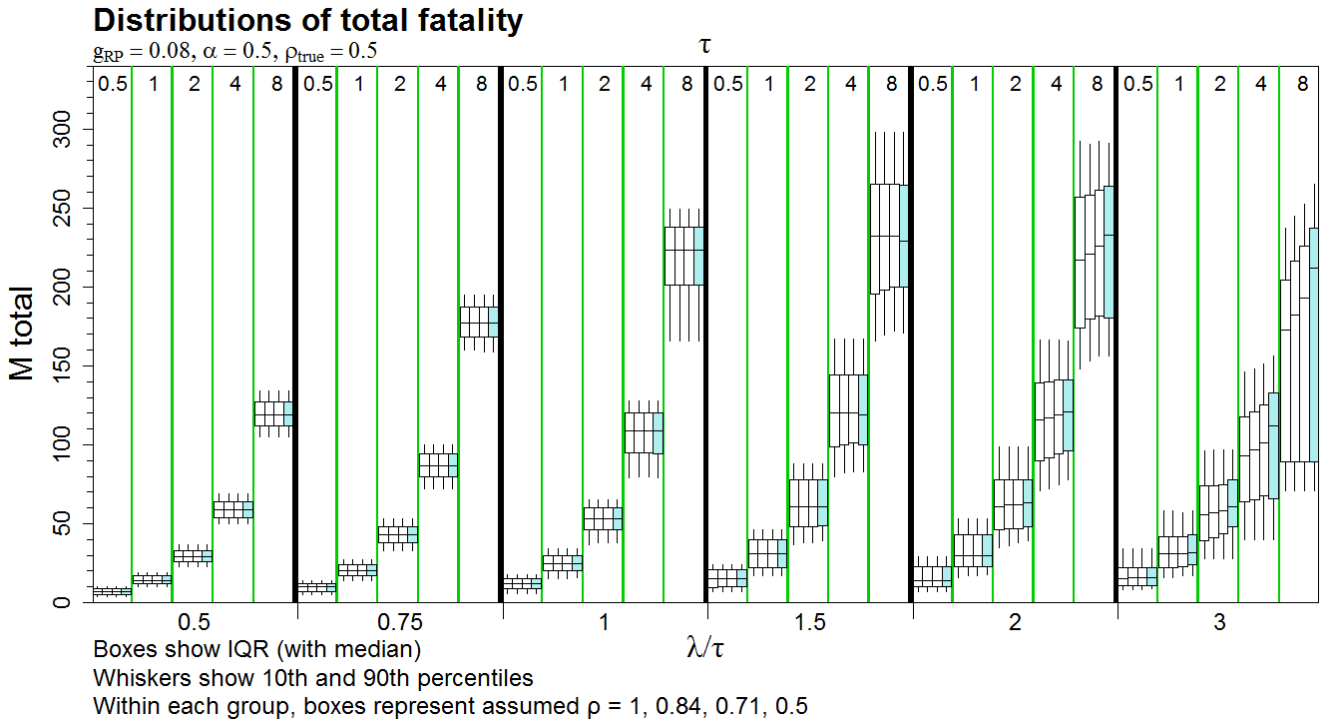

Figure 39. Distribution of total number of fatalities after misspecification of ρ in estimation; $\rho_{\text{true}} = 0.5$, $\alpha = 0.50$, $g = 0.08$ in years 4–30. In all scenarios, $g = 0.3$ in years 1–3. Boxes with ρ specified correctly are colored blue. See table 1 for explanation of terms used here.

The assumed weights only come into play when the short-term trigger is fired. This rarely happens when $\lambda \leq \tau$, in which case the overall effect of misspecification of weights is negligible. When the incremental AMA is ineffective (that is, $\rho_{\text{true}} = 1$), wrongly assuming $\rho = 0.841, 0.707,$ or 0.5 has little bearing on the final fatality numbers. The effect of misspecification is greatest when incremental AMAs are most effective ($\rho = 0.5$) and $\lambda \gg \tau$. In this case, the AMAs effectively cut the fatality rate to low enough levels to justify substantial delay in AMA for full avoidance, but overly pessimistic assumptions about effectiveness discount that justification and lead to earlier trigger firings and fatality numbers that fall far short of permitted levels.

Relative errors (difference between median number of fatalities when ρ is misspecified and median when ρ is not misspecified on a proportional scale) were less than 1% in most cases and exceeded 10% only when $\lambda/\tau = 3$ (so the short-term trigger fires early), $\tau = 4$ or 8, AMAs were highly effective ($\rho = 0.5$) and grossly misspecified (assumed $\rho = 1$ or 0.841).

Comparable figures for $g = 0.12$ and 0.15 are given in figures 40–47. The consequences of misspecification are less severe in these scenarios because the differences in detection probability among years are less pronounced.

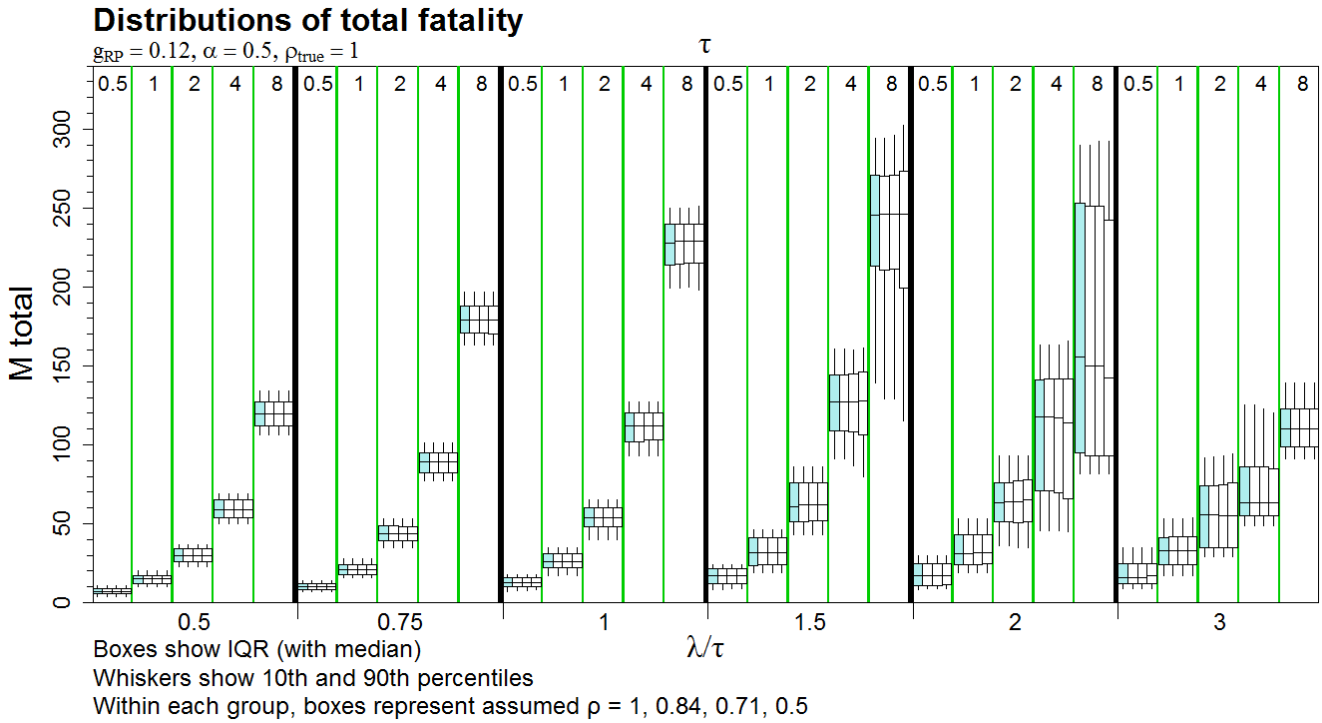

Figure 40. Distribution of total number of fatalities after misspecification of ρ in estimation; $\rho_{\text{true}} = 1$, $\alpha = 0.50$, $g = 0.12$ in years 4–30. In all scenarios, $g = 0.3$ in years 1–3. Boxes with ρ specified correctly are colored blue. See table 1 for explanation of terms used here.

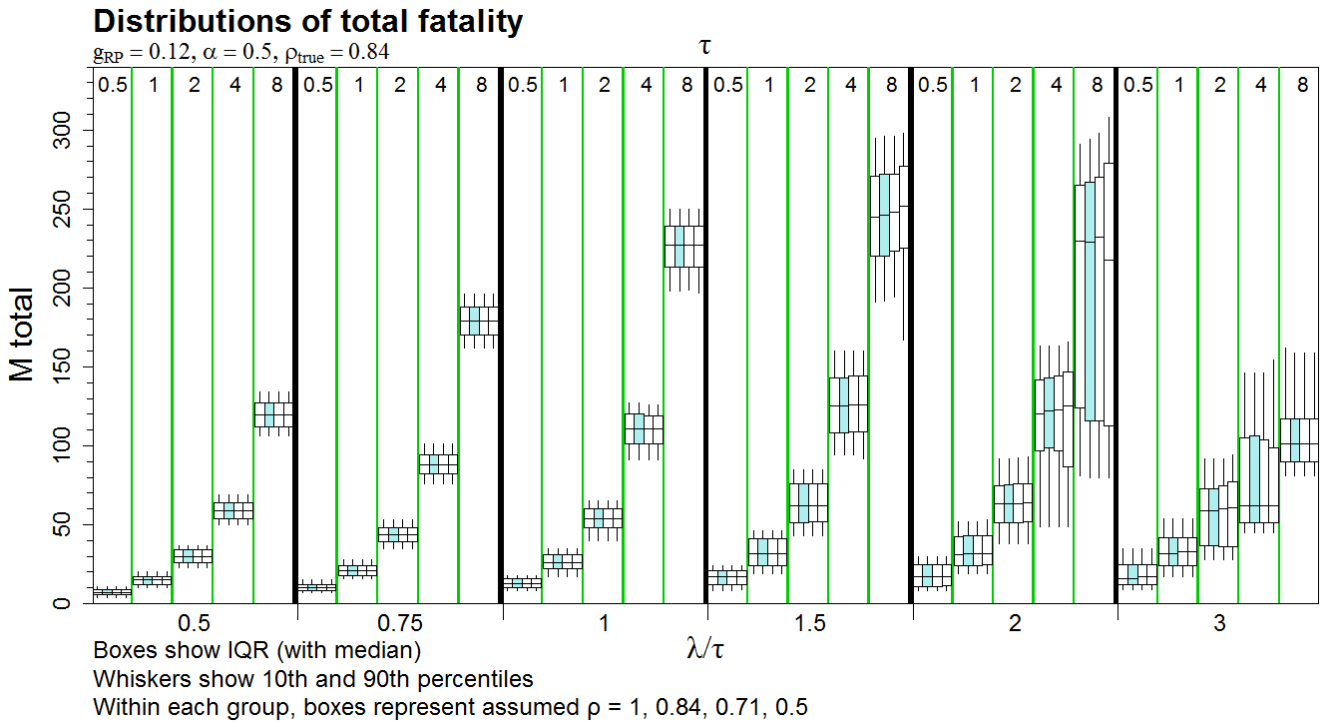

Figure 41. Distribution of fatalities after misspecification of ρ in estimation; $\rho_{\text{true}} = 0.84$, $\alpha = 0.50$, $g = 0.12$ in years 4–30. In all scenarios, $g = 0.3$ in years 1–3. Boxes with ρ specified correctly are colored blue.

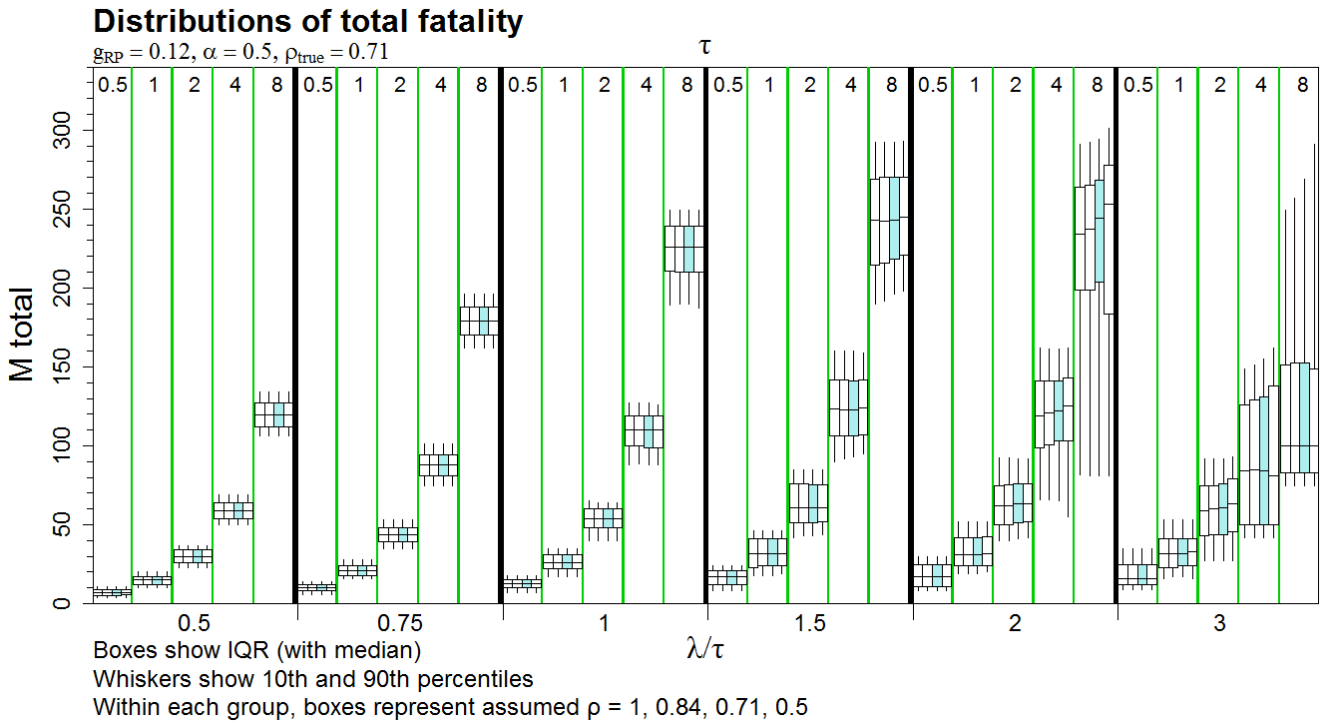

Figure 42. Distribution of total number of fatalities after misspecification of ρ in estimation; $\rho_{\text{true}} = 0.71$, $\alpha = 0.50$, $g = 0.12$ in years 4–30. In all scenarios, $g = 0.3$ in years 1–3. Boxes with ρ specified correctly are colored blue. See table 1 for explanation of terms used here.

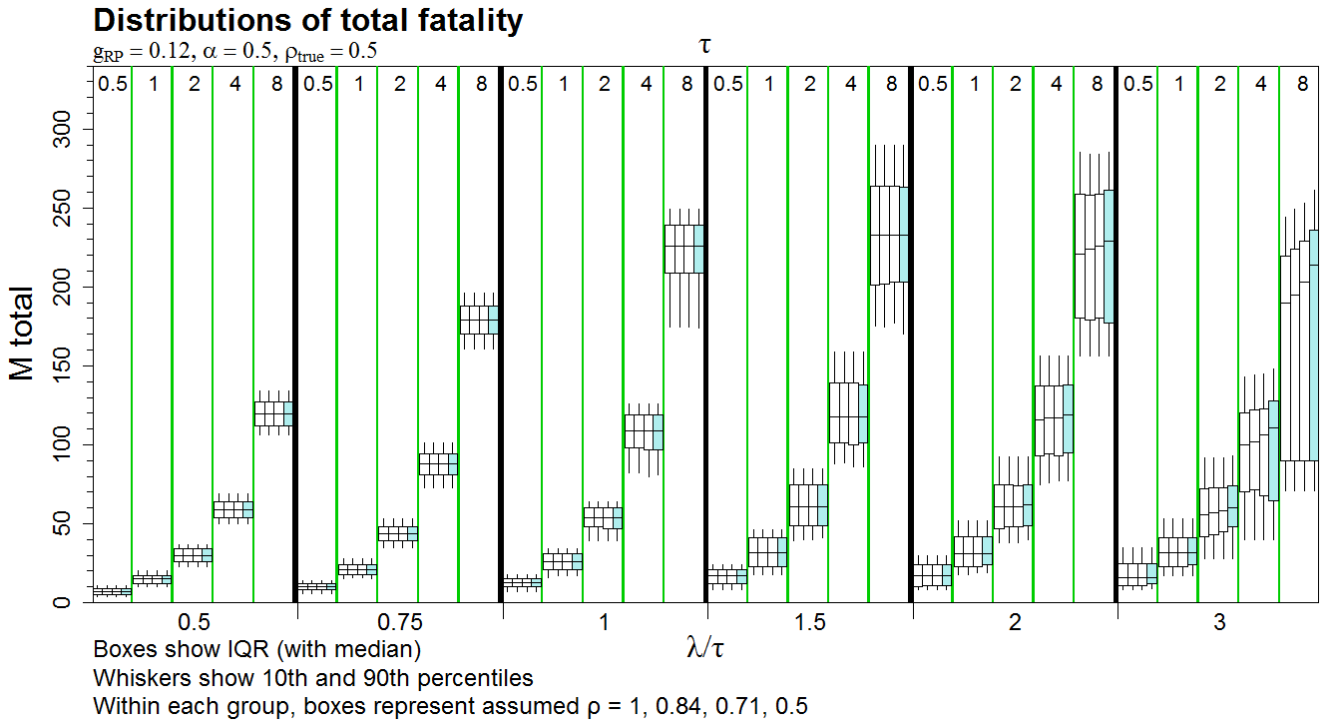

Figure 43. Distribution of total number of fatalities after misspecification of ρ in estimation; $\rho_{\text{true}} = 0.50$, $\alpha = 0.50$, $g = 0.12$ in years 4–30. In all scenarios, $g = 0.3$ in years 1–3. Boxes with ρ specified correctly are colored blue. See table 1 for explanation of terms used here.

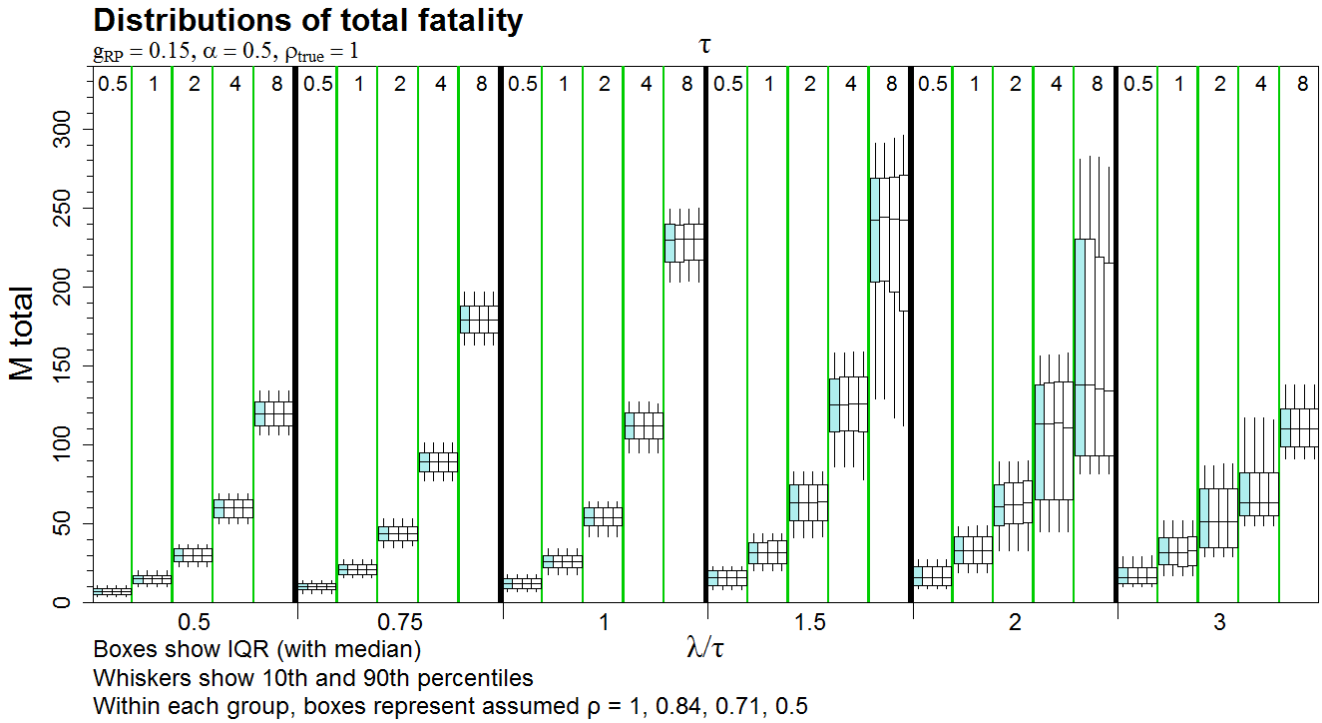

Figure 44. Distribution of fatalities after misspecification of ρ in estimation; $\rho_{\text{true}} = 1, \alpha = 0.50, g = 0.15$ in years 4–30. In all scenarios, $g = 0.3$ in years 1–3. Boxes with ρ specified correctly are colored blue. See table 1 for explanation of terms used here.

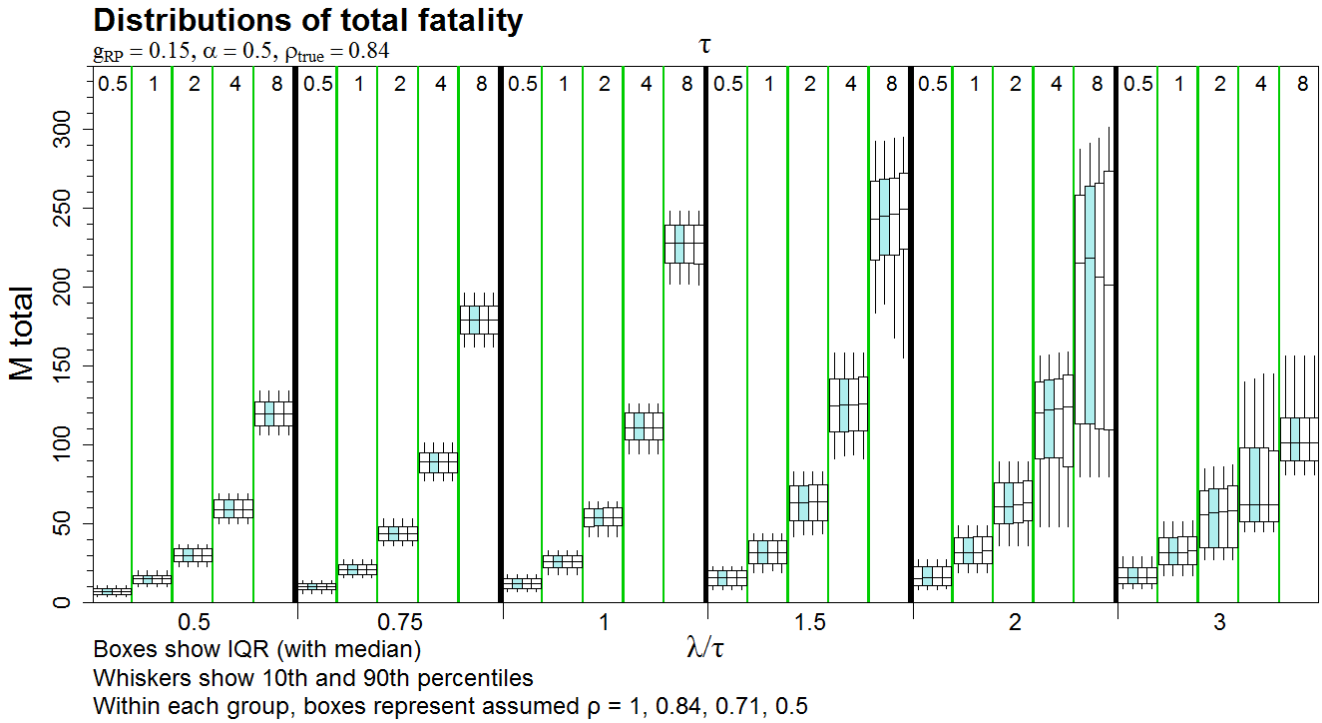

Figure 45. Distribution of fatalities after misspecification of ρ in estimation; $\rho_{\text{true}} = 0.84$, $\alpha = 0.50$, $g = 0.15$ in years 4–30. In all scenarios, $g = 0.3$ in years 1–3. Boxes with ρ specified correctly are colored blue.

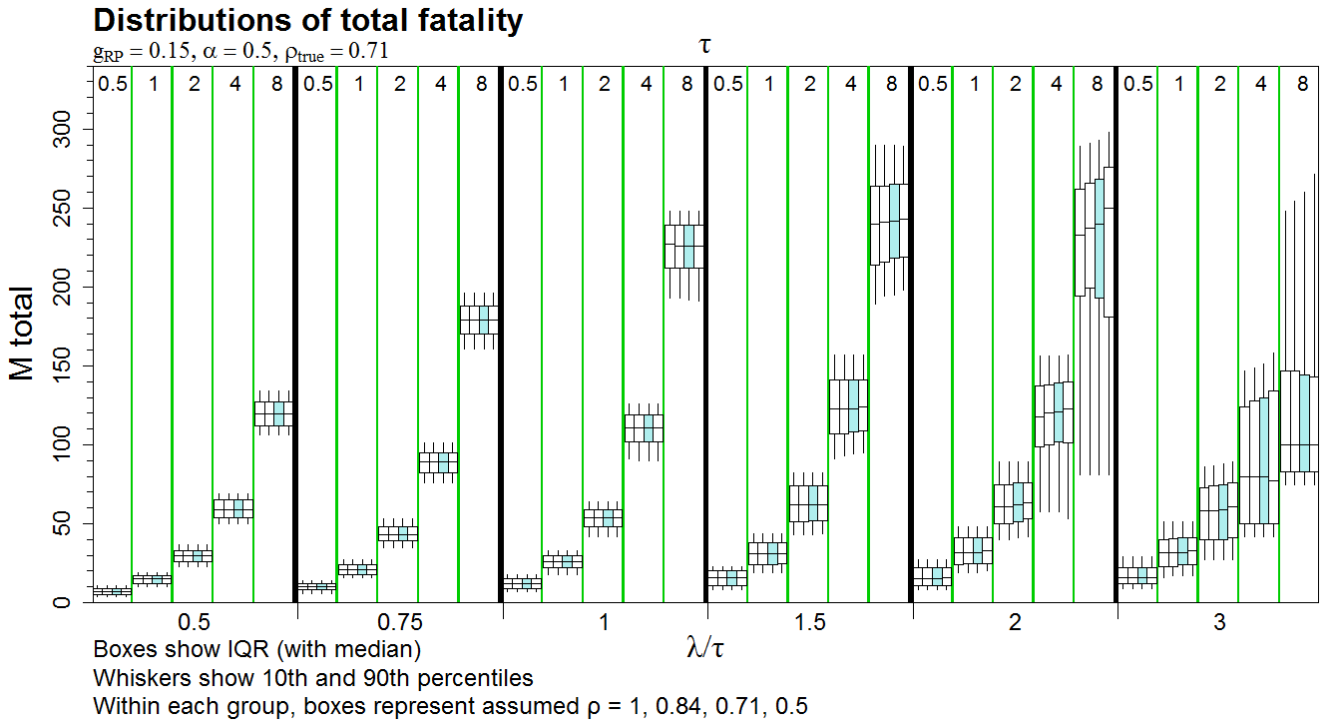

Figure 46. Distribution of fatalities after misspecification of ρ in estimation; $\rho_{\text{true}} = 0.71$, $\alpha = 0.50$, $g = 0.15$ in years 4–30. In all scenarios, $g = 0.3$ in years 1–3. Boxes with ρ specified correctly are colored blue. See table 1 for explanation of terms used here.

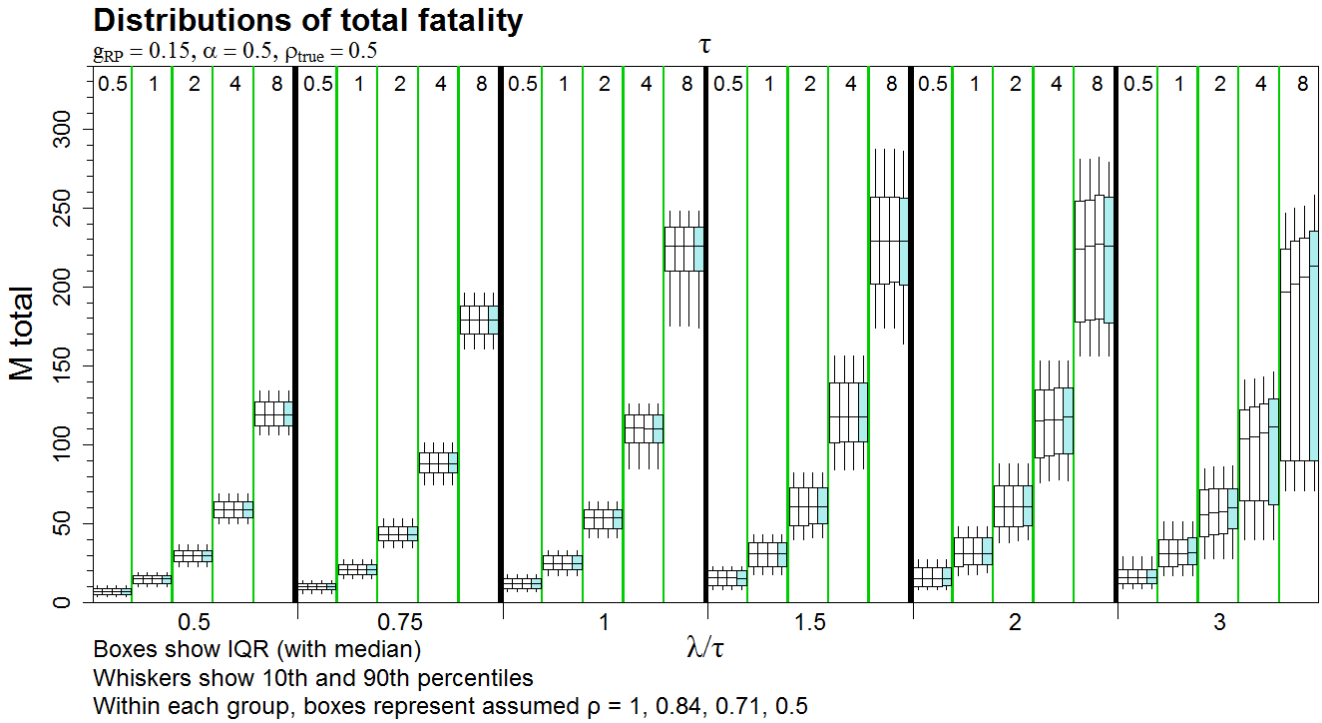

Figure 47. Distribution of fatalities after misspecification of ρ in estimation; $\rho_{\text{true}} = 0.5$, $\alpha = 0.50$, $g = 0.15$ in years 4–30. In all scenarios, $g = 0.3$ in years 1–3. Boxes with ρ specified correctly are colored blue. See table 1 for explanation of terms used here.

How Many Fatalities Could Occur and Not Fire the Short-Term Trigger?

By design, to account for natural random variation among years, the short-term trigger is minimally sensitive to short-term fluctuations and may allow actual take to exceed the permitted average rate of τ for a few years. In this section, the potential for high levels of take to occur without firing the short-term trigger is explored. There is one graph for each combination of parameter values $\tau = 0.5,1,2,4,8$; $g = 0.08, 0.12, 0.15, 0.3$ (for all 3 years); and $\alpha' = 0.01, 0.05, 0.10$) with separate lines for different values of λ/τ. For example, in figure 48, for parameters $\tau = 4$ per year (or 12 in 3 years), $g = 0.08$, and $\alpha' = 0.05$, the heavy black line represents the case where $\lambda = \tau$ and shows the probability that values on the *x*-axis would be met or exceeded without the short-term trigger firing. For example, for $m = 0$, the line shows the probability that $M \geq 0$ and the trigger does not fire. But M is always going to be at least 0, so the *y*-value at $m = 0$ is the probability that the trigger does not fire, which, when $\lambda = \tau$, should be approximately $1 - \alpha'$. Also note that the probability that there are 15 or more fatalities in a 3-year period and the trigger does not fire is about 20% when $\lambda = 1\tau$, and there is a 10% chance there would be 17 or more fatalities in a 3-year period. Thus, when the permitted average rate is $3\tau = 12$ in 3 years, the probability that there will be 17 or more fatalities and the short-term trigger does not fire is 10%. Similarly, if the original take rate is 3 times the permitted level ($\lambda = 3\tau$), there is a 10% chance that there would be 39 or more fatalities that pass unnoticed by the short-term trigger.

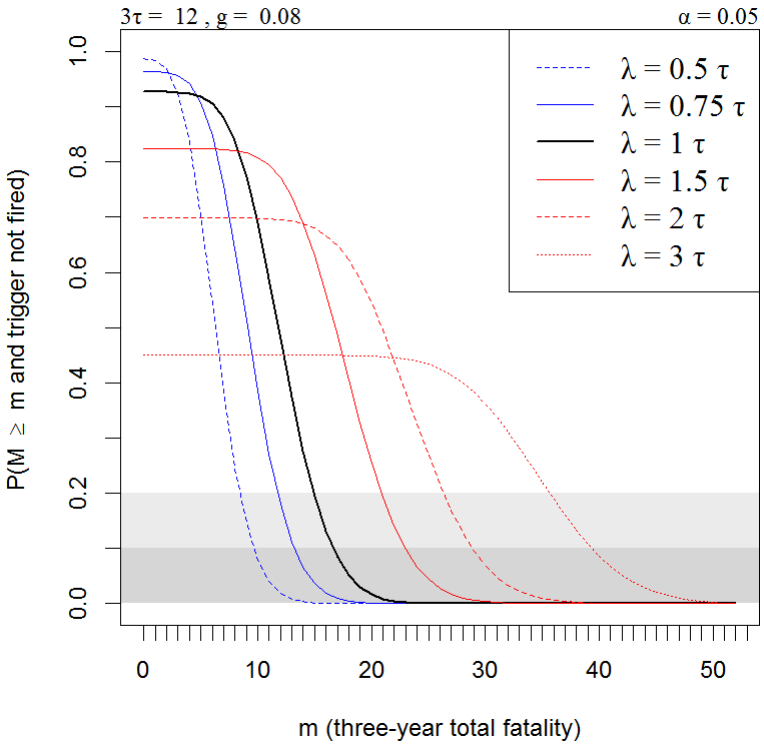

Figure 48. Potential short-term fatality breakout, with $\tau = 4$, $g = 0.08$, $\alpha' = 0.05$. See table 1 for explanation of terms used here.

Curves for all the familiar parameter combinations from previous sections are given below.

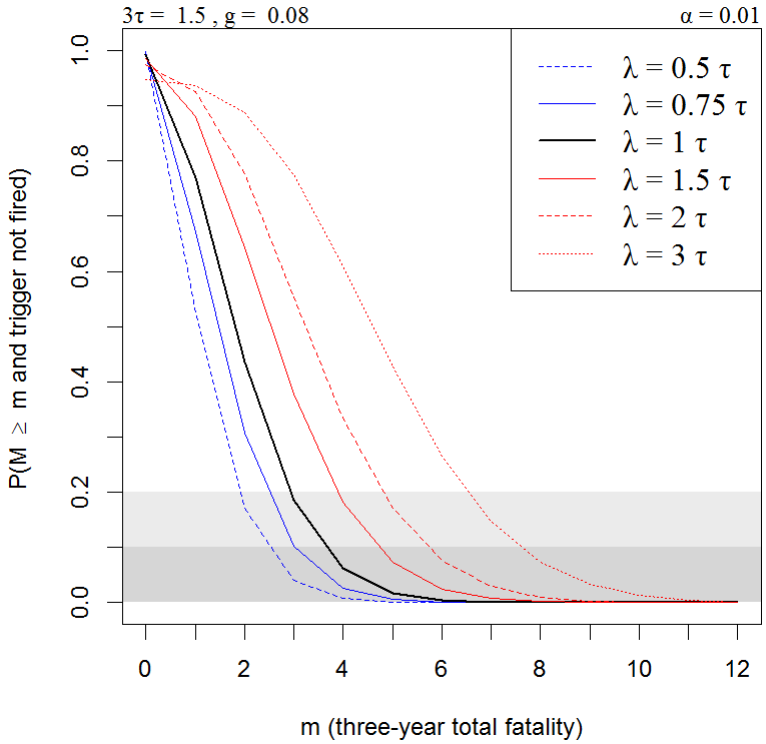

Figure 49. Potential short-term fatality breakout, with $\tau = 0.5$, $g = 0.08$, $\alpha' = 0.01$. See table 1 for explanation of terms used here.

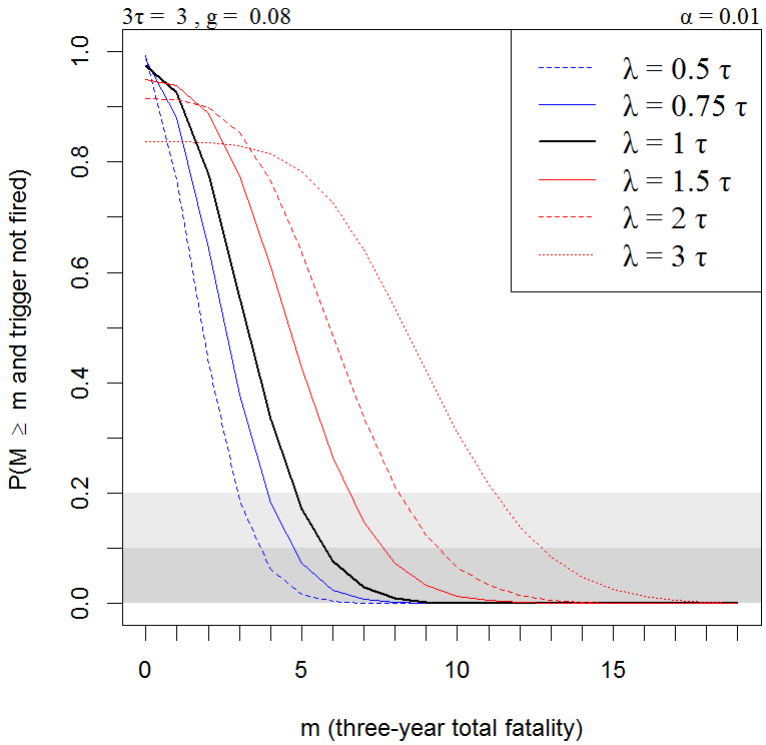

Figure 50. Potential short-term fatality breakout, with $\tau = 1$, $g = 0.08, \alpha' = 0.01$. See table 1 for explanation of terms used here.

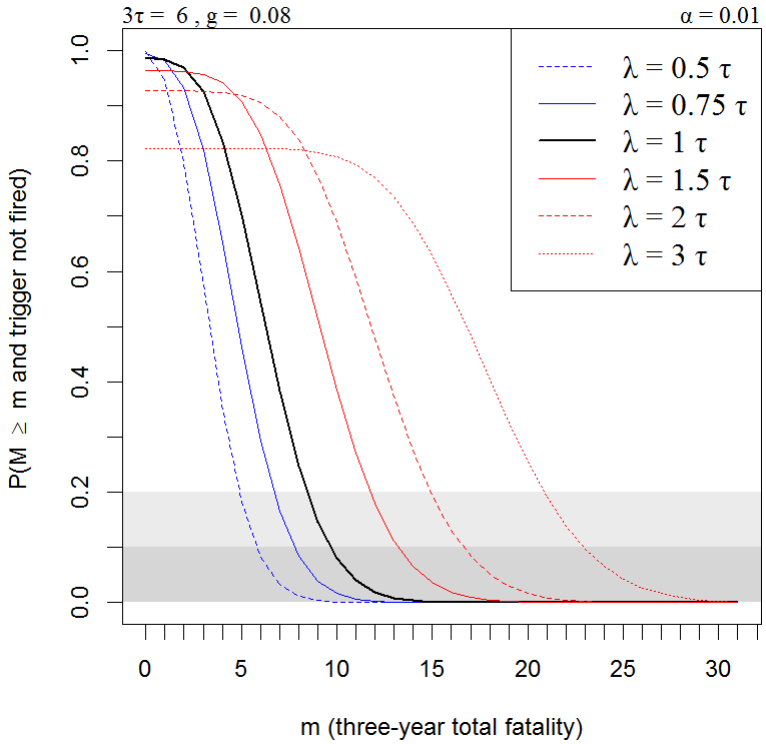

Figure 51. Potential short-term fatality breakout, with $\tau = 2$, $g = 0.08, \alpha' = 0.01$. See table 1 for explanation of terms used here.

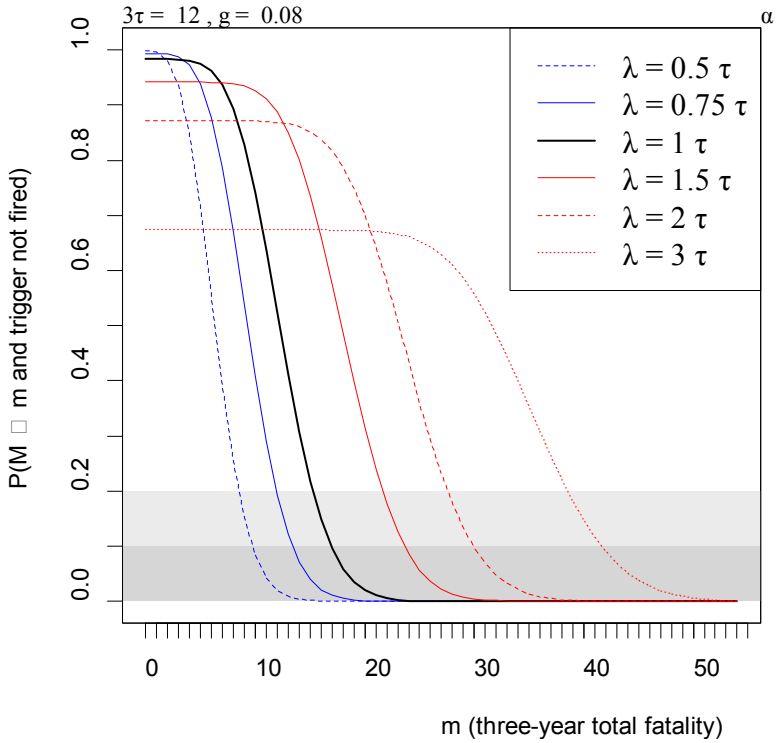

Figure 52. Potential short-term fatality breakout, with $\tau = 4$, $g = 0.08, \alpha' = 0.01$. See table 1 for explanation of terms used here.

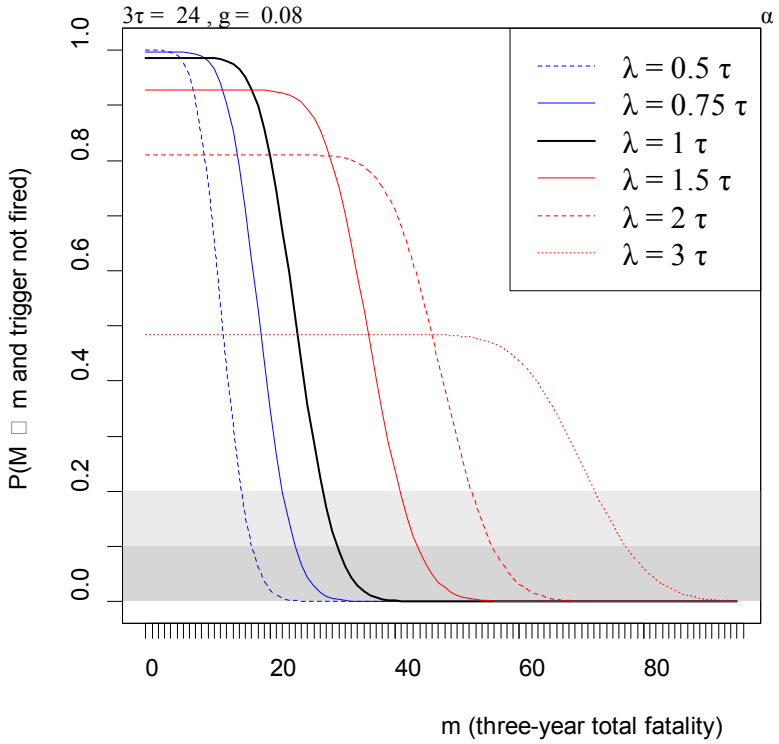

Figure 53. Potential short-term fatality breakout, with $\tau = 8$, $g = 0.08, \alpha' = 0.01$. See table 1 for explanation of terms used here.

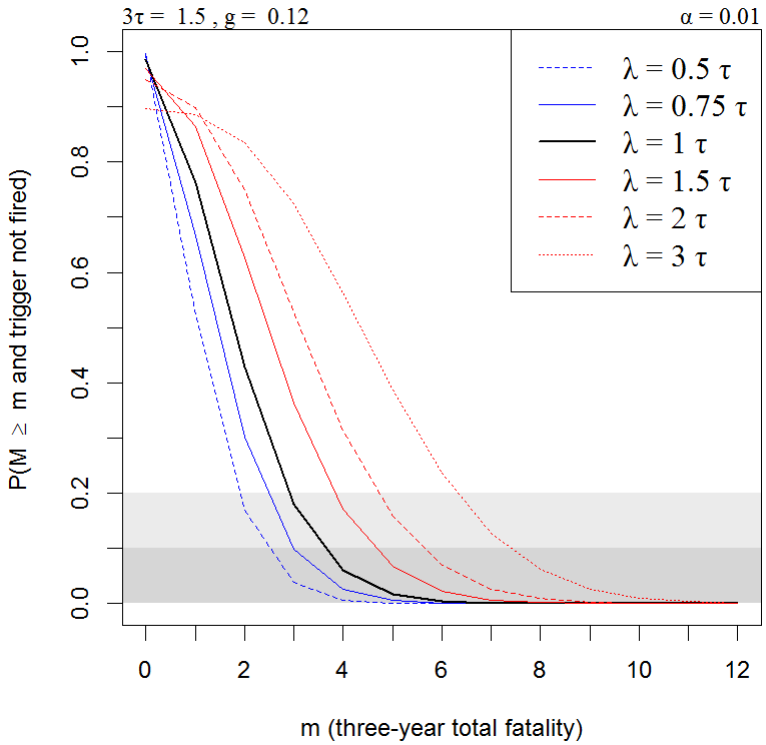

Figure 54. Potential short-term fatality breakout, with $= 0.5\ g = 0.12, \alpha' = 0.01$. See table 1 for explanation of terms used here.

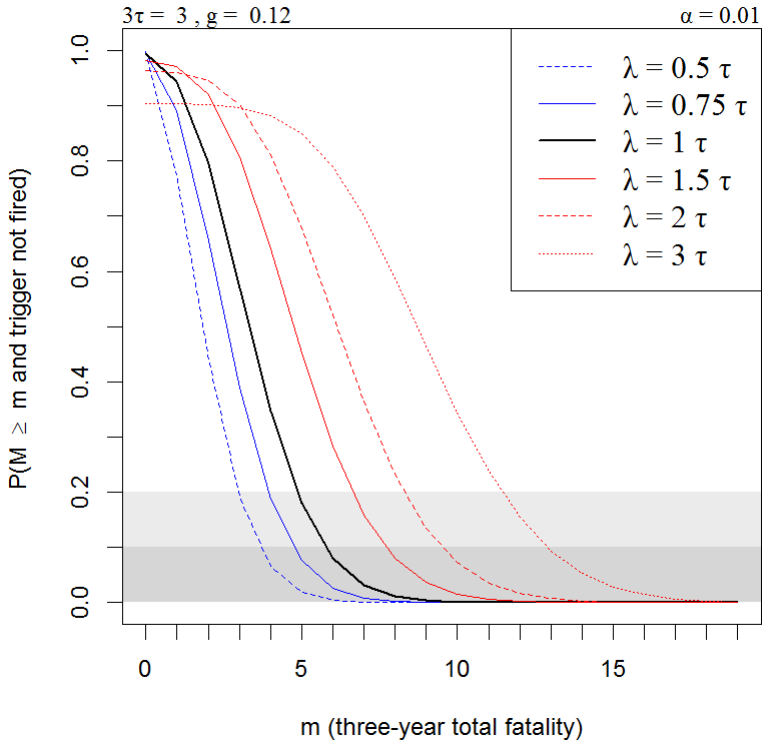

Figure 55. Potential short-term fatality breakout, with $\tau = 1, g = 0.12, \alpha' = 0.01$. See table 1 for explanation of terms used here.

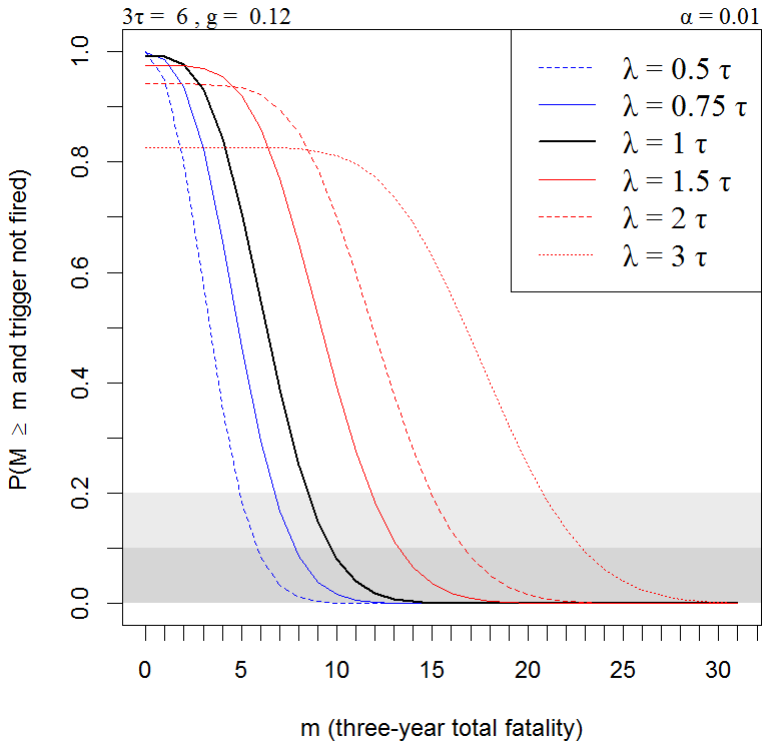

Figure 56. Potential short-term fatality breakout, with $\tau = 2$, $g = 0.12, \alpha' = 0.01$. See table 1 for explanation of terms used here.

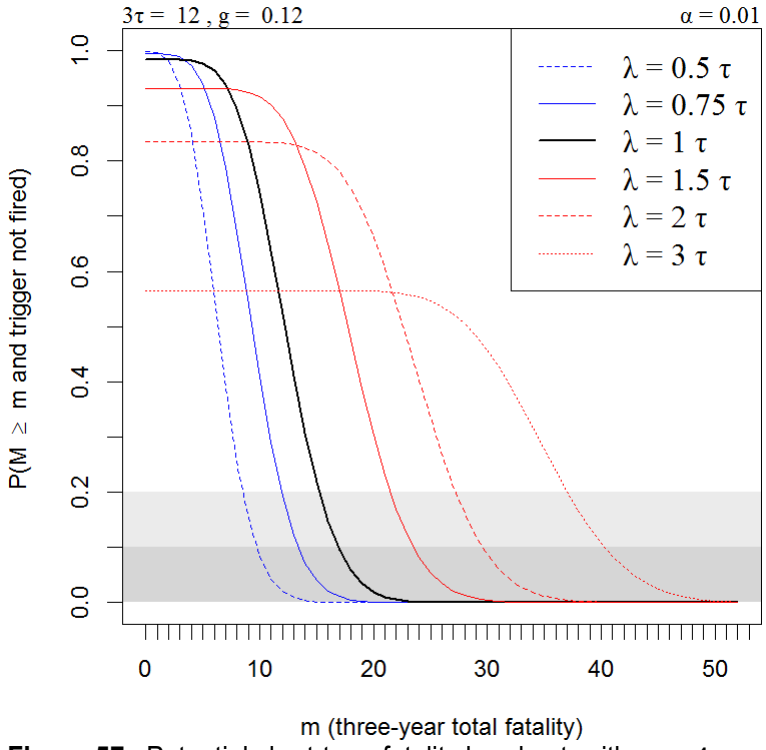

Figure 57. Potential short-term fatality breakout, with $\tau = 4$, $g = 0.12, \alpha' = 0.01$. See table 1 for explanation of terms used here.

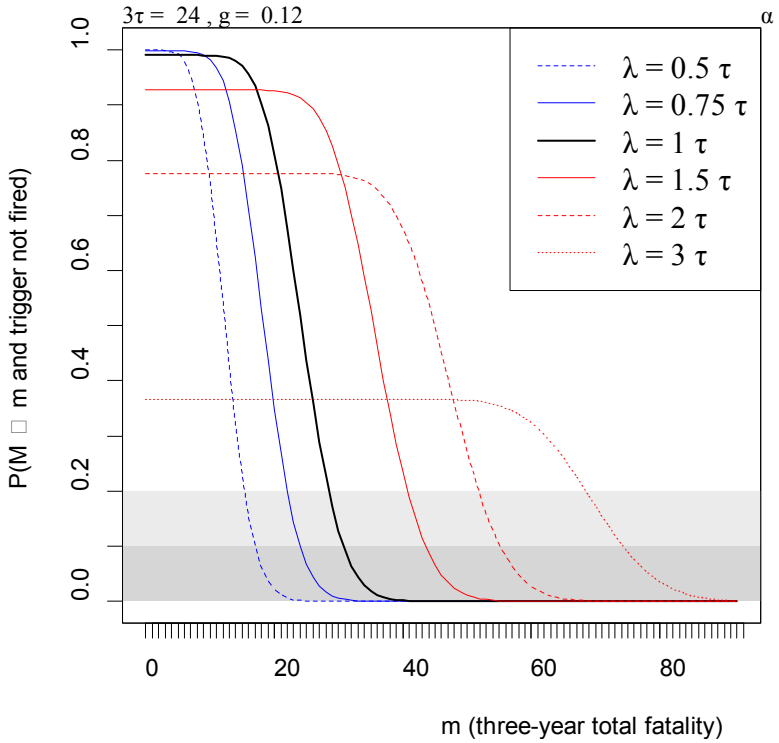

Figure 58. Potential short-term fatality breakout, with $\tau = 8, g = 0.12, \alpha' = 0.01$. See table 1 for explanation of terms used here.

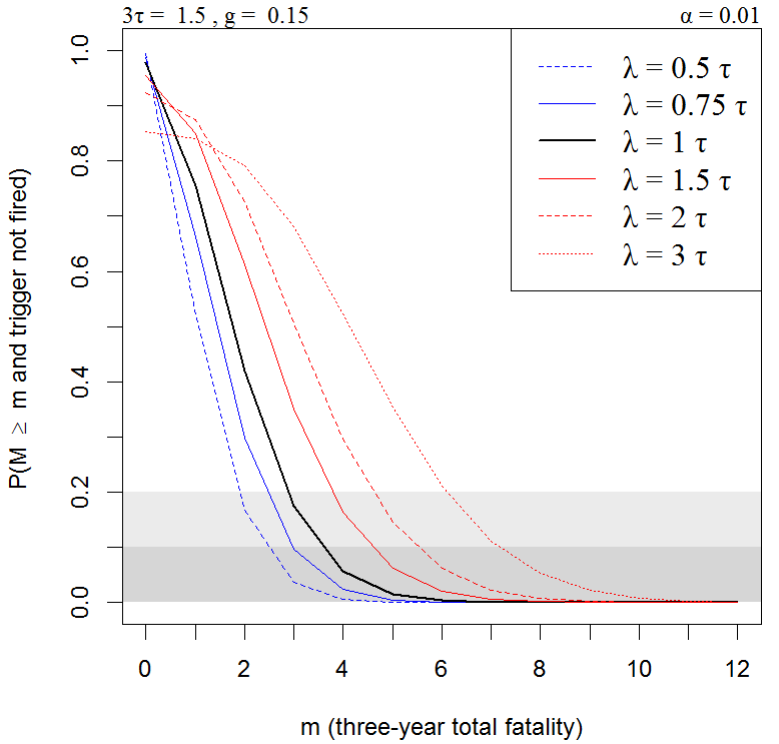

Figure 59. Potential short-term fatality breakout, with $\tau = 0.5, g = 0.15, \alpha' = 0.01$. See table 1 for explanation of terms used here.

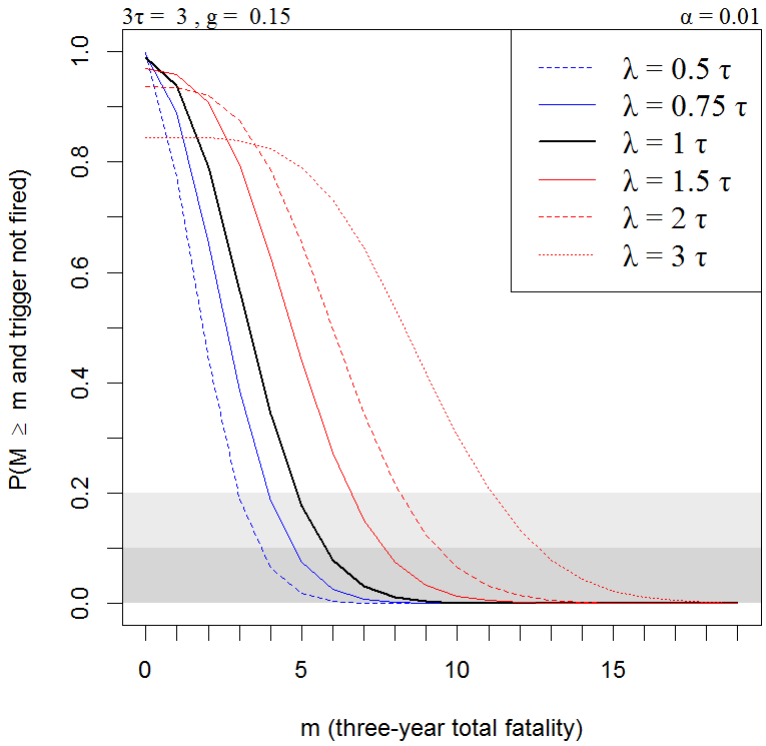

Figure 60. Potential short-term fatality breakout, with $\tau = 1, g = 0.15, \alpha' = 0.01$. See table 1 for explanation of terms used here.

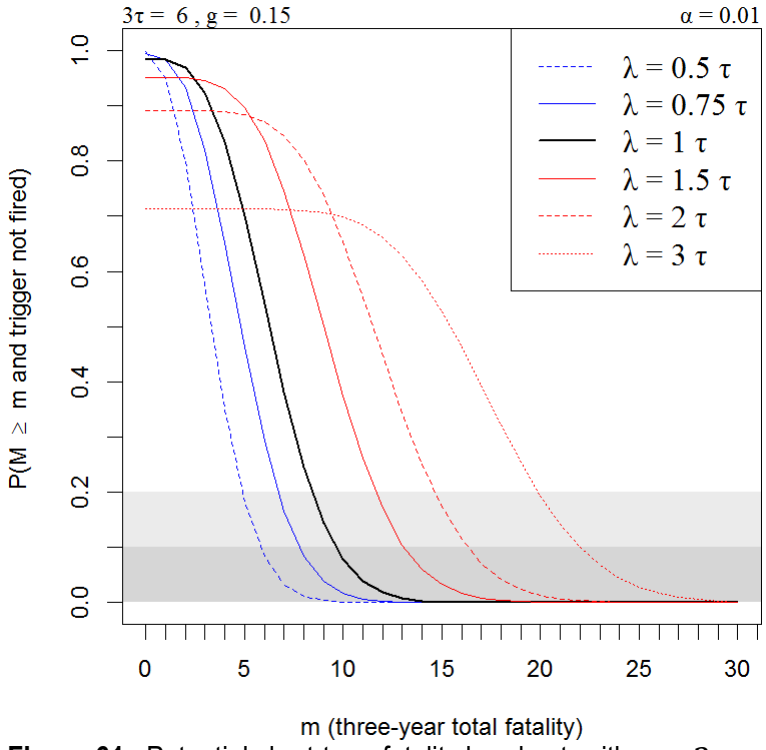

Figure 61. Potential short-term fatality breakout, with $\tau = 2, g = 0.15, \alpha' = 0.01$. See table 1 for explanation of terms used here.

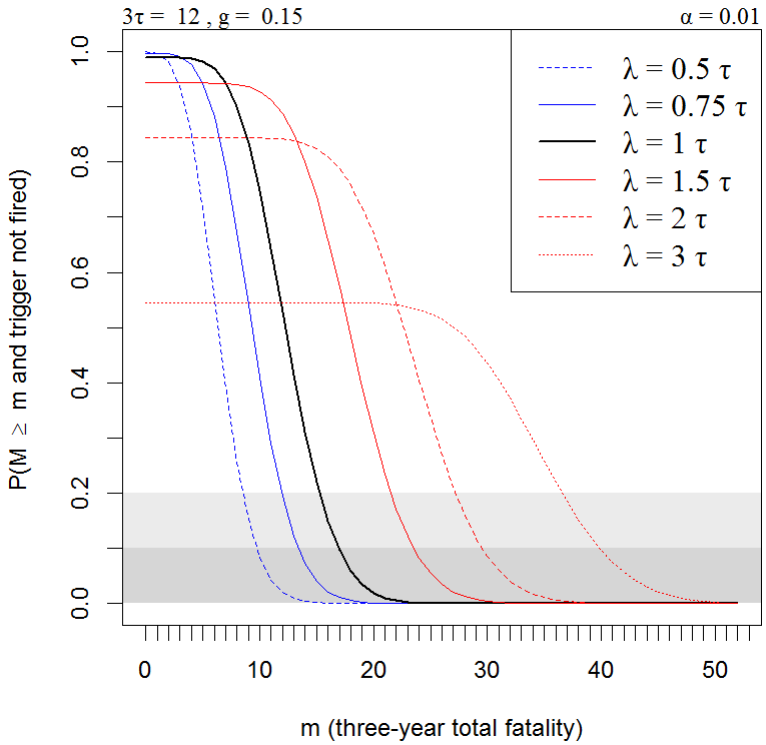

Figure 62. Potential short-term fatality breakout, with $\tau = 4$, $g = 0.15, \alpha' = 0.01$. See table 1 for explanation of terms used here.

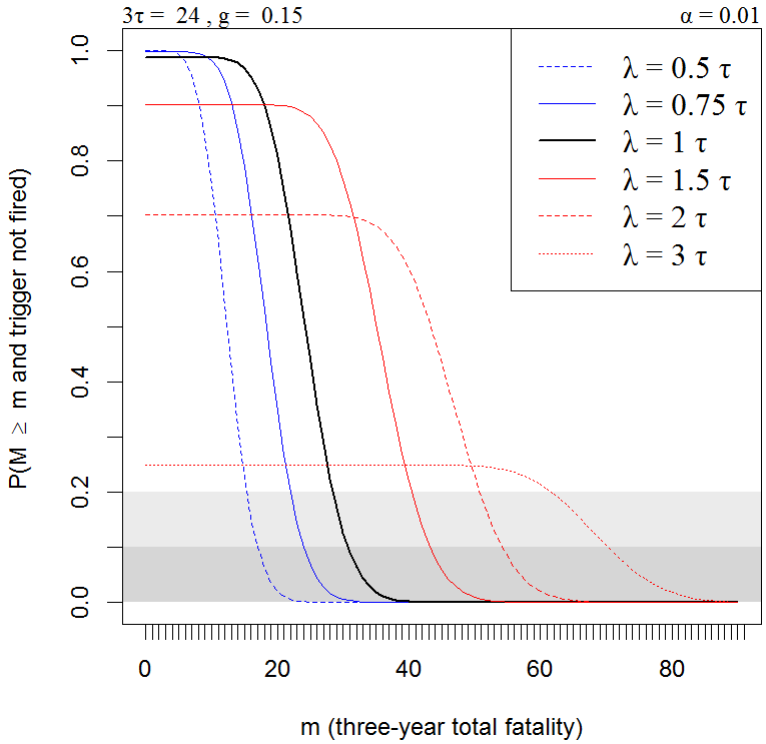

Figure 63. Potential short-term fatality breakout, with $\tau = 8$, $g = 0.15, \alpha' = 0.01$. See table 1 for explanation of terms used here.

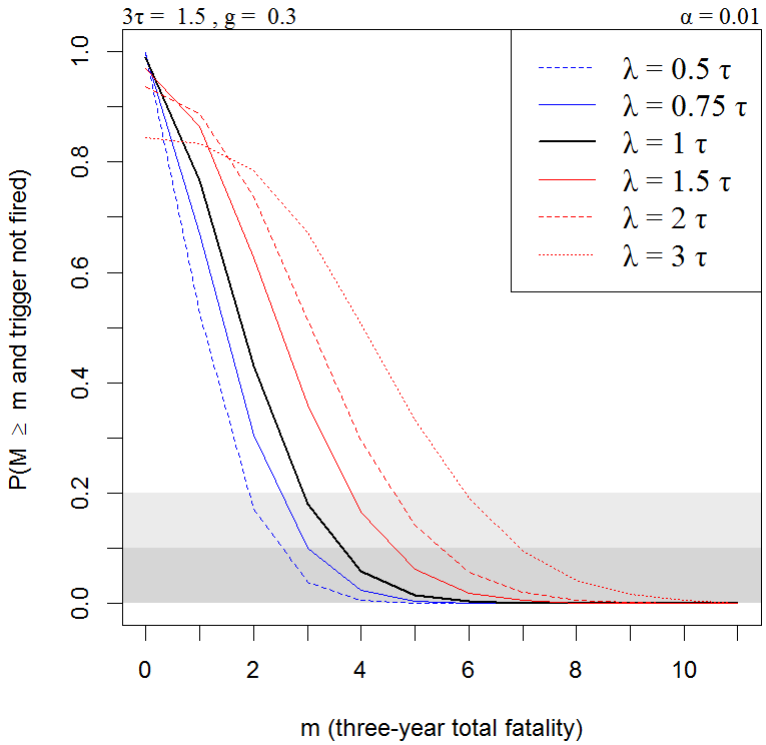

Figure 64. Potential short-term fatality breakout, with $\tau = 0.5$, $g = 0.3$, $\alpha' = 0.01$. See table 1 for explanation of terms used here.

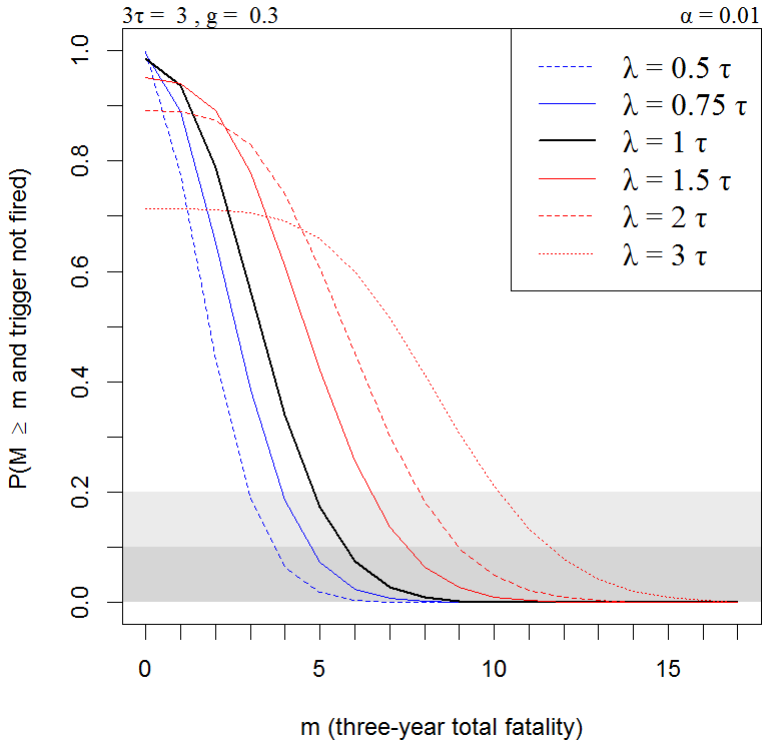

Figure 65. Potential short-term fatality breakout, with $\tau = 1$, $g = 0.3$, $\alpha' = 0.01$. See table 1 for explanation of terms used here.

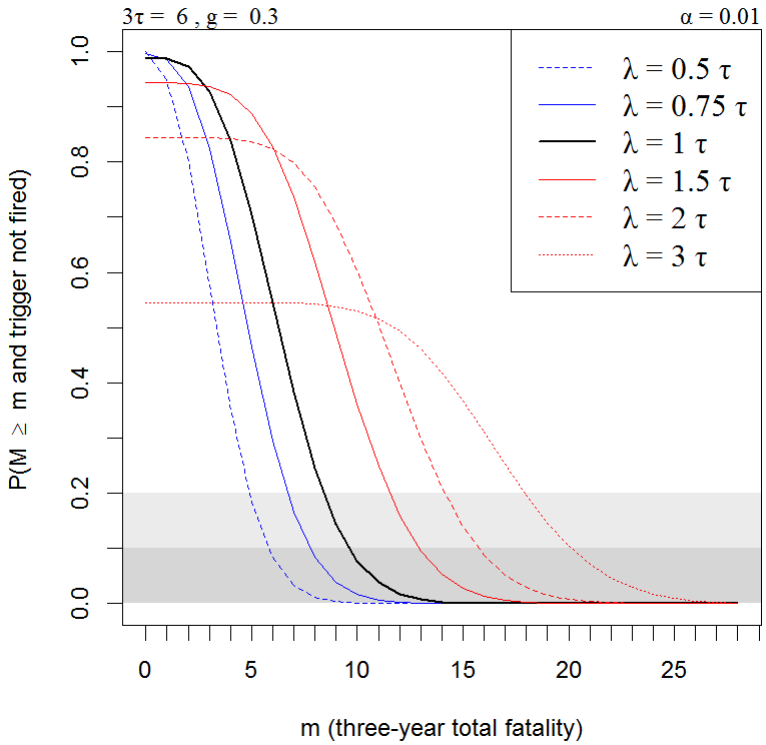

Figure 66. Potential short-term fatality breakout, with $\tau = 2$, $g = 0.3, \alpha' = 0.01$. See table 1 for explanation of terms used here.

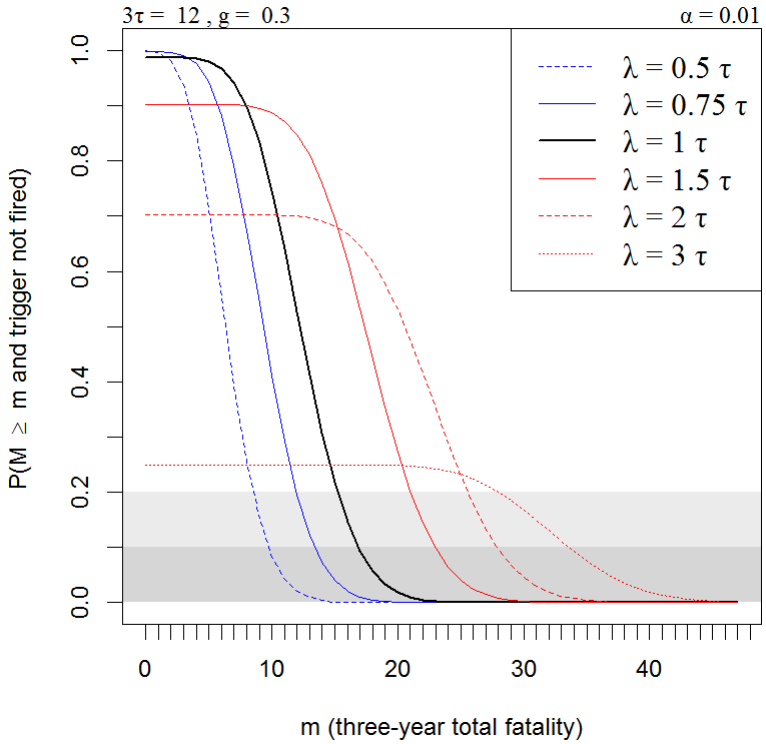

Figure 67. Potential short-term fatality breakout, with $\tau = 4$, $g = 0.3, \alpha' = 0.01$. See table 1 for explanation of terms used here.

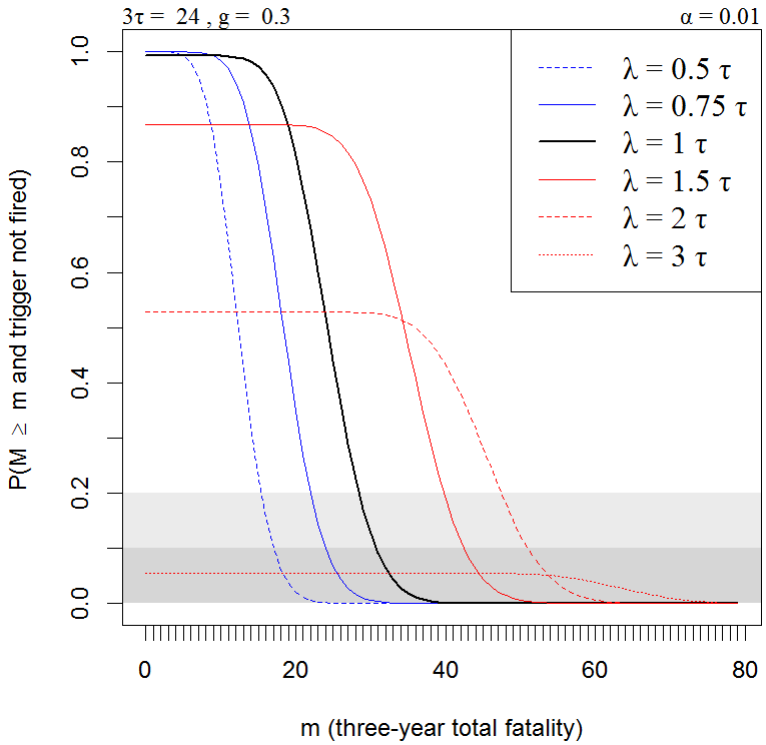

Figure 68. Potential short-term fatality breakout, with $= 8, g = 0.3, \alpha' = 0.01$. See table 1 for explanation of terms used here.

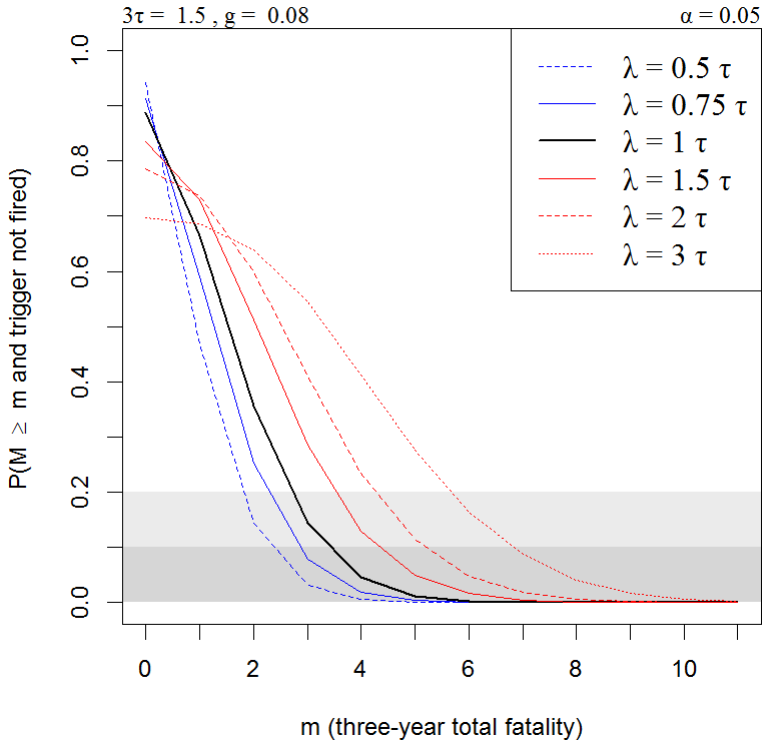

Figure 69. Potential short-term fatality breakout, with $= 0.5, g = 0.08, \alpha' = 0.05$. See table 1 for explanation of terms used here.

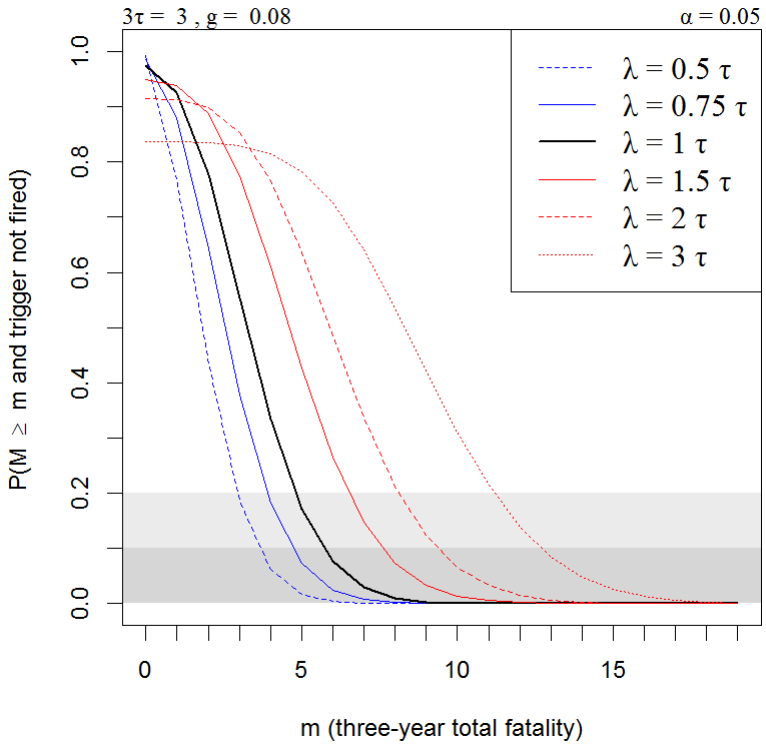

Figure 70. Potential short-term fatality breakout, with $= 1$, $g = 0.08, \alpha' = 0.05$. See table 1 for explanation of terms used here.

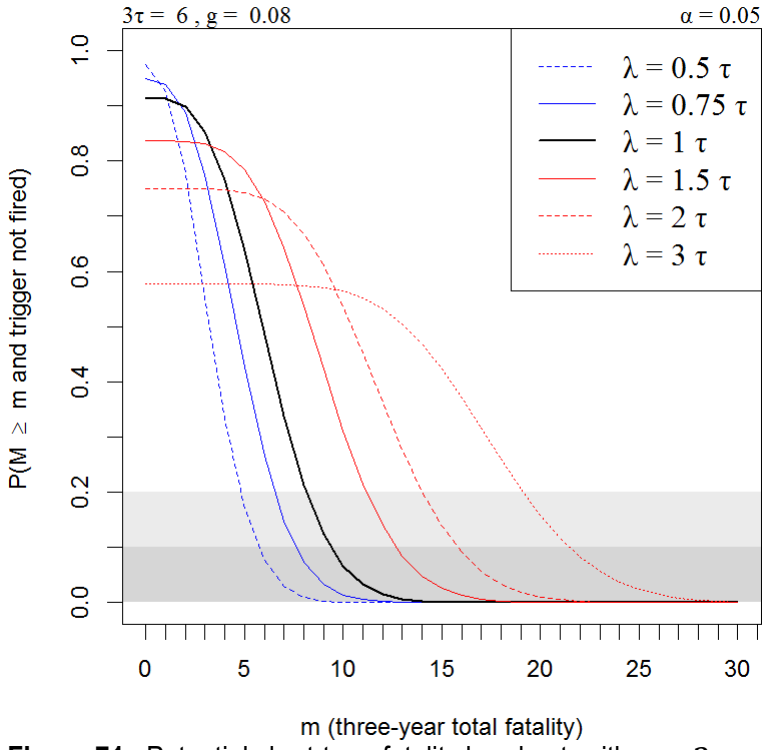

Figure 71. Potential short-term fatality breakout, with $\tau = 2$ $g = 0.08, \alpha' = 0.05$. See table 1 for explanation of terms used here.

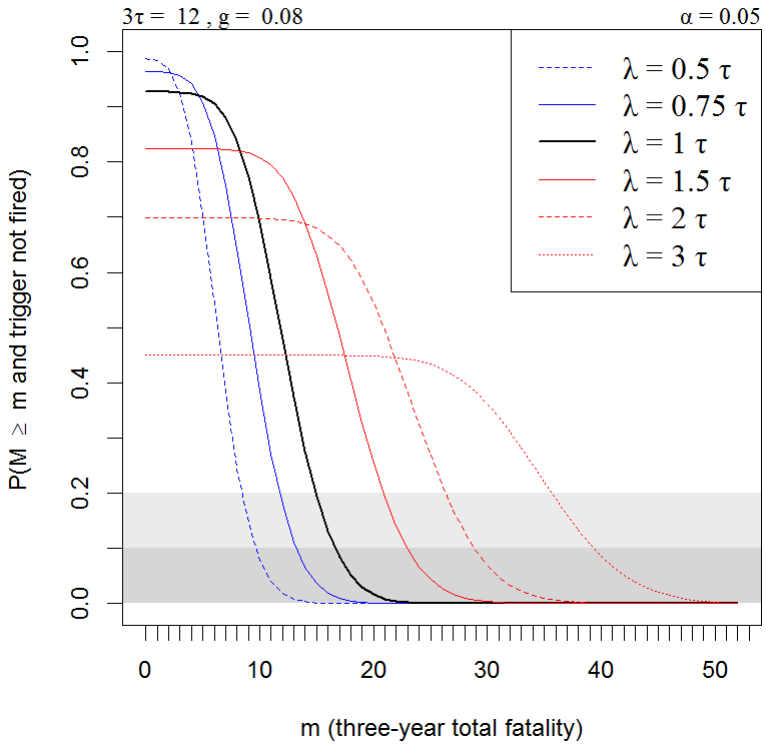

Figure 72. Potential short-term fatality breakout, with $\tau = 4$, $g = 0.08, \alpha' = 0.05$. See table 1 for explanation of terms used here.

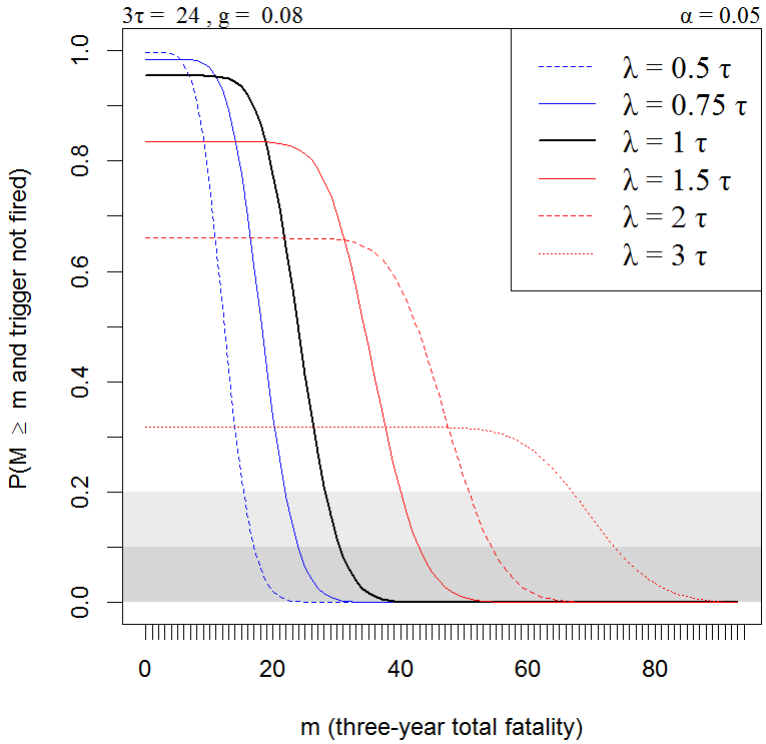

Figure 73. Potential short-term fatality breakout, with $= 8$, $g = 0.08, \alpha' = 0.05$. See table 1 for explanation of terms used here.

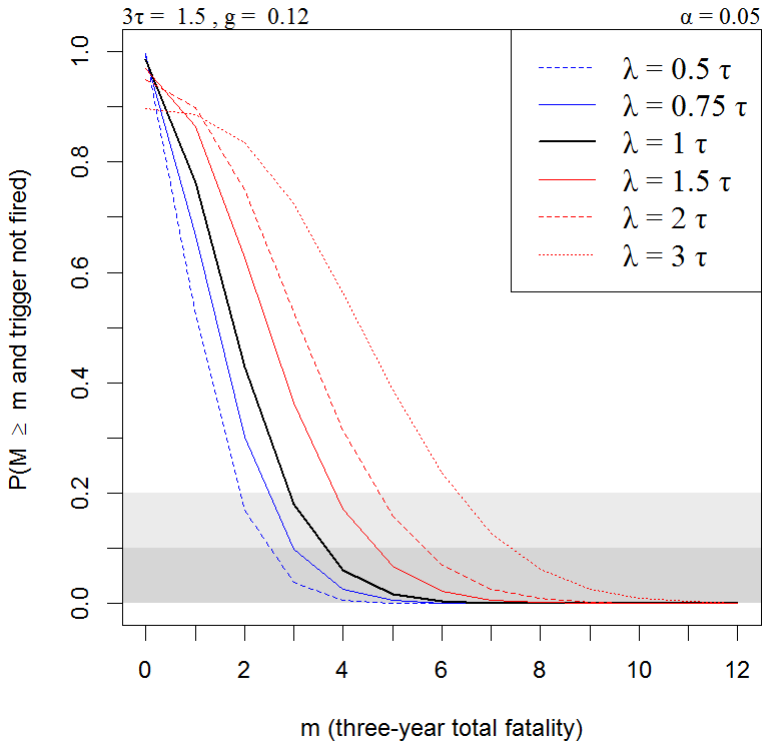

Figure 74. Potential short-term fatality breakout, with $= 0.5, g = 0.12, \alpha' = 0.05$. See table 1 for explanation of terms used here.

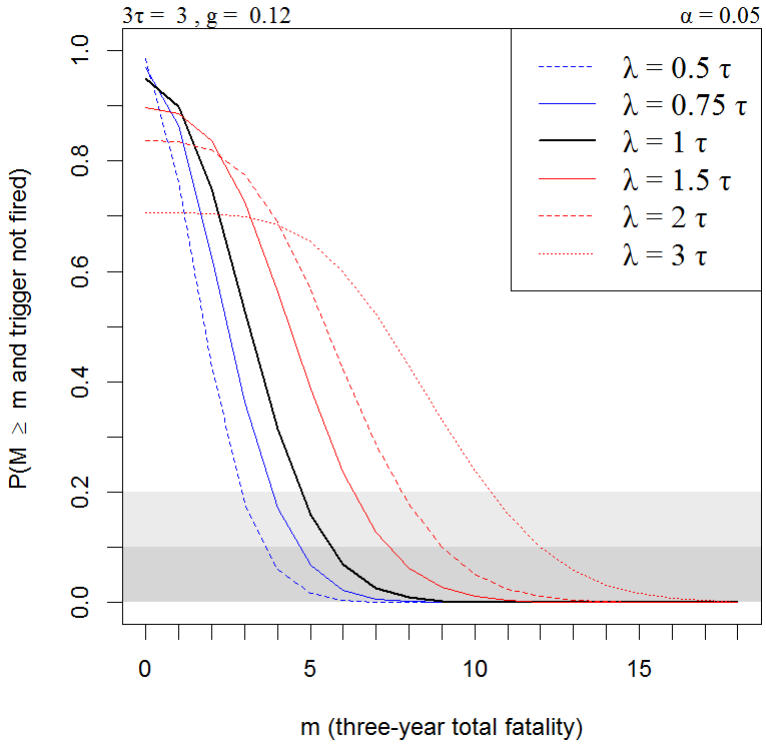

Figure 75. Potential short-term fatality breakout, with $= 1, g = 0.12, \alpha' = 0.05$. See table 1 for explanation of terms used here.

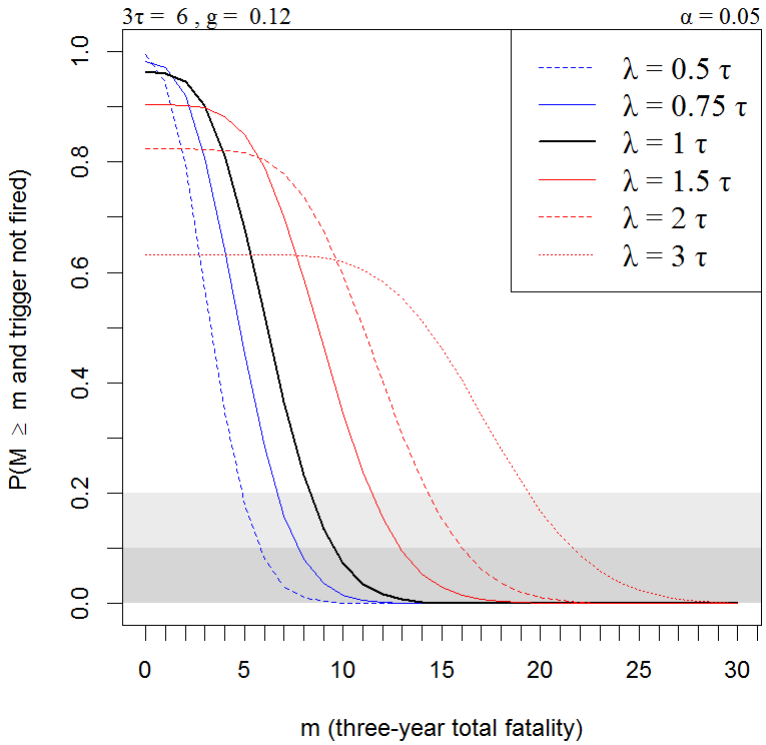

Figure 76. Potential short-term fatality breakout, with $= 2, g = 0.12, \alpha' = 0.05$. See table 1 for explanation of terms used here.

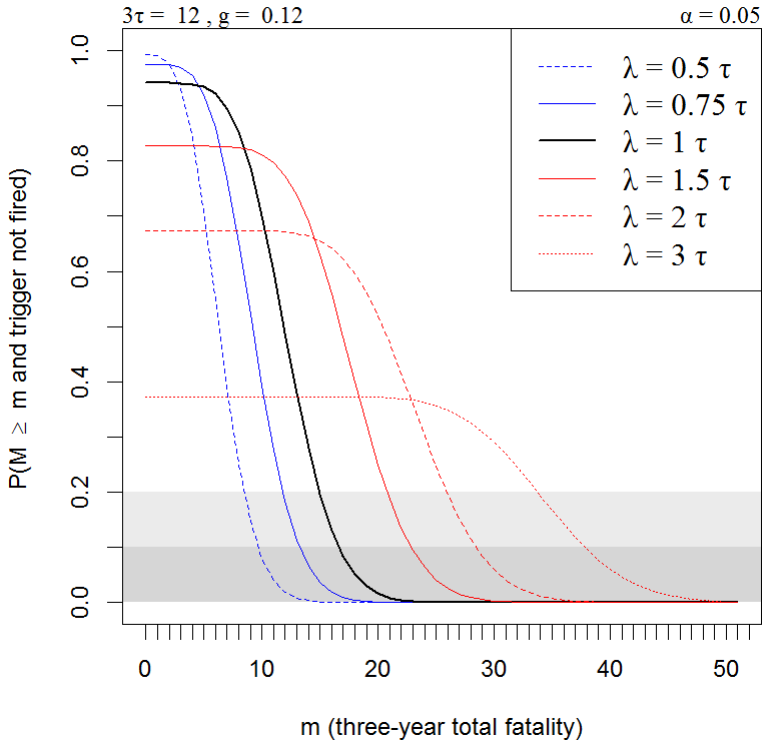

Figure 77. Potential short-term fatality breakout, with $\tau = 4, g = 0.12, \alpha' = 0.05$. See table 1 for explanation of terms used here.

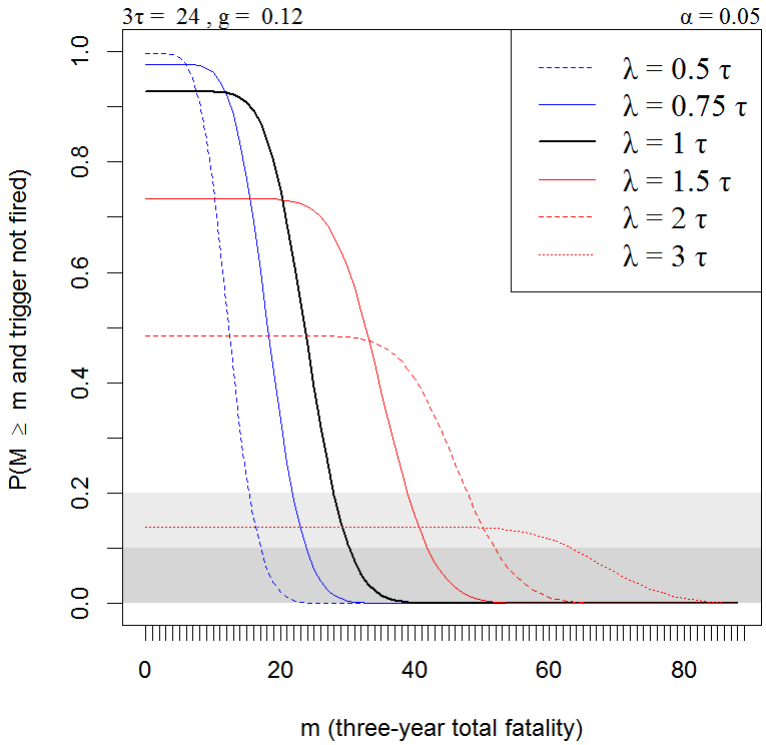

Figure 78. Potential short-term fatality breakout, with $= 8, g = 0.12, \alpha' = 0.05$. See table 1 for explanation of terms used here.

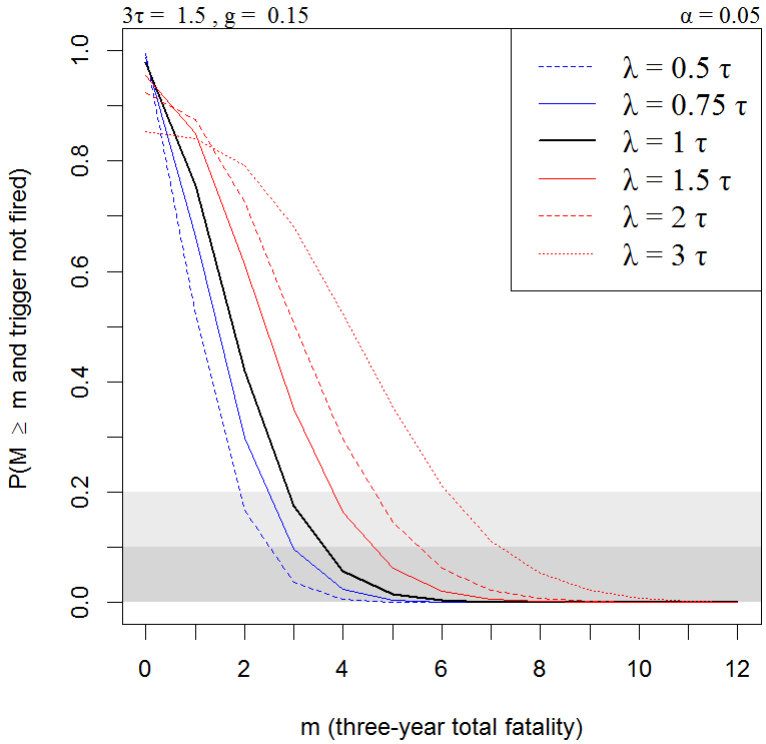

Figure 79. Potential short-term fatality breakout, with $= 0.5, g = 0.15, \alpha' = 0.05$. See table 1 for explanation of terms used here.

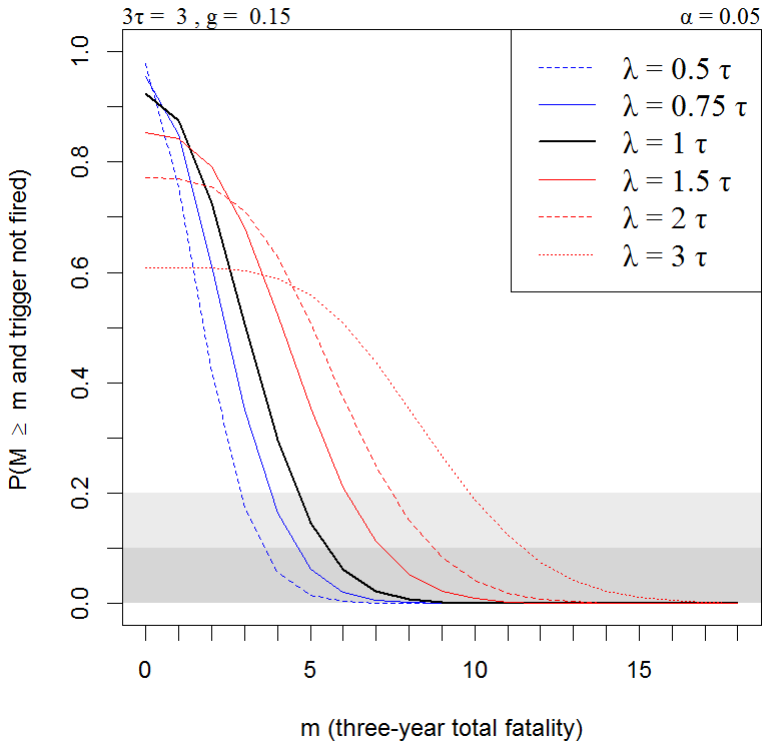

Figure 80. Potential short-term fatality breakout, with $= 1, g = 0.15, \alpha' = 0.05$. See table 1 for explanation of terms used here.

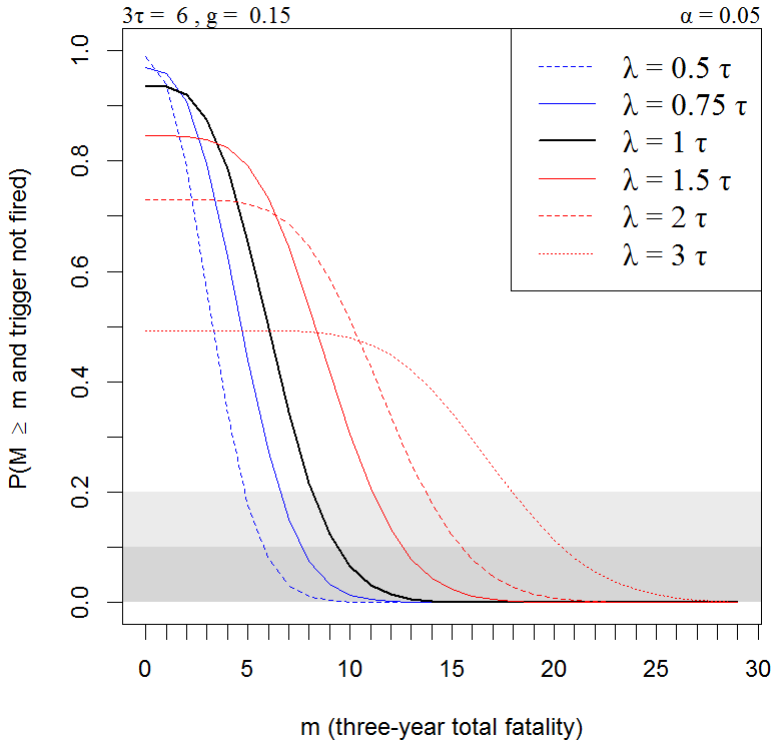

Figure 81. Potential short-term fatality breakout, with $= 2, g = 0.15, \alpha' = 0.05$. See table 1 for explanation of terms used here.

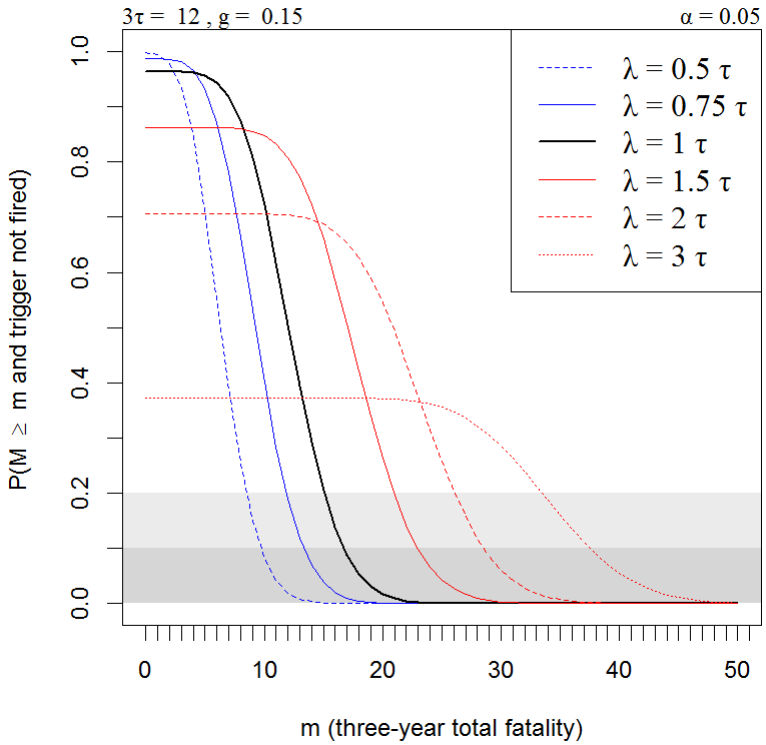

Figure 82. Potential short-term fatality breakout, with $= 4, g = 0.15, \alpha' = 0.05$. See table 1 for explanation of terms used here.

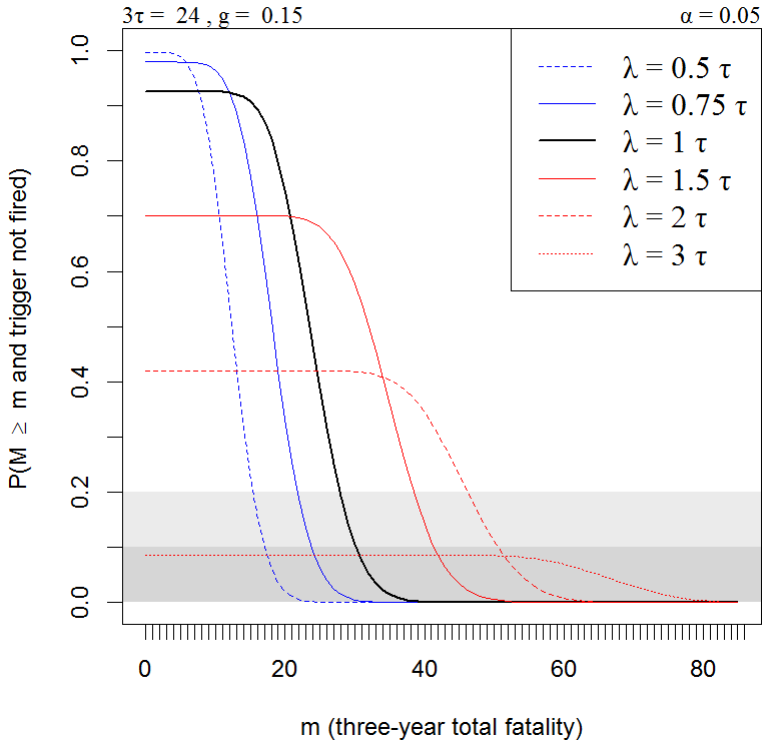

Figure 83. Potential short-term fatality breakout, with $= 8, g = 0.15, \alpha' = 0.05$. See table 1 for explanation of terms used here.

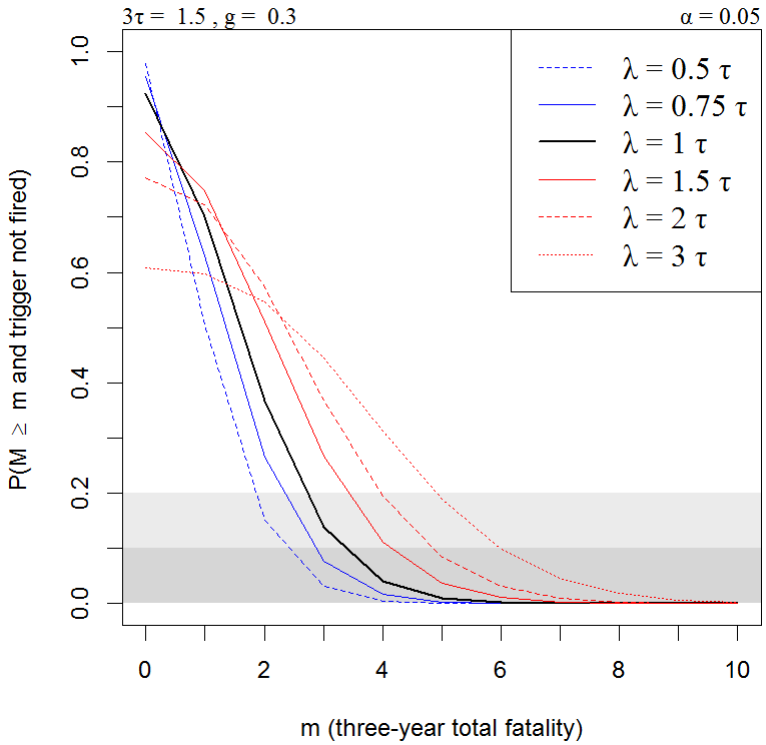

Figure 84. Potential short-term fatality breakout, with $= 0.5, g = 0.3, \alpha' = 0.05$. See table 1 for explanation of terms used here.

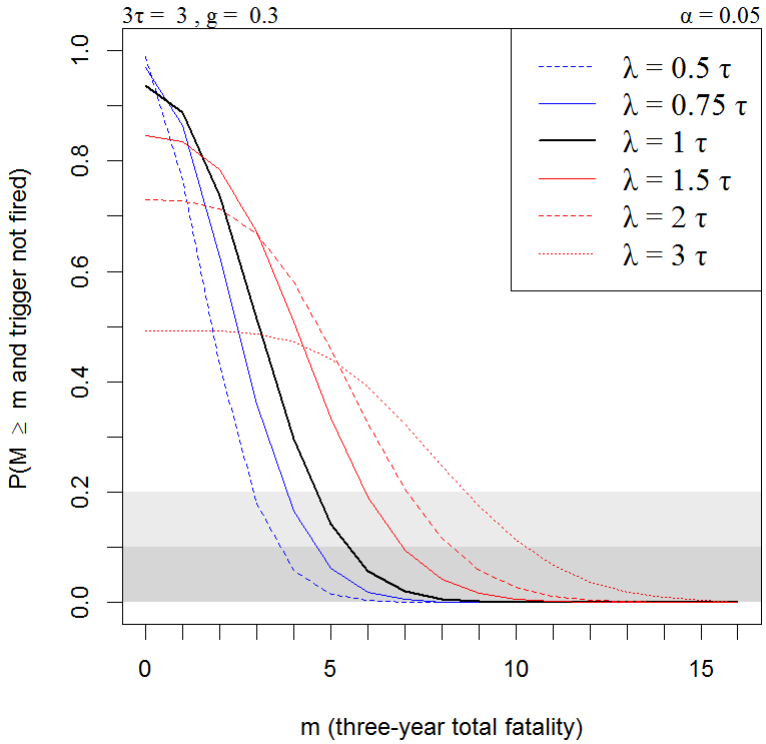

Figure 85. Potential short-term fatality breakout, with $= 1, g = 0.3, \alpha' = 0.05$. See table 1 for explanation of terms used here.

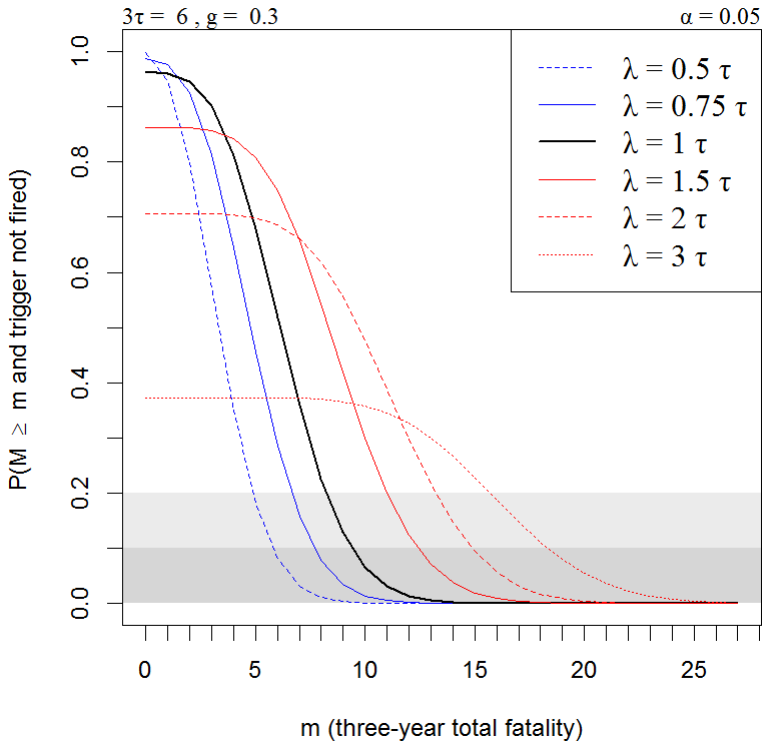

Figure 86. Potential short-term fatality breakout, with $= 2$, $g = 0.3, \alpha' = 0.05$. See table 1 for explanation of terms used here.

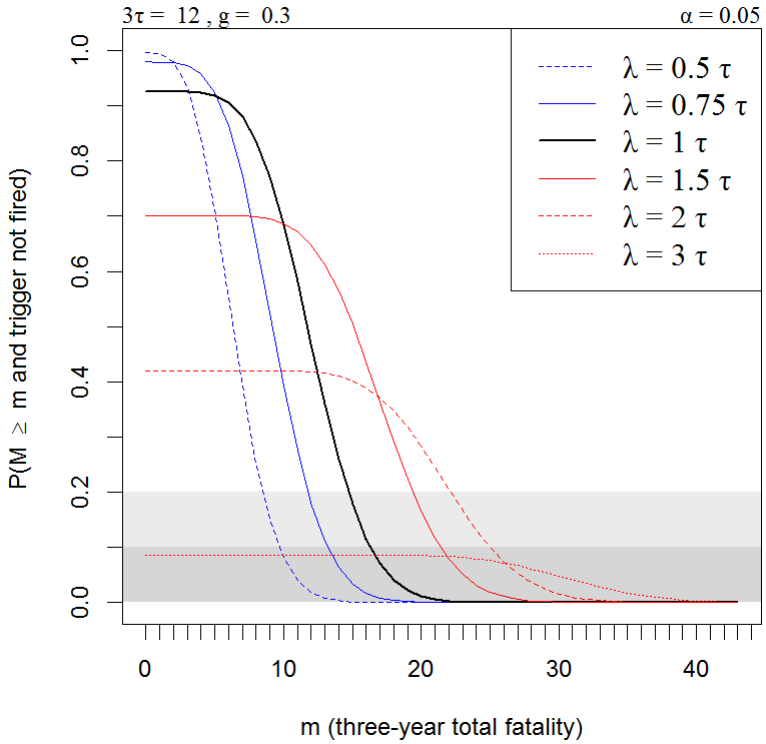

Figure 87. Potential short-term fatality breakout, with $= 4$, $g = 0.3, \alpha' = 0.05$. See table 1 for explanation of terms used here.

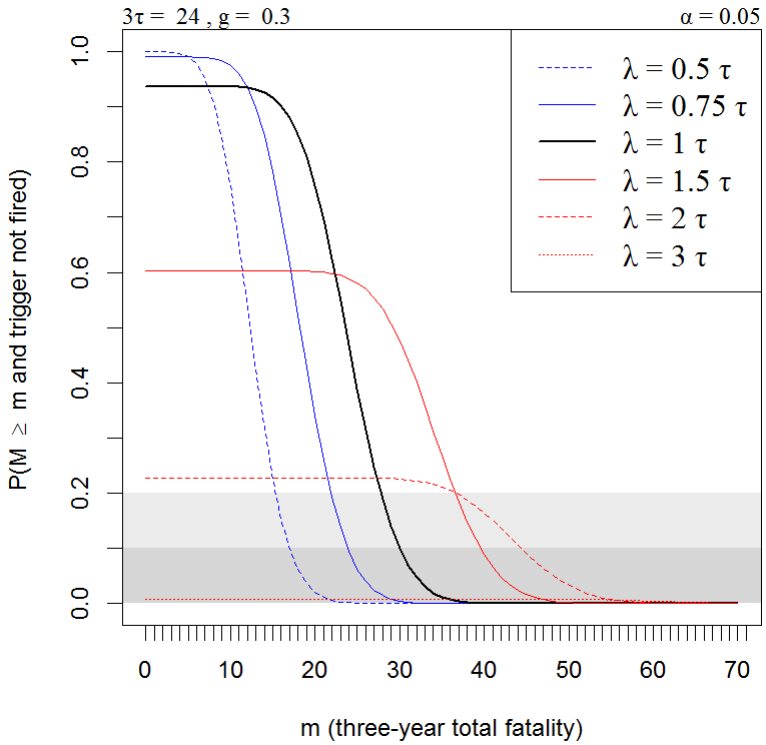

Figure 88. Potential short-term fatality breakout, with $= 8$, $g = 0.3, \alpha' = 0.05$. See table 1 for explanation of terms used here.

Reversion Trigger

The probability of reversion after i years for the given scenarios and four different choices of α (0.5, 0.2, 0.1, 0.05) are shown in figures 89–100.

In each figure, the distribution of the number of years of operation before reversion is displayed with the actual fatality rate (λ/yr) on the x-axis and the years until reversion on the y-axis for values of $\lambda = \frac{\tau\rho}{2}, \tau\rho, \frac{\tau(\rho+1)}{2}, \tau$. In the scenarios with $\lambda = \tau\rho$ (second major subdivision in each figure), reversion would (presumably) raise the average fatality rate to the permitted level of τ. Each figure represents a unique combination of α and ρ.

In the first scenario (fig. 89), the AMA under consideration has assumed effectiveness of $\rho = 0.5$, and the test is conducted with a significance level of $\alpha = 0.5$. When the fatality rate was one-half of what was required for reversion ($\lambda = \tau\rho/2$), reversion was common in the first few years of a project, but reversion occurred later for smaller values of τ and for lower detection probabilities. As expected, reversion was less common and tended to occur later for larger values of λ.

When $\lambda = \tau$ and reversion was not justified, reversion still occurred in a sizeable fraction of projects, especially with the smaller thresholds ($\tau < 2$). Decreasing the value of α made the reversion trigger less sensitive (figs. 90–92) resulting in later (and less frequent) reversion.

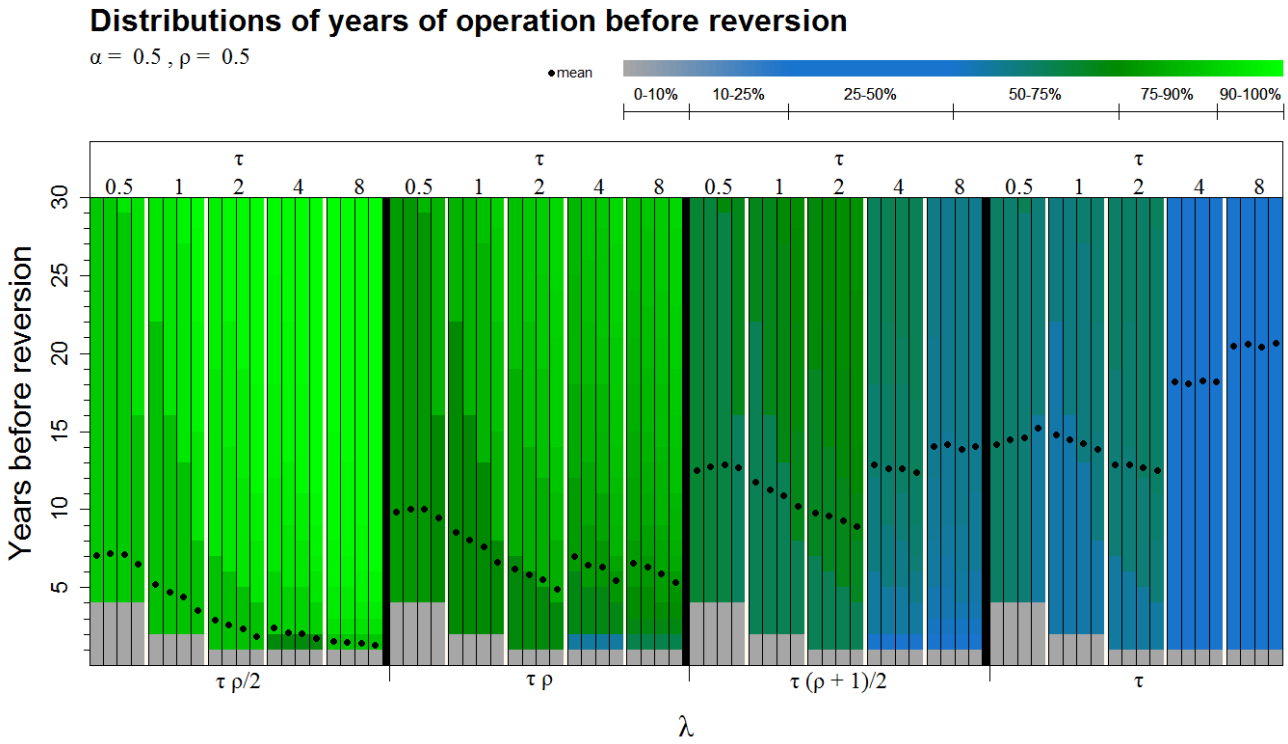

Figure 89. Distribution of years before reversion, with $\rho = 0.50, \alpha = 0.50$. The four bars within each subgroup represent $g = 0.08, 0.12, 0.15, 0.3$, respectively, in years 4–27. In all scenarios, $g = 0.3$ in years 1–3. See table 1 for explanation of terms used here.

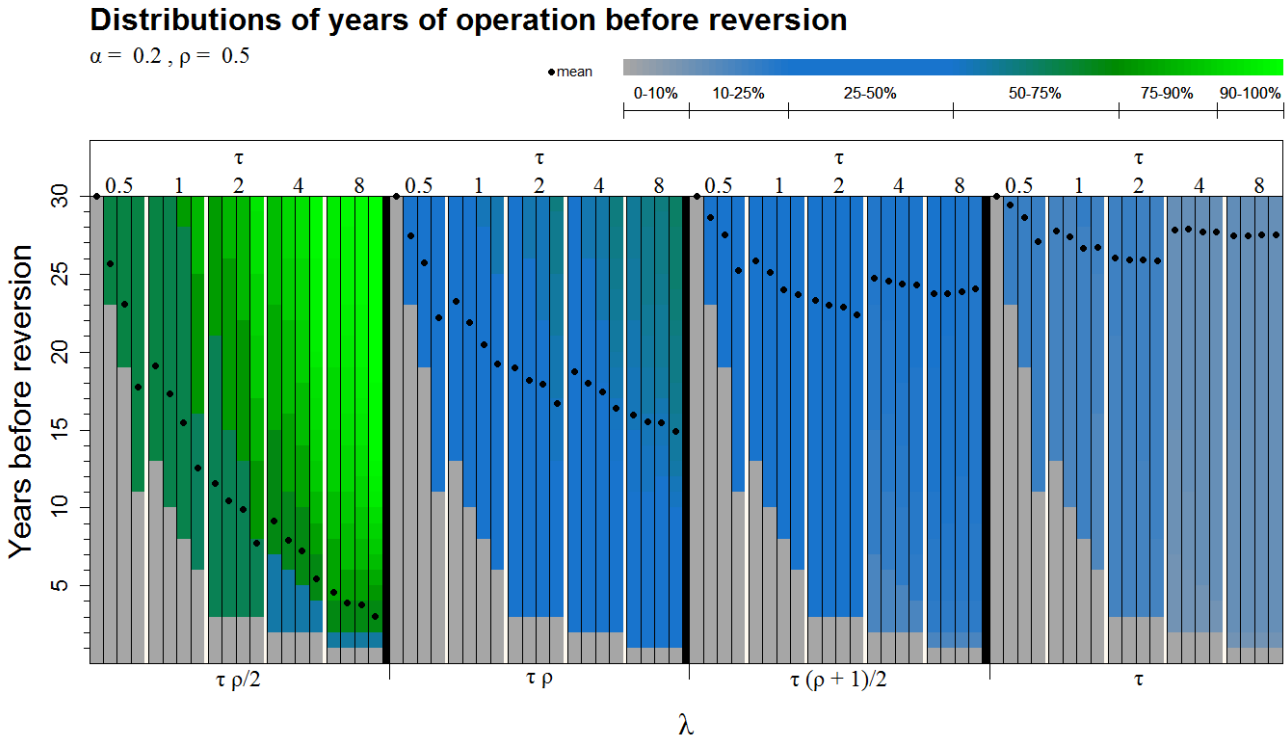

Figure 90. Distribution of years before reversion, with $\rho = 0.50, \alpha = 0.20$. The four bars within each subgroup represent $g = 0.08, 0.12, 0.15, 0.3$, respectively, in years 4–27. In all scenarios, $g = 0.3$ in years 1–3. See table 1 for explanation of terms used here.

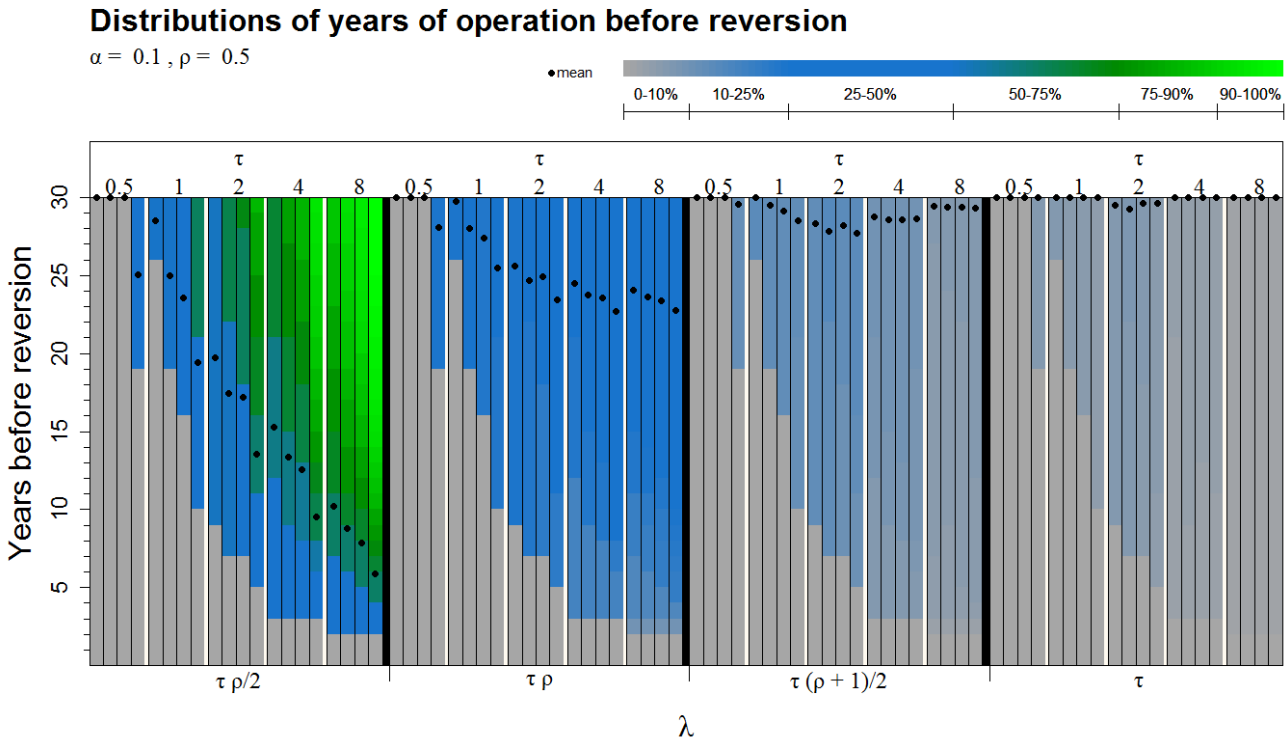

Figure 91. Distribution of years before reversion, with $\rho = 0.50, \alpha = 0.10$.The four bars within each subgroup represent $g = 0.08, 0.12, 0.15, 0.3$, respectively, in years 4–27. In all scenarios, $g = 0.3$ in years 1–3. See table 1 for explanation of terms used here.

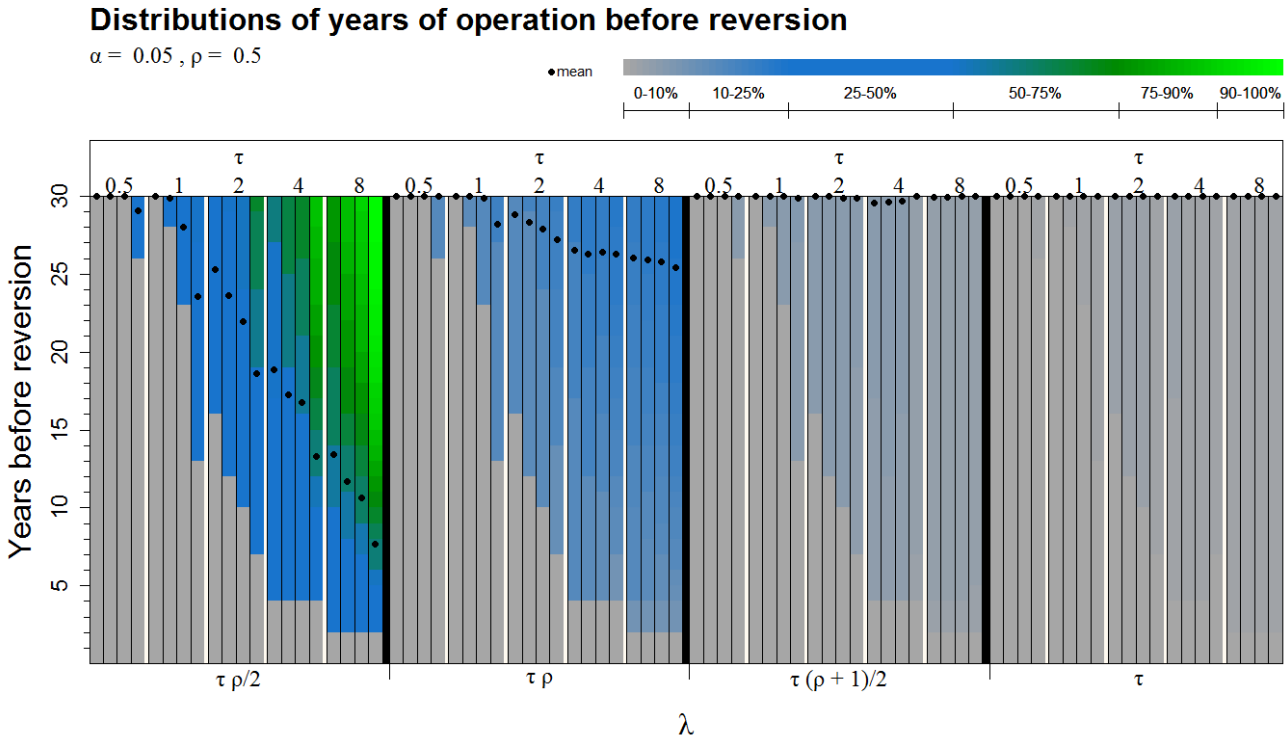

Figure 92. Distribution of years before reversion, with $\rho = 0.50, \alpha = 0.05$. The four bars within each subgroup represent $g = 0.08, 0.12, 0.15, 0.3$, respectively, in years 4–27. In all scenarios, $g = 0.3$ in years 1–3. See table 1 for explanation of terms used here.

As the effectiveness of the AMA to be reversed decreased (that is, ρ increased), reversion became increasingly likely and occurred earlier (figs. 93–100).

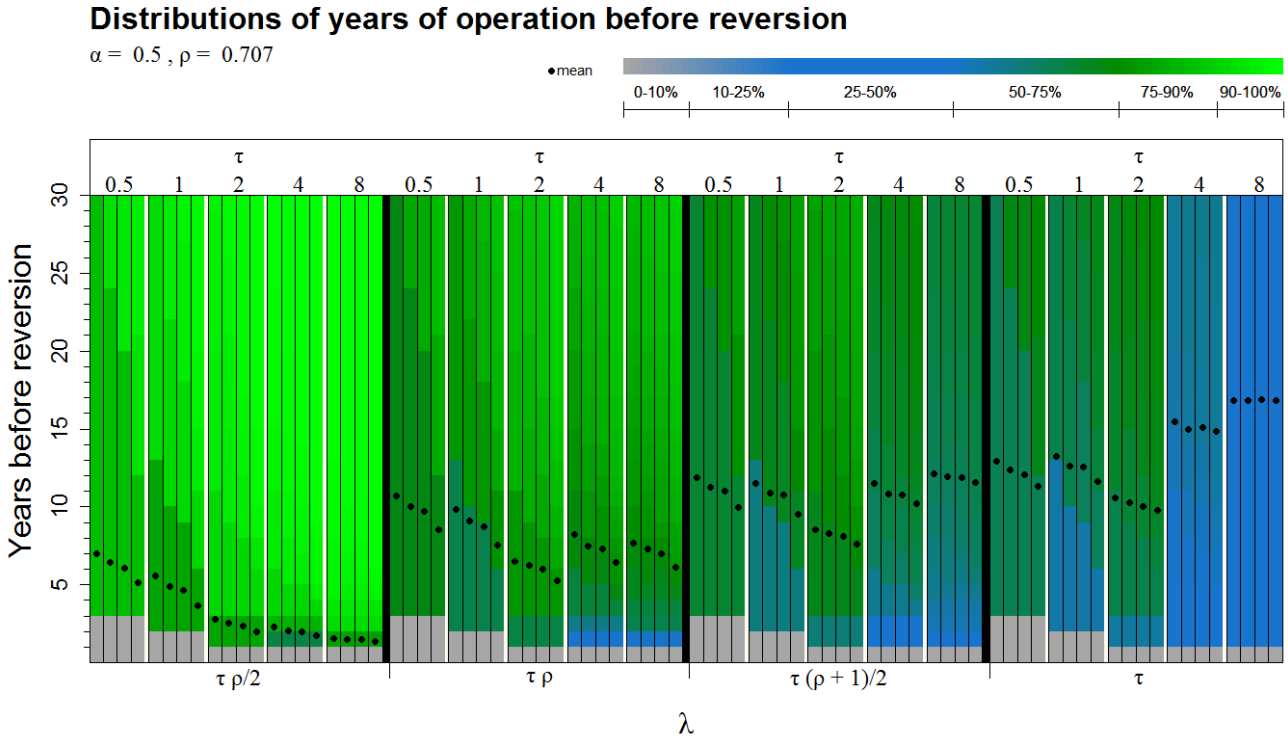

Figure 93. Distribution of years before reversion, with $\rho = 0.71, \alpha = 0.5$. The four bars within each subgroup represent $g = 0.08, 0.12, 0.15, 0.3$, respectively, in years 4–27. In all scenarios, $g = 0.3$ in years 1–3. See table 1 for explanation of terms used here.

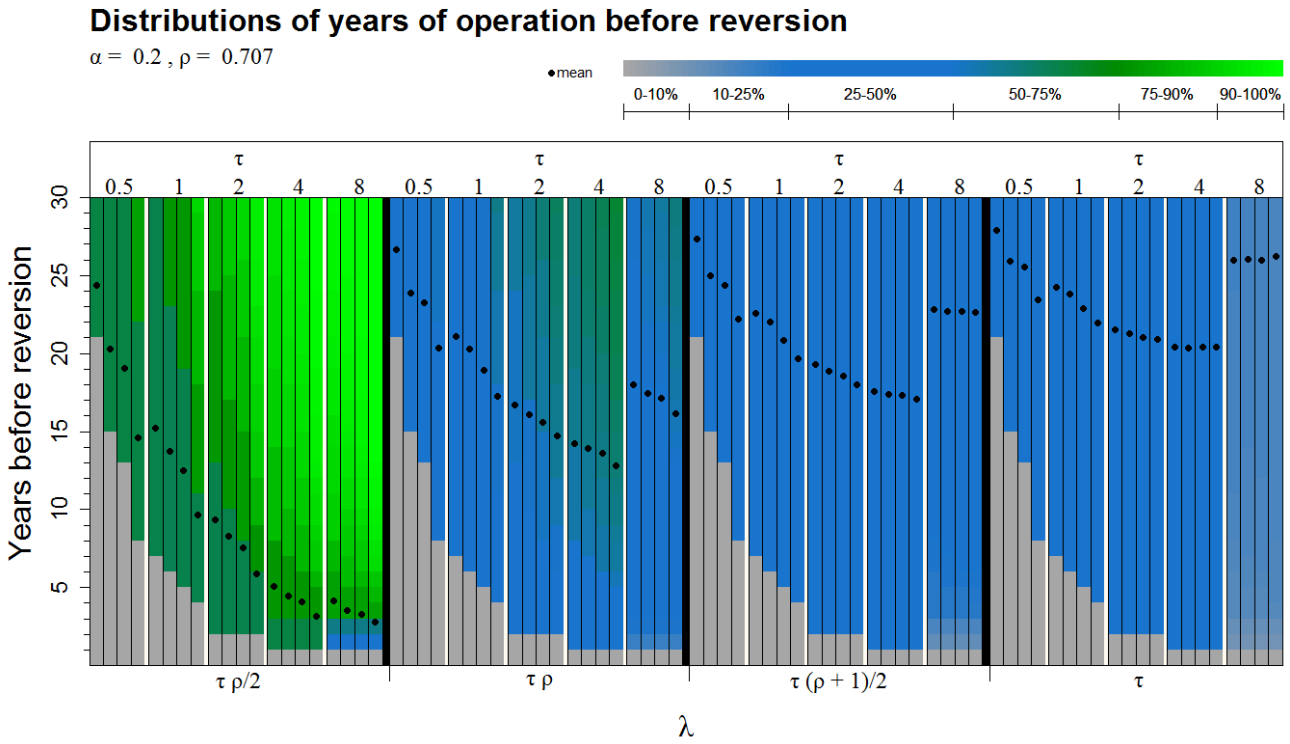

Figure 94. Distribution of years before reversion, with $\rho = 0.71, \alpha = 0.2$.The four bars within each subgroup represent $g = 0.08, 0.12, 0.15, 0.3$, respectively, in years 4–27. In all scenarios, $g = 0.3$ in years 1–3. See table 1 for explanation of terms used here.

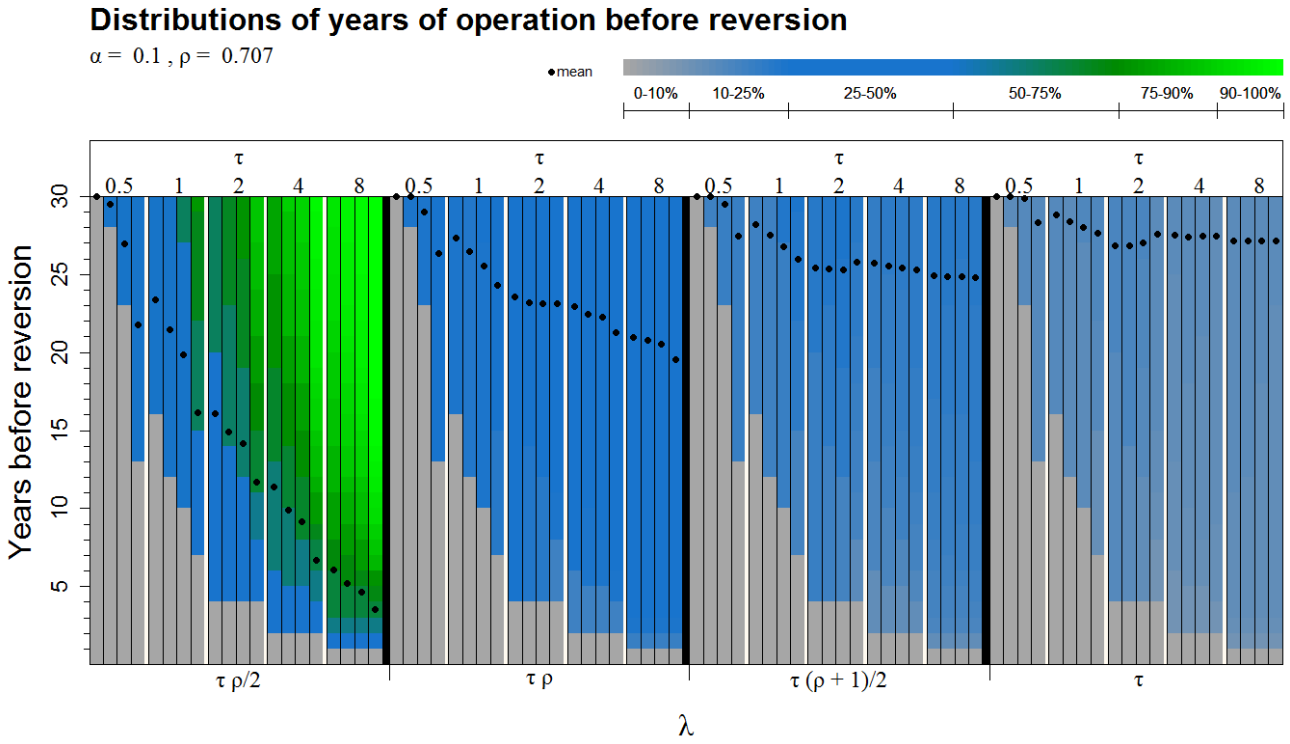

Figure 95. Distribution of years before reversion, with $\rho = 0.71, \alpha = 0.1$. The four bars within each subgroup represent $g = 0.08, 0.12, 0.15, 0.3$, respectively, in years 4–27. In all scenarios, $g = 0.3$ in years 1–3. See table 1 for explanation of terms used here.

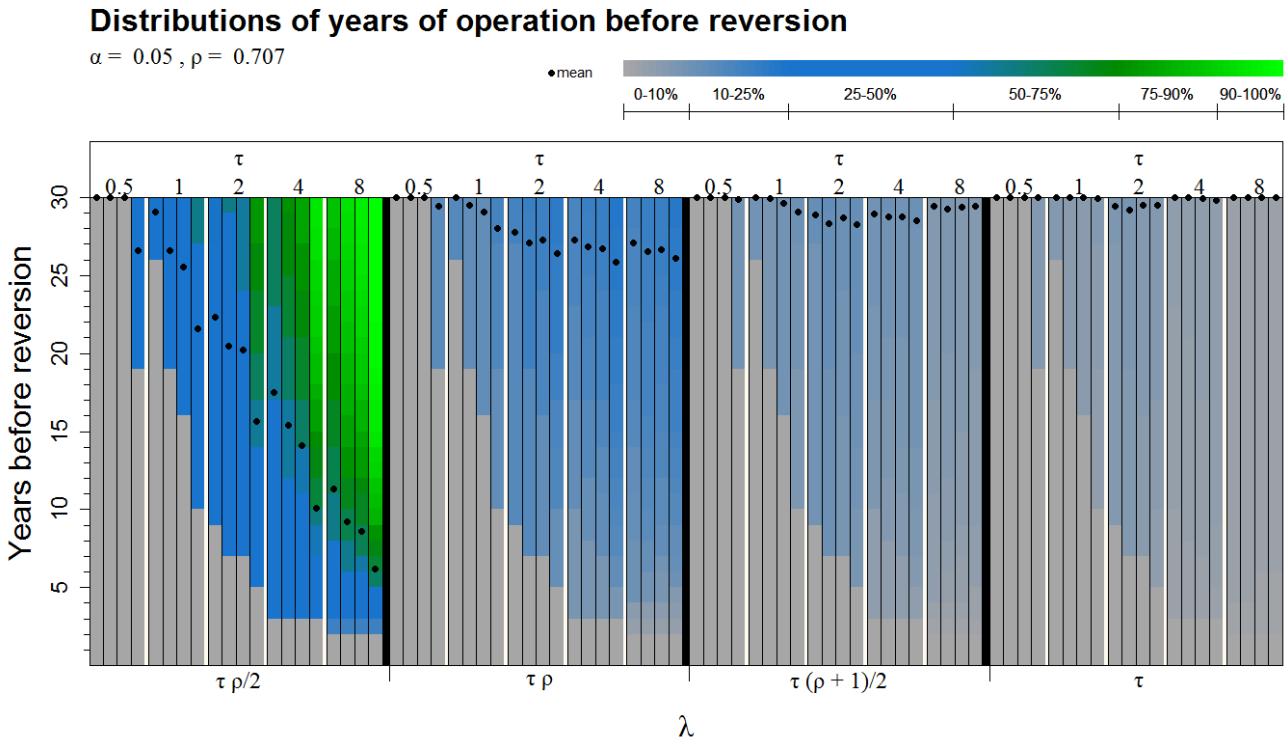

Figure 96. Distribution of years before reversion, with $\rho = 0.71, \alpha = 0.05$. The four bars within each subgroup represent $g = 0.08, 0.12, 0.15, 0.3$, respectively, in years 4–27. In all scenarios, $g = 0.3$ in years 1–3. See table 1 for explanation of terms used here.

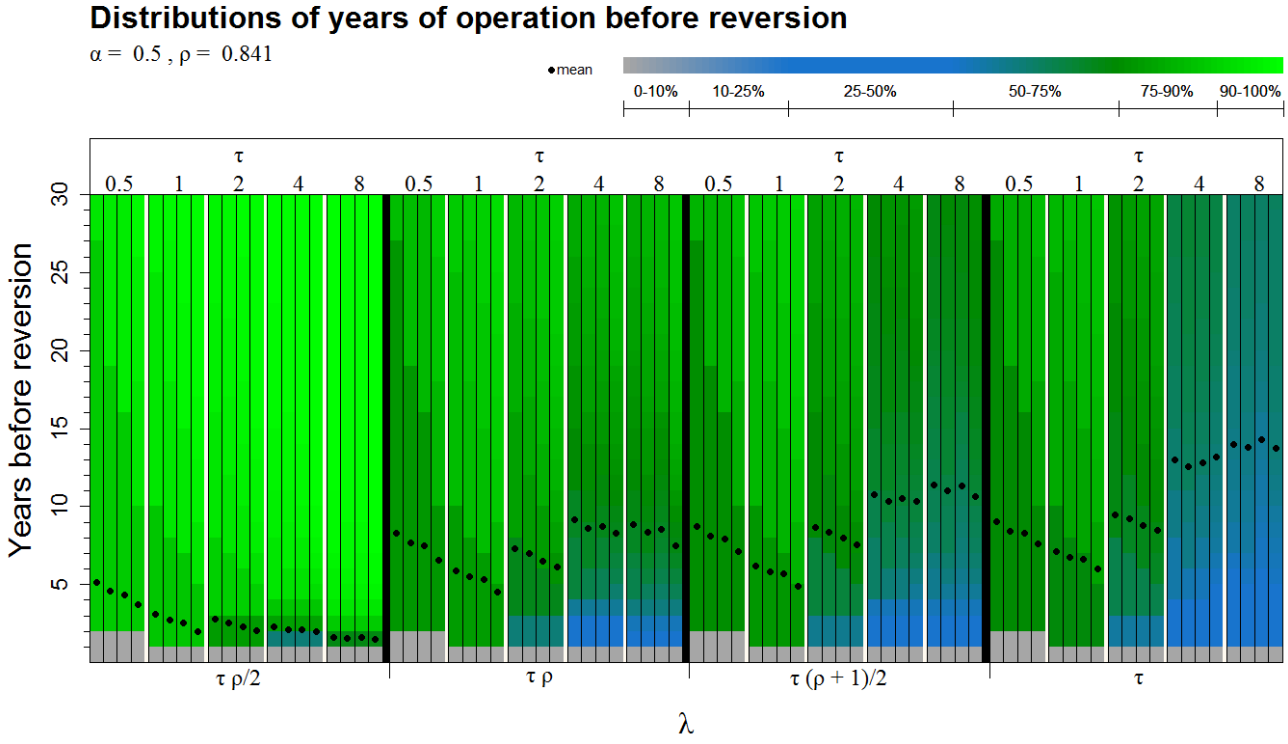

Figure 97. Distribution of years before reversion, with $\rho = 0.84, \alpha = 0.5$.The four bars within each subgroup represent $g = 0.08, 0.12, 0.15, 0.3$, respectively, in years 4–27. In all scenarios, $g = 0.3$ in years 1–3. See table 1 for explanation of terms used here.

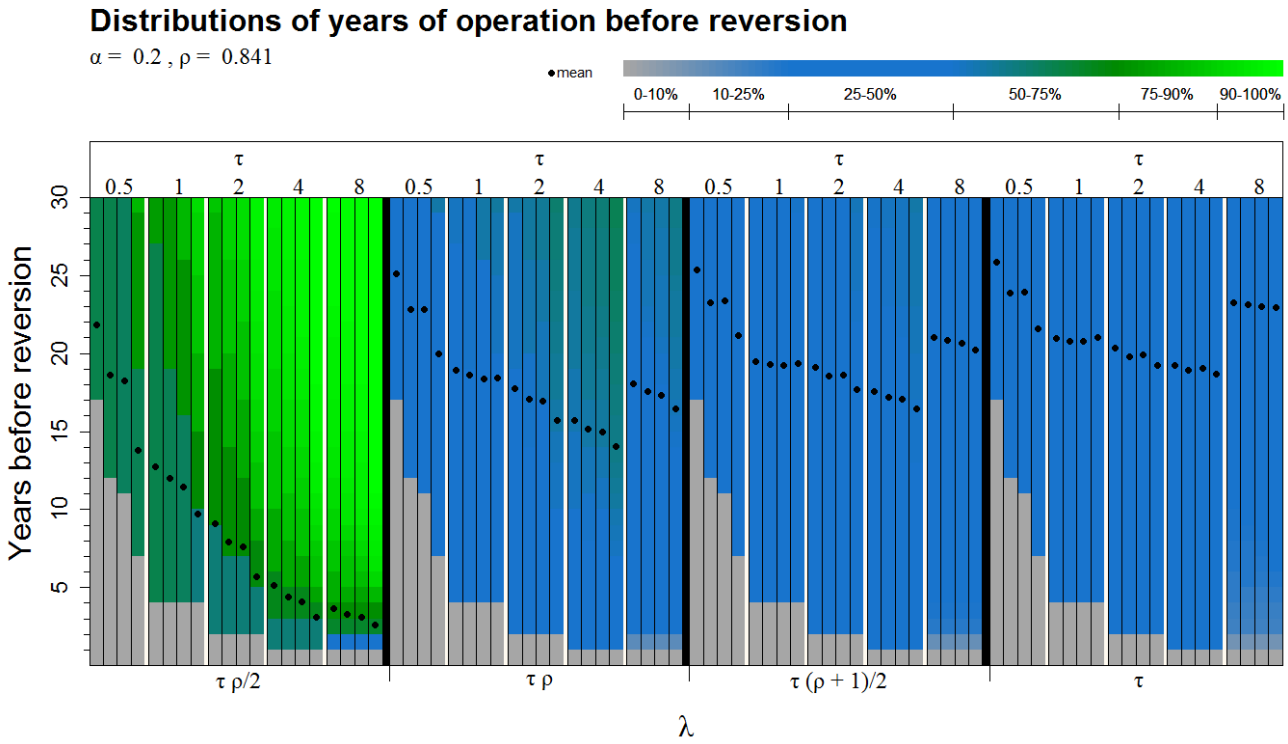

Figure 98. Distribution of years before reversion, with $\rho = 0.84, \alpha = 0.2$.The four bars within each subgroup represent $g = 0.08, 0.12, 0.15, 0.3$, respectively, in years 4–27. In all scenarios, $g = 0.3$ in years 1–3. See table 1 for explanation of terms used here.

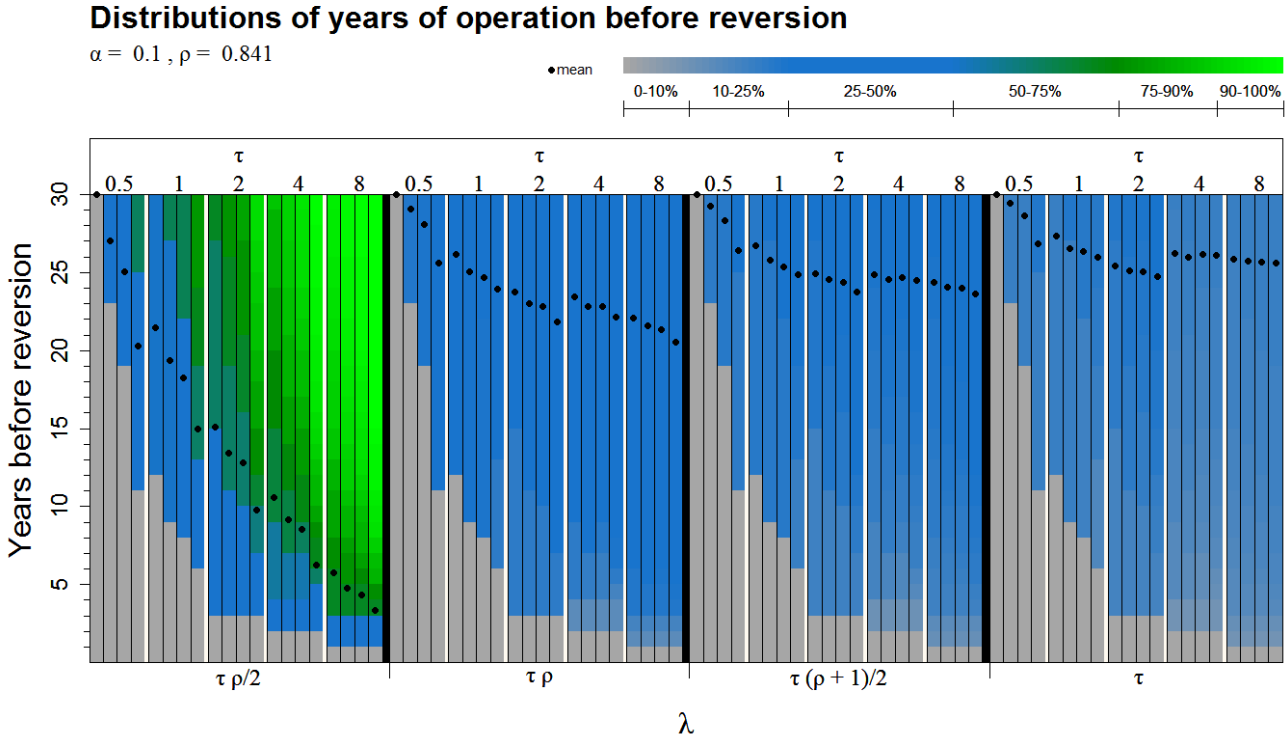

Figure 99. Distribution of years before reversion, with $\rho = 0.84, \alpha = 0.1$. The four bars within each subgroup represent $g = 0.08, 0.12, 0.15, 0.3$, respectively, in years 4–27. In all scenarios, $g = 0.3$ in years 1–3. See table 1 for explanation of terms used here.

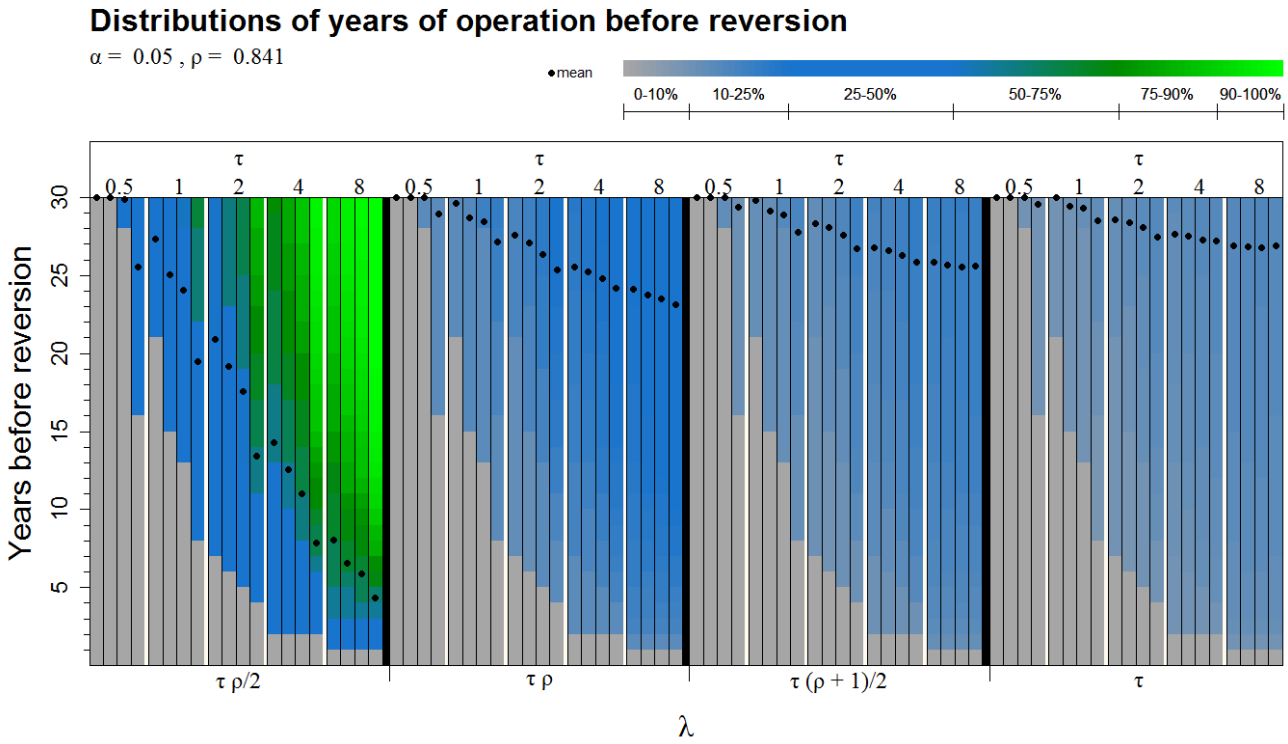

Figure 100. Distribution of years before reversion, with $\rho = 0.84, \alpha = 0.05$. The four bars within each subgroup represent $g = 0.08, 0.12, 0.15, 0.3$, respectively, in years 4–27. In all scenarios, $g = 0.3$ in years 1–3. See table 1 for explanation of terms used here.

As expected, less effective constraints were more commonly reversed.

Acknowledgments

This study benefitted tremendously from lively discussions and insightful comments and analysis from many people. Special thanks go to T.J. Miller (USFWS, retired), who spent many hours and days devouring all the details and offering a never-ending stream of constructive thoughts, questions, and comments. The work involved lengthy technical discussions with dozens of people, whose attention and assistance were welcome and much appreciated. Particularly valuable in shaping the work were the discussions with joint industry/government working groups that met in Indianapolis in February 2015 and in Portland, Oregon, in October 2015. Participants included T.J. Miller, Rick Amidon, Forest Clark, Sean Marsan, Scott Pruitt, and Megan Seymour (USFWS, Region 3), Tara Calloway (USFWS, Region 8), Ben Cowen (Locke Lord LLP), Christina Calabrese (EDP Renewables), Karyn Coppinger (Invenergy LLC), Mike Speerschneider (EverPower Wind Holdings, Inc.), John Anderson (American Wind Energy Association), Jerry Roppe (Iberdrola Renewables), Jim Lynch (K & L Gates LLP), Milani Chaloupka (Ecological Modelling Services Pty Ltd), Paul Rabie (Western Ecosystems Technology, Inc), and John Skalski (University of Washington). Leslie New's (Washington State University) insightful comments during and after a visit to Corvallis opened our eyes to nuances that we would otherwise have missed. Many thanks!

References Cited

Berger, J.O., Bernardo, J.M., and Sun, D., 2012, Objective priors for discrete parameter spaces: Journal of the American Statistical Association, v. 107, p. 636–648. DOI: 10.1080/01621459.2012.682538

Bispo, R., Bernardino, J., Marques, T.A., and Pestana, D., 2013, Modeling carcass removal time for avian mortality assessment in wind farms using survival analysis: Environmental and Ecological Statistics, v. 20, no. 1, p. 147–165, doi:10.1007/s10651-012-0212-5.

Cryan, P.M., Gorresen, P.M., Hein, C.R., Schirmacher, M.R., Diehl, R.H., Huso, M.M., Hayman, D.T.S., Fricker, P.D., Bonaccorso, F.J., Johnson, D.H., Heist, K., and Dalton, D.C., 2014, Behavior of bats at wind turbines: Proceedings of the National Academy of Sciences of the United States of America, v. 111, no. 42, p. 15126-15131, doi:10.1073/pnas.1406672111.

Dalthorp, D., Huso, M., Dail, D., and Kenyon, J., 2014, Evidence of absence software user guide: U.S. Geological Survey Data Series 881, p. 34, http://dx.doi.org/10.3133/ds881.

Erickson, W.P., Strickland, M.D., Johnson, G.D., and Kern, J.W., 1998, Examples of statistical methods to assess risks of impacts to birds from wind plants *in* Proceedings of the National Avian-Wind Power Planning Meeting III, San Diego, California, May 1998: Prepared for the Avian Subcommittee of the National Wind Coordinating Committee by LGL, Limited, King City, Ontario, p. 172–182.

Etterson, M.A., 2013, Hidden Markov models for estimating animal mortality from anthropogenic hazards: Ecological Applications, v. 23, p. 1915–1925, http://dx.doi.org/10.1890/12-1166.1.

Evans, W.R., 2012, An evaluation of the potential for using acoustic monitoring to remotely assess aerial vertebrate collisions at industrial wind energy facilities: New York State Energy Research and Development Authority, report 12-26, 19 p.

Huso, M.M.P., 2011, An estimator of wildlife fatality from observed carcasses: Environmetrics, v. 22, p. 318–329.

Huso, M.M.P., and Dalthorp, D., 2014, Accounting for unsearched areas in estimating wind turbine-caused fatality: Journal of Wildlife Management, v. 78, no. 2, p. 347–358, doi:10.1002/jwmg.663.

Huso, M.M.P., Dalthorp, D., Dail, D., and Madsen, L., 2015, Estimating wind-turbine caused bird and bat fatality when zero carcasses are observed: Ecological Applications, v. 25, no. 5, p. 1213–1225, doi:10.1890/14-0764.1.

Huso, M.M.P., Dalthorp, D., and Miller, T.J., in press, Wind energy development–Methods for assessing post-construction bird and bat mortality: Human-Wildlife Interactions.

Korner-Nievergelt, F., Korner-Nievergelt, P., Behr, O., Niermann, I., Brinkmann, R., and Hellriegel, B., 2011, A new method to determine bird and bat fatality at wind energy turbines from carcass searches: Wildlife Biology, v. 17, no. 4, p. 350–363, http://dx.doi.org/10.2981/10-121.

Meinke, C., Rabie, P., and Baker, Q., 2014, Fitting a square peg in a round hole–Applying the USGS evidence of absence model to habitat conservation plan compliance: Poster session *of* Joint Wind Wildlife Research Meeting of the National Wind Coordinating Collaborative and American Wind Wildlife Institute, Broomfield, Colorado.

Morrison, M., 2002, Searcher bias and scavenging rates in bird/wind energy studies: National Research Energy Laboratory, Golden, Colorado, NREL/SR-500-30876.

Pandey, A., Hermence, J., and Harness, R., 2007, Development of a cost-effective system to monitor wind turbines for bird and bat collisions—Phase I—Sensor system feasibility study: California Energy Commission, PIER Energy-Related Environmental Research, CEC-500-2007-004.

Péron, G., Hines, J.E., Nichols, J.D., Kendall, W.L., Peters, K.A., and Mizrahi, D.S., 2013, Estimation of bird and bat mortality at wind-power farms with superpopulation model: Journal of Applied Ecology, v. 50, no. 4, p. 902–911.

R Core Team, 2013, R: A language and environment for statistical computing. R Foundation for Statistical Computing, Vienna, Austria, http://www.R-project.org/.

Shoenfeld, P.S., 2004, Suggestions regarding avian mortality extrapolation: West Virginia Highlands Conservancy, Davis, West Virginia, accessed August 12, 2015, at http://www.wvhighlands.org/Birds/SuggestionsRegardingAvianMortalityExtrapolation.pdf.

Schulz, A., 2014, pBrackets: Plot Brackets. R package version 1.0. http://CRAN.R-project.org/package=pBrackets.

Wolpert, R.L., 2015, ACME: A Partially Periodic Estimator of Avian & Chiropteran Mortality at Wind Turbines: Web page, Cornell University Library, http://arxiv.org/abs/1507.00749.

Yee, T.W., 2010, The VGAM Package for Categorical Data Analysis. Journal of Statistical Software, v. 32, no. 10, p. 1-34, http://www.jstatsoft.org/v32/i10/.

Publishing support provided by the U.S. Geological Survey
Science Publishing Network, Tacoma Publishing Service Center

For more information concerning the research in this report, contact the
Director, Forest and Rangeland Ecosystem Science Center
U.S. Geological Survey
777 NW 9th St., Suite 400
Corvallis, Oregon 97330
http://fresc.usgs.gov/

ISSN 2331-1258 (online)
http://dx.doi.org/10.3133/ofr20151227